

---

# **Emissions and Fuel Economy of a Vehicle with a Spark-Ignition, Direct-Injection Engine: Mitsubishi Legnum GDI™**

---



**Center for Transportation Research  
Argonne National Laboratory**

Operated by The University of Chicago,  
under Contract W-31-109-Eng-38, for the

**United States Department of Energy**

---

# **Emissions and Fuel Economy of a Vehicle with a Spark-Ignition, Direct-Injection Engine: Mitsubishi Legnum GDI™**

---

by R.L. Cole, R.B. Poola, and R. Sekar

The Center for Transportation Research, Energy Systems Division,  
Argonne National Laboratory, 9700 South Cass Avenue, Argonne, Illinois 60439

February 1999

Work sponsored by United States Department of Energy,  
Office of Energy Efficiency and Renewable Energy, under Contract W-31-109-ENG-38

## Contents

ACKNOWLEDGMENTS .....	vii
ABSTRACT .....	1
1 INTRODUCTION .....	3
2 EXPERIMENTAL SETUP .....	4
2.1 Vehicle Specifications .....	4
2.2 Test Cycles and Series .....	6
2.3 Fuel Analysis .....	6
2.4 Test Matrix .....	9
3 TEST RESULTS .....	10
3.1 Fuel Economy and Greenhouse Gas Emissions .....	10
3.2 Mass Emissions .....	12
3.2.1 Engine-Out Emissions from SIDI Engine for Five Fuels .....	12
3.2.2 Engine-Out Emissions from SIDI and PFI Engines Using Indolene .....	15
3.2.3 Tailpipe Emissions from SIDI Engine for Five Fuels .....	15
3.2.4 Particulate Emissions from SIDI Engine .....	19
3.2.5 Tailpipe Emissions from SIDI and PFI Vehicles on Indolene (A) .....	20
3.2.6 Catalyst Efficiencies for SIDI and PFI Vehicles .....	22
3.2.7 FTP Emissions from SIDI and PFI Vehicles Compared with PNGV Goals .....	23
3.3 Second-by-Second Emissions .....	24
3.3.1 Engine-Out Emissions from SIDI Engine for Three Fuels .....	24
3.3.2 Engine-Out Emissions from SIDI and PFI Engines on Indolene .....	31
3.3.3 Tailpipe Emissions from SIDI Vehicle for Three Fuels .....	38
3.3.4 Tailpipe Emissions from SIDI and PFI Vehicles on Indolene .....	46
3.3.5 FTP Emissions from SIDI Vehicle, Measured at ATL .....	53
3.4 Hydrocarbon Speciation .....	62
3.5 Ozone-Forming Potential .....	66
3.6 Catalyst Efficiency .....	71
4 CONCLUSIONS .....	84
4.1 Fundamental Conclusions .....	84
4.2 Fuel Economy and Greenhouse Gas Emissions .....	85
4.3 Mass Emissions .....	85
4.4 Second-by-Second Emissions .....	87
4.5 Hydrocarbon Speciation .....	88
4.6 Ozone-Forming Potential .....	88
4.7 Catalyst Efficiency and Warm-Up Time .....	88
5 REFERENCES .....	90
APPENDIX: Test Results for Top 20 Hydrocarbon Species .....	91

## Tables

1	Specifications of Mitsubishi Legnum and Dodge Neon .....	5
2	Emissions Measurement Instruments Used at Amoco .....	7
3	Emissions Measurement Instruments Used at ATL .....	7
4	Fuel Properties.....	8
5	Test Matrix for the Mitsubishi .....	9
6	Test Matrix for the Neon .....	9
7	Comparison of Catalyst Efficiencies on the Basis of Weighted-Average Emissions.....	22

## Figures

1	Mitsubishi Legnum GDI™ Station Wagon .....	4
2	Dodge Neon on Chassis Dynamometer .....	5
3	Comparison of Fuel Economy Results .....	11
4	Histogram of Exhaust Oxygen Content .....	11
5	Carbon Dioxide Emissions.....	12
6	Engine-Out Emissions Obtained from Different Fuels during FTP-75 Test Cycle.....	13
7	Comparison of Engine-Out Emissions for Mitsubishi-SIDI and Neon-PFI Vehicles during FTP-75 Cycle.....	16
8	Comparison of Tailpipe Emissions from Mitsubishi-SIDI with Five Different Fuels during FTP-75 Cycle.....	18
9	Particulate Emissions from Mitsubishi SIDI during FTP-75 Cycle.....	20
10	Comparison of Tailpipe Emissions from Mitsubishi-SIDI and Neon-PFI during FTP-75 Cycle .....	21
11	Mitsubishi-SIDI's Challenge in Meeting PNGV Goals .....	23
12	Comparison of Engine-Out Emissions for Three Gasolines during FTP Cold Phase .....	25
13	Comparison of Engine-Out Emissions from Three Gasolines during Second Phase of FTP .....	27

## Figures (Cont.)

14	Comparison of Engine-Out Emissions from Three Gasolines during Third Phase of FTP .....	29
15	Comparison of Engine-Out Emissions from Mitsubishi-SIDI and Neon-PFI Vehicles during FTP Cold Phase.....	32
16	Comparison of Engine-Out Emissions from Mitsubishi-SIDI and Neon-PFI Vehicles during Second Phase of FTP.....	34
17	Comparison of Engine-Out Emissions from Mitsubishi-SIDI and Neon-PFI Vehicles during Third Phase of FTP.....	36
18	Comparison of Tailpipe Emissions for Three Gasolines during FTP Cold Phase .....	39
19	Comparison of Tailpipe Emissions from Three Gasolines during Second Phase of FTP .....	41
20	Comparison of Tailpipe Emissions from Three Gasolines during Third Phase of FTP .....	43
21	Comparison of Tailpipe Emissions from Mitsubishi-SIDI and Neon-PFI Vehicles during FTP Cold Phase.....	47
22	Comparison of Tailpipe Emissions from Mitsubishi-SIDI and Neon-PFI during Second Phase of FTP .....	49
23	Comparison of Tailpipe Emissions from Mitsubishi-SIDI and Neon-PFI during Third Phase of FTP .....	51
24	Comparison of Tailpipe and Engine-Out Emissions for Two Gasolines during the First Phase of the FTP .....	54
25	Comparison of Emissions for Two Gasolines during the Second Phase of the FTP .....	58
26	Comparison of Tailpipe and Engine-Out Emissions for Two Gasolines during the Third Phase of the FTP .....	63
27	Tailpipe Hydrocarbon Composition with Indolene (A).....	67
28	Tailpipe Hydrocarbon Composition for Mitsubishi-SIDI .....	68
29	Comparison of Ozone-Forming Potential of Indolene (A), Ultimate, and Low-Sulfur Gasolines in SIDI Vehicle.....	69
30	Comparison of Ozone-Forming Potential of SIDI vs. PFI Vehicles.....	70
31	Catalyst Conversion Efficiencies for THC, CO, and NO <sub>x</sub> for Three Gasolines during First Phase of FTP .....	72

## Figures (Cont.)

32	Catalyst Conversion Efficiencies for THC, CO, and NO <sub>x</sub> for Three Gasolines during Second Phase of FTP .....	74
33	Catalyst Conversion Efficiencies for THC, CO, and NO <sub>x</sub> for Three Gasolines during Third Phase of FTP .....	76
34	Catalyst Conversion Efficiencies for THC, CO, and NO <sub>x</sub> during First Phase of FTP .....	78
35	Catalyst Conversion Efficiencies for THC, CO, and NO <sub>x</sub> during Second Phase of FTP .....	80
36	Catalyst Conversion Efficiencies for THC, CO, and NO <sub>x</sub> during Third Phase of FTP .....	82
37	Converter Inlet Temperatures during First Phase of FTP .....	83

## **Acknowledgments**

The work that constitutes the basis of this report was supported by the U.S. Department of Energy, Office of Energy Efficiency and Renewable Energy, under Contract W-31-109-ENG-38.

Amoco Petroleum Products provided the two vehicles used in these tests. The first series of tests was performed at Amoco's facility in Naperville, Illinois. We thank David Tatterson, Alan Leard, John O'Keefe, James Doorhy, Jean Chen, and Larry Robinson of Amoco for their assistance in performing the tests.

Additional tests were performed at Automotive Testing Laboratories, Inc. (ATL), of East Liberty, Ohio. We thank Wendy Clark, Rick Jackson, and Walter Dudak of ATL for their assistance in performing these tests.

**Emissions and Fuel Economy of a Vehicle with a  
Spark-Ignition, Direct-Injection Engine:  
Mitsubishi Legnum GDI™**

by

R.L. Cole, R.B. Poola, and R. Sekar

**Abstract**

A 1997 Mitsubishi Legnum station wagon with a 150-hp, 1.8-L, spark-ignition, direct-injection (SIDI) engine was tested for emissions by using the FTP-75, HWFET, SC03, and US06 test cycles and four different fuels. The purpose of the tests was to obtain fuel-economy and emissions data on SIDI vehicles and to compare the measurements obtained with those of a port-fuel-injection (PFI) vehicle. The PFI vehicle chosen for the comparison was a 1995 Dodge Neon, which meets the Partnership for a New Generation of Vehicles (PNGV) emissions goals of nonmethane hydrocarbons (NMHC) less than 0.125 g/mi, carbon monoxide (CO) less than 1.7 g/mi, nitrogen oxides (NO<sub>x</sub>) less than 0.2 g/mi, and particulate matter (PM) less than 0.01 g/mi. The Mitsubishi was manufactured for sale in Japan and was not certified to meet current U.S. emissions regulations.

Results show that the SIDI vehicle can provide up to 24% better fuel economy than the PFI vehicle does, with correspondingly lower greenhouse gas emissions. The SIDI vehicle as designed does not meet the PNGV goals for NMHC or NO<sub>x</sub> emissions, but it does meet the goal for CO emissions. Meeting the goal for PM emissions appears to be contingent upon using low-sulfur fuel and an oxidation catalyst. One reason for the difficulty in meeting the NMHC and NO<sub>x</sub> goals is the slow (200 s) warm-up of the catalyst. Catalyst warm-up time is primarily a matter of design. The SIDI engine produces more NMHC and NO<sub>x</sub> than the PFI engine does, which puts a greater burden on the catalyst to meet the emissions goals than is the case with the PFI engine. Oxidation of NMHC is aided by unconsumed oxygen in the exhaust when the SIDI engine operates in stratified-charge mode, but the same unconsumed oxygen inhibits chemical reduction of NO<sub>x</sub>. Thus, meeting the NO<sub>x</sub> emissions goal is likely to be the greatest challenge for the SIDI engine.





## 1 Introduction

This report describes tests that were conducted on a spark-ignition, direct-ignition (SIDI) vehicle, a 1997 Mitsubishi Legnum station wagon with a 1.8-L GDI™ engine, and on a comparison vehicle, a 1995 Dodge Neon sedan. The purpose of these tests was to provide emissions data on SIDI vehicles and to compare the SIDI emissions with those of a port-fuel-injection (PFI) vehicle. The PFI comparison vehicle was chosen as one that meets the Partnership for a New Generation of Vehicles (PNGV) emissions goals, namely, nonmethane hydrocarbons (NMHC) less than 0.125 g/mi, carbon monoxide (CO) less than 1.7 g/mi, nitrogen oxides (NO<sub>x</sub>) less than 0.2 g/mi, and particulate matter (PM) less than 0.01 g/mi.

The Mitsubishi Legnum was tested under the FTP-75, HWFET, SC03, and US06 test cycles with four different fuels. The results were compared with those for the Neon, which was tested only under the FTP-75 and HWFET cycles, using Indolene as the fuel. In addition to the normal measurements of NO<sub>x</sub>, total hydrocarbons (THC), methane (CH<sub>4</sub>), CO, and carbon dioxide (CO<sub>2</sub>) on a bag-wise basis, these gases and the exhaust gas temperature were measured on a second-by-second basis and the hydrocarbons were speciated. For some of the Mitsubishi tests, the exhaust-gas oxygen (O<sub>2</sub>) and PM were also measured.

The results show that the SIDI engine is a potential alternative to the compression-ignition, direct-injection (CIDI) engine (that is, the diesel engine) as a PNGV prime mover. However, meeting the NO<sub>x</sub> limit will be as challenging for the SIDI engine as it is for the CIDI engine. Meeting the NMHC limit will also be a challenge, but not to the degree that meeting the NO<sub>x</sub> limit is. Whether the SIDI engine can meet the PM limit will depend on the type of fuel used. This report also contains recommendations for future research.

## 2 Experimental Setup

### 2.1 Vehicle Specifications

The subject vehicle of this series of tests is a 1997 Mitsubishi Legnum with a 1.8-L spark-ignition, direct-injection (SIDI) engine. The vehicle, shown in Figure 1, is a five-passenger station wagon that is available to the Japanese public. The vehicle is certified to meet Japanese emissions and safety regulations but is not certified under U.S. regulations. At the beginning of testing, the vehicle had about 1,440 km (900 mi) on the odometer. A sedan version of the vehicle, called the Galant, is also available in Japan with the SIDI engine. The U.S. version of the Galant does not offer the SIDI engine.

The Mitsubishi uses a dual catalyst system, with both catalysts located under the floor. The first catalyst is an iridium-based selective-reduction  $\text{NO}_x$  catalyst that was developed jointly by Mitsubishi and Nippon Shokubai Corp. This catalyst extends the range of  $\text{NO}_x$ -reduction to leaner air/fuel ratios than a conventional three-way catalyst can handle. The second catalyst is a conventional three-way catalyst, which oxidizes hydrocarbons and carbon monoxide and can reduce  $\text{NO}_x$  during homogeneous-mode operation.

For comparison, a 1995 Dodge Neon sedan with a 2.0-L PFI engine was tested. The Neon was chosen as a comparison vehicle because it meets the PNGV emissions goals, and it is approximately the same size as the Legnum. The Neon has been certified for U.S. emissions and safety standards. It also meets the Tier II (year 2004) emissions standards, which are the emissions goals for the PNGV program. The Neon is shown in Figure 2. Specifications of both vehicles are compared in Table 1. At the beginning of testing, the comparison vehicle had about 88,320 km (55,200 mi) on the odometer. The Neon is 306 mm shorter, 165 mm lower, 34 mm narrower, and



**FIGURE 1 Mitsubishi Legnum GDI™ Station Wagon  
(Argonne National Laboratory photo)**



**FIGURE 2 Dodge Neon on Chassis Dynamometer (Argonne National Laboratory photo)**

**TABLE 1 Specifications of Mitsubishi Legnum and Dodge Neon**

	Mitsubishi Legnum	Dodge Neon
Engine type	1.8-L I4	2.0-L I4
Maximum power	112 kW @ 6500 rpm	98 kW @ 6000 rpm
Maximum torque	128 N-m @ 5000 rpm	174 N-m @ 5000 rpm
Bore	81.0 mm	87.5 mm
Stroke	89.0 mm	83.0 mm
Displacement	1834 cm <sup>3</sup>	1995 cm <sup>3</sup>
Compression ratio	12.0:1	9.8:1
Cylinder head	Pentroof, DOHC, 4 valves per cylinder	Pentroof, SOHC, 4 valves per cylinder
Piston	Asymmetrical, with hemispherical bowl in crown	Symmetrical
Intake port	Upright, located between the camshafts	Horizontal
Fuel system	Direct injection, 5.0 MPa pressure	Port injection
Transmission	4-speed automatic	3-speed automatic
Vehicle height	1510 mm	1345 mm
Vehicle length	4670 mm	4364 mm
Vehicle width	1740 mm	1706 mm
Wheelbase	2635 mm	2642 mm
Weight	1260 kg	1080 kg
Seating capacity	5	5

180 kg lighter than the Mitsubishi. However, the vehicles are close enough in size than these differences do not invalidate the test results.

The catalyst used on the Neon is a conventional three-way catalyst. It is located close to the exhaust manifold to provide fast warm-up.

## **2.2 Test Cycles and Series**

Both the Mitsubishi Legnum and the Dodge Neon were tested under the FTP-75 and Highway Fuel-Economy (HWFET) procedures established by the U.S. Environmental Protection Agency (EPA); this series of tests was conducted in a laboratory owned by Amoco Petroleum Products of Naperville, Illinois. (Amoco is the owner of both vehicles.) A second series of tests of the Mitsubishi only was conducted at Automotive Testing Laboratories, Inc. (ATL), of East Liberty, Ohio. The ATL tests included the FTP-75, HWFET, SC03, and US06 test cycles. The tests were supervised by an ANL engineer.

Instruments used for the tests are indicated in Tables 2 and 3. In addition to measurements made with those instruments, the exhaust-gas temperature was measured at the catalytic converter inlet, at the catalytic converter outlet, and (at the Amoco laboratory only) immediately before the exhaust gas entered the constant-volume system (CVS). Both engine-out and tailpipe measurements were taken. For the engine-out measurements, dummy catalytic converters were fabricated and installed in place of the catalytic converters. Each dummy catalytic converter had a backpressure valve that was adjusted to give the same backpressure at 50 miles per hour (mph) as that produced by the catalytic converter.

The following data were measured for each cycle of each test: total hydrocarbons, methane, carbon monoxide, carbon dioxide, oxides of nitrogen, and speciated hydrocarbons. Second-by-second data were also measured for the following: total hydrocarbons, methane, carbon monoxide, carbon dioxide, oxides of nitrogen, and exhaust-gas temperatures (measured at converter inlet, converter outlet, and, at Amoco only, inlet to CVS.) Additional measurements at ATL only included exhaust oxygen content at the inlet of the catalytic converter or dummy converter and particulate matter (PM<sub>10</sub>), which was measured for the FTP-75, HWFET, and SC03 tests only. In addition fuel properties were analyzed for each fuel used.

## **2.3 Fuel Analysis**

Three fuels were used for the tests at the Amoco laboratory. The Mitsubishi was run on Indolene (A), Amoco Premium Ultimate, and a low-sulfur blend. The Dodge Neon was run on Indolene (A) only. Two fuels were used at ATL. California phase-2 reformulated gasoline (RFG) was used for all four test cycles, and Indolene (B) was used only for the FTP-75 and US06 test cycles.

**TABLE 2 Emissions Measurement Instruments Used at Amoco**

Measurement	Instrument
Dynamometer	Clayton DC-90 Hydrokinetic Power Absorber
CO, high range, second-by-second	2 Beckman Model 864
CO, low range, second-by-second	2 Beckman Model 865 IR
CO <sub>2</sub> , second-by-second	2 Beckman Model 868
Hydrocarbons, second-by-second	4 Beckman Model 400A
NO/NO <sub>x</sub> , second-by-second	2 Beckman Model 951A
Exhaust-gas speciation	2 HP 5840 Series II Gas Chromatograph
Exhaust aldehydes and ketones	High-pressure liquid chromatography (HPLC)

**TABLE 3 Emissions Measurement Instruments Used at ATL**

Measurement	Instrument	
	FTP, SC03, and HWFET	US06
Dynamometer	Clayton ECE-50	Horiba DMA-20-86-150hp
CO	Horiba AIA-210 and 220	Rosemount 864
CO <sub>2</sub>	Horiba AIA-220	Rosemount 880
Hydrocarbons	Horiba FIA-220 and Beckman 402	Rosemount 400A
NO <sub>x</sub>	Horiba CLA-220	Rosemount 951
CH <sub>4</sub>	Horiba GFA-220	Horiba GFA-220
O <sub>2</sub>	Horiba Mexa λ and MB200	Horiba Mexa λ and MB200
Catalyst temp.	Omega type K	Omega type K
CVS	Horiba CVS	Horiba CVS-46 CFV
Particulates	Gelman #2200 holder and T60A20 filter	—

The designations (A) and (B) for Indolene are used in this report to distinguish these fuels, which have slightly different properties. Indolene was chosen because it is the standard reference fuel; however, it has 154-161 ppm of sulfur. Japanese fuel specifications limit sulfur to a maximum of 30 ppm.

Premium Ultimate was chosen as being representative of American premium gasolines. The 12.0:1 compression ratio of the SIDI engine makes a premium fuel desirable, although Mitsubishi claims the engine will run on Japanese regular-grade gasoline. The 77-ppm sulfur content of Premium Ultimate also exceeds the maximum sulfur specification for Japanese fuel. The Premium

Ultimate is a winter gasoline and has the highest Reid vapor pressure, 12.62 psi, of the three gasolines.

The low-sulfur gasoline is a blend based on racing fuel. It has a sulfur content of 20 ppm and a low Reid vapor pressure, 7.92 psi. It also has a high aromatic content, 63.908%, the narrowest boiling range ( $T_{90} - T_{10} = 84^{\circ}\text{C}$ ), and a high oxygenate content, 11.273%.

The RFG has a sulfur content of 30.2 ppm; the lowest Reid vapor pressure, 6.9 psi; a narrow boiling range ( $T_{90} - T_{10} = 88^{\circ}\text{C}$ ); and the highest oxygenate content, 11.273%. The properties of the low-sulfur fuel and RFG are similar, except for aromatic content. Fuel properties for all of the gasolines are summarized in Table 4.

**TABLE 4 Fuel Properties**

Property	Indolene (A)	Premium Ultimate	Low-Sulfur Fuel	Indolene (B)	California Phase 2 RFG
Heating value, Btu/lb	18,497	18,286	18,109	18,467	18,163
API gravity	59.05	67.7	49.3	59.3	
Sp. gr. @ 15.5°C	0.7426	0.7127	0.7839	0.7415	0.7380
Reid vapor, psi	8.34	12.62	7.92	8.73	6.9
Octane no., (R+M)/2	91.5	93.0	99.9	92.1	92.0
Carbon, wt %	85.35	83.90	86.07	86.43	84.29
Hydrogen, wt %	13.40	14.70	12.10	13.41	13.71
Oxygen, wt %	0.20	1.52	2.56	Not reported	Not reported
Sulfur, ppm	154	77	20	161	30.2
$T_{10}$ , °C	54	40	60	50	61
$T_{50}$ , °C	104	85	104	100	94
$T_{90}$ , °C	165	148	144	158	149
Paraffins, %	65.0 <sup>a</sup>	5.396	4.725	64 <sup>a</sup>	67.1 <sup>a</sup>
Iso-paraffins, %		28.909	18.442		
Naphthenes, %		4.103	1.304		
Aromatics, %	27.5	50.243	63.908	29	27.2
Olefins, %	7.5	4.722	0.259	7	5.7
$\text{C}_{14+}$ , %	0.000	0.000	0.500		
Unknowns, wt %	0.788	2.049	0.089		
Oxygenates, wt %	0.000	4.578	11.273		11.11

<sup>a</sup> Includes all saturates.

## 2.4 Test Matrix

The test matrix for the Mitsubishi is shown in Table 5, and that for the Neon is shown in Table 6. Duplicate tests for each point on the test matrix were run; the results presented here are averages of the two runs, unless otherwise specified.

**TABLE 5 Test Matrix for the Mitsubishi<sup>a</sup>**

Test Cycle	Indolene (A)	Premium Ultimate	Low-Sulfur Fuel	Indolene (B)	California Phase 2 RFG
FTP-75	A	A	A	B	B
HWFET	A	A	A		B
SC03					B
US06				B	B

<sup>a</sup> A = tests at Amoco; B = tests at ATL.

**TABLE 6 Test Matrix for the Neon<sup>a</sup>**

Test Cycle	Indolene (A)	Premium Ultimate	Low-Sulfur Fuel
FTP-75	A	A	A
HWFET	A	A	A

<sup>a</sup> A = tests at Amoco.



### 3 Test Results

Test results range from broad overall results to detailed results. In this report, the overall results, such as fuel economy and greenhouse gas emissions, are presented first; these are followed by presentation of the more detailed results. The results presented include fuel economy and greenhouse gas emissions, mass emissions, second-by-second emissions, hydrocarbon speciation, ozone-forming potential, and catalyst efficiency.

#### 3.1 Fuel Economy and Greenhouse Gas Emissions

Fuel economy for the FTP and HWFET (“Highway”) cycles is shown in Figure 3. Both vehicles used Indolene fuel. The normal dynamometer settings were 1477 kg (3250 lb) inertia and 4.1 kW (5.5 hp) load for the Mitsubishi SIDI and 1307 kg (2875 lb) inertia and 5.0 kW (6.7 hp) load for the Neon. A third case, in which the Mitsubishi (SIDI) was run at the Neon (PFI) inertia and load, is also shown in Figure 3 to determine whether the difference in fuel economy is due to differences in the engines or differences in dynamometer settings.

Figure 3 shows that, at Amoco, the FTP fuel economy of 35 miles per gallon (mpg) for the SIDI using Indolene (A) was about 22% more than the PFI’s 28.5 mpg using the same fuel. Highway fuel economy of 53 mpg for the SIDI was about 24% more than the PFI’s 43 mpg. Using the PFI’s dynamometer settings increased the SIDI’s FTP fuel economy by 1 mpg and decreased its highway fuel economy by 2 mpg. These differences are insignificant, compared with the differences in fuel economy between the SIDI and the PFI.

The spark-ignition direct-injection engine in the SIDI vehicle is primarily responsible for its high fuel economy, compared to the port fuel-injection engine in the PFI vehicle. The high fuel economy of the SIDI vehicle can be attributed to (1) its relatively low intake pumping losses, made possible by the stratified-charge mode of operation, and (2) the 12.0:1 compression ratio. According to Mitsubishi, the high compression ratio is made possible by the knock suppression characteristics of direct injection.<sup>1</sup>

The SIDI vehicle was also tested with the FTP cycle, using Indolene (B), at ATL. Its fuel economy of 30 mpg at ATL was 14% less than the 35 mpg measured at Amoco. Although this discrepancy was larger than expected, it does serve to illustrate the difference between the two laboratories.

The SIDI engine can display higher fuel economy than the PFI engine can because the former operates in the stratified-charge mode for a significant amount of time. It is also capable of switching between the homogeneous-charge mode, when the engine must produce high power, and the stratified-charge mode, when the engine is lightly loaded. Figure 4 shows a histogram of exhaust oxygen for an entire FTP-75 cycle, excluding the 10-minute soak when the engine was not

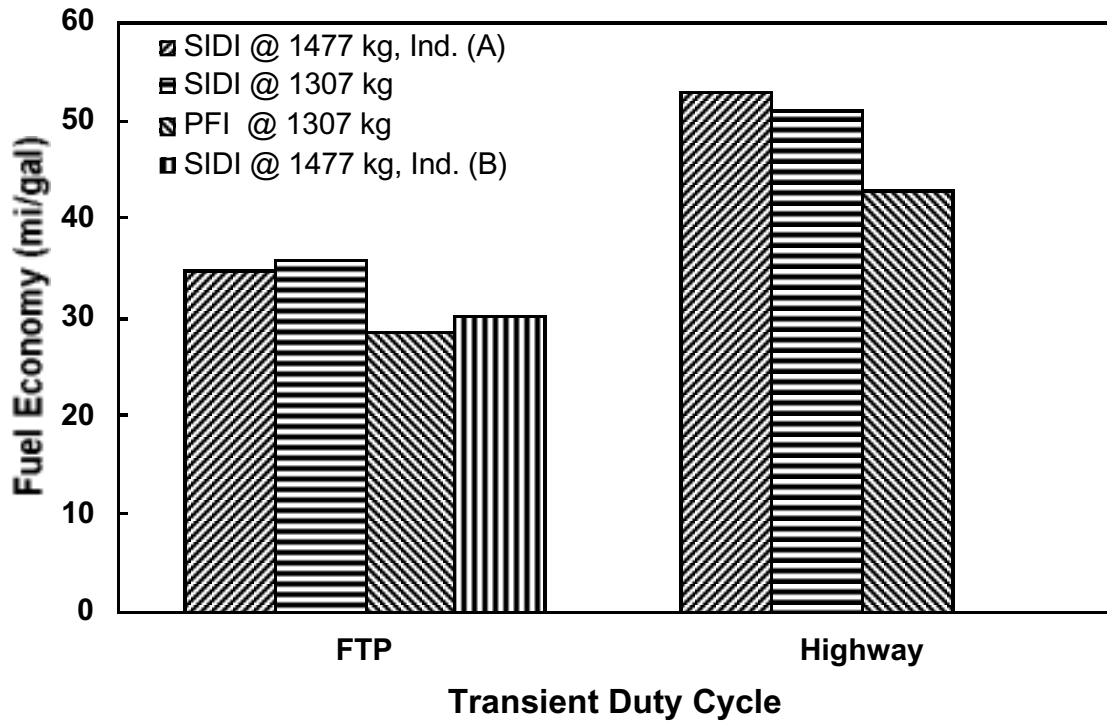


FIGURE 3 Comparison of Fuel Economy Results

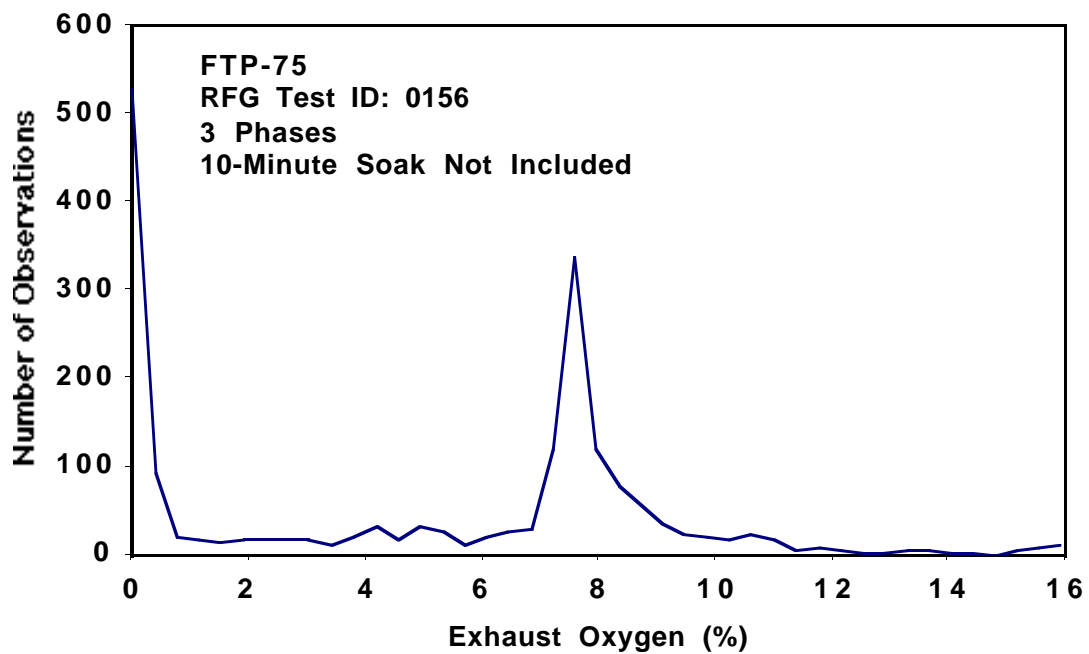


FIGURE 4 Histogram of Exhaust Oxygen Content

running. Exhaust oxygen was recorded every second, and Figure 4 plots the number of observations against exhaust oxygen content. The figure shows a bimodal distribution of oxygen content with peaks at 0% and 7.9%. Exhaust oxygen of 0% corresponds to a stoichiometric (that is, homogeneous charge) air/fuel ratio, and exhaust oxygen of 7.9% corresponds to a lean (that is, stratified charge) air/fuel ratio.

Figure 5 compares the emissions of carbon dioxide, an important greenhouse gas, associated with the SIDI Mitsubishi and the PFI Neon. Carbon dioxide emissions are closely related to fuel economy for gasoline- and diesel-fueled vehicles. As shown, the weighted-average carbon dioxide emissions from the SIDI vehicle are about 23% less than those from the PFI vehicle.

## 3.2 Mass Emissions

### 3.2.1 Engine-Out Emissions from SIDI Engine for Five Fuels

Engine-out emissions from the SIDI engine running on the five different fuels are shown in Figure 6. Weighted-average total-hydrocarbon emissions are 15% higher for the low-sulfur fuel than for Indolene (A), 6% lower for Ultimate than for Indolene (A), and 12% lower for RFG than

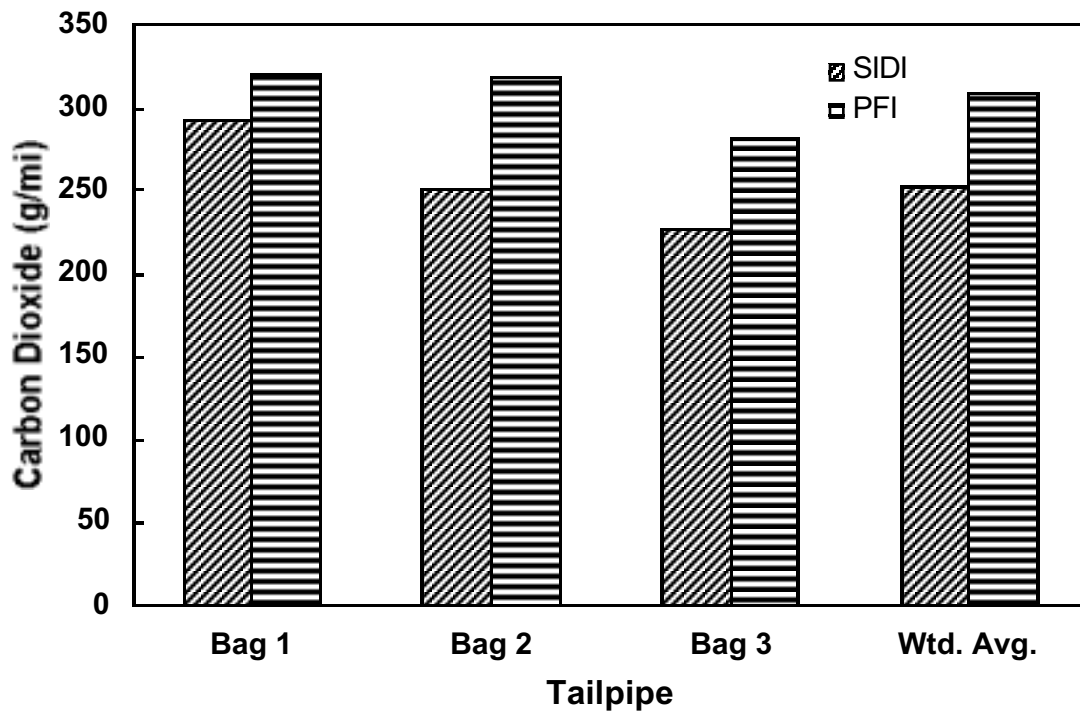


FIGURE 5 Carbon Dioxide Emissions

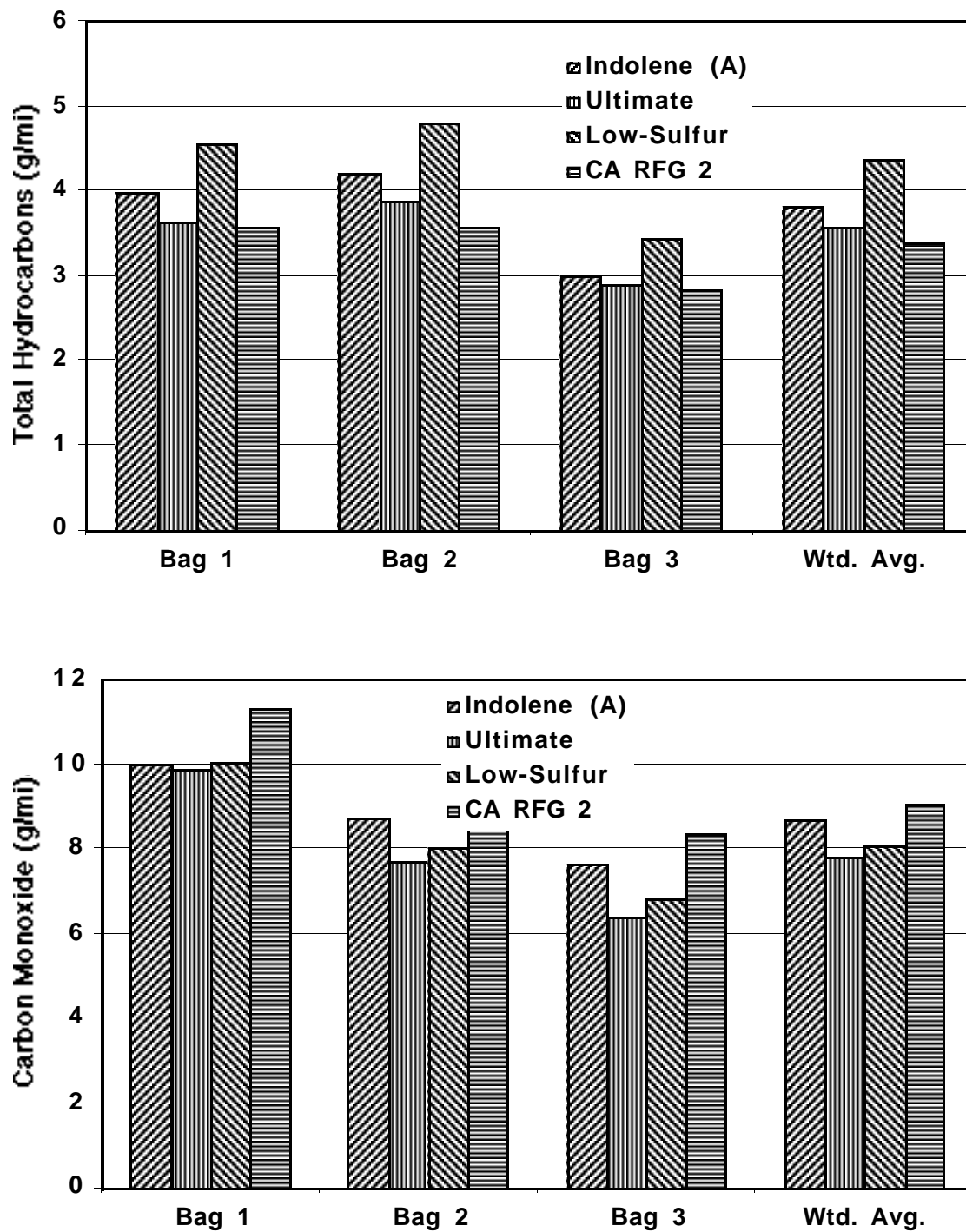
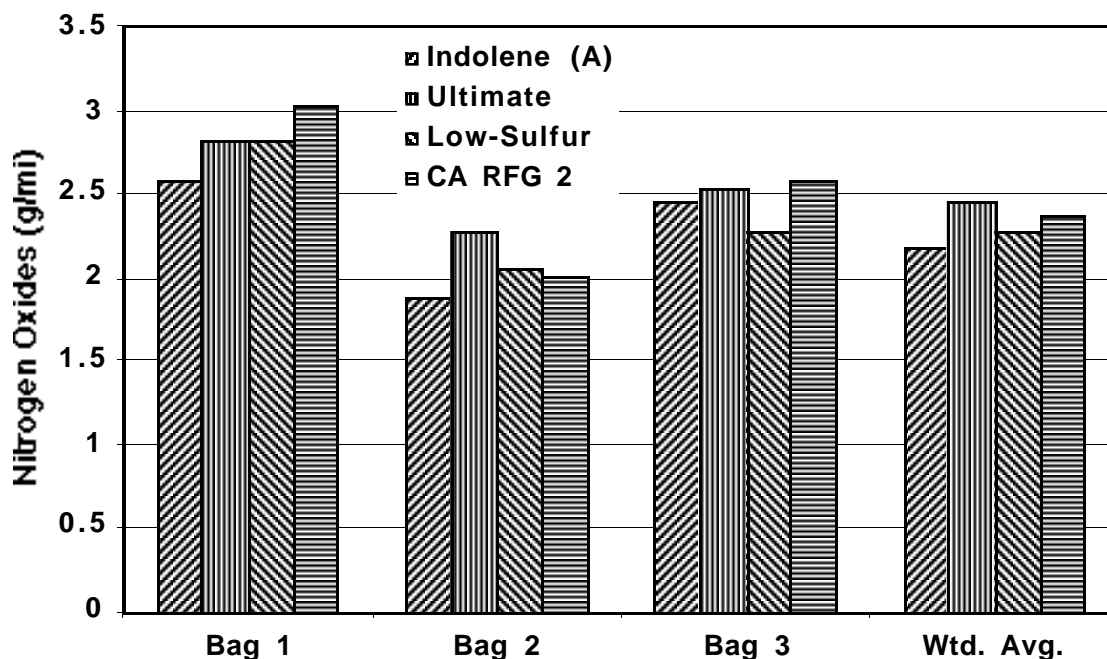


FIGURE 6 Engine-Out Emissions Obtained from Different Fuels during FTP-75 Test Cycle



**FIGURE 6 (Cont.)**

for Indolene (A). The disparity between the low-sulfur fuel and the RFG is noteworthy because the properties of the two fuels are similar except for the aromatic content. Low-sulfur fuel has 63.9% aromatics, but RFG has 27.2% aromatics. The two fuels have similar low Reid vapor pressures (7.92 and 6.9 psi), similar narrow boiling ranges (84 and 88°C), and similar high oxygenate contents (11.273 and 11.11%). See Table 4. The hypothesis that high aromatic content is associated with high hydrocarbon emissions is not completely borne out, because Ultimate has high aromatic content (50.243%) with low hydrocarbon emissions. The effect of the cold start is shown by comparing hydrocarbon emissions from bag 1 to those from bag 3. Hydrocarbon emissions from bag 1 are 1.25 to 1.33 times more than those from bag 3.

Weighted-average engine-out CO emissions with the Ultimate fuel are 10% less, low-sulfur fuels are 7% less, and RFG are 4.5% more than CO emissions with Indolene (A). As was the case for hydrocarbons, there is a significant difference in CO emissions between low-sulfur fuel and RFG, which differ mainly in aromatic content. The CO emissions with the high-aromatic low-sulfur fuel are less than those of the low-aromatic RFG. In this case, Ultimate, which has a high aromatic content, also has low CO emissions. The effect of the cold start on CO emissions was similar to that on hydrocarbon emissions. CO emissions from bag 1 are 1.30-1.55 times more than those from bag 3.

Weighted-average engine-out NO<sub>x</sub> emissions with Ultimate are 13% higher, those with low-sulfur fuel are 4% higher, and those with RFG are 8.8% higher than NO<sub>x</sub> emissions with Indolene (A). Indolene (A) has the lowest aromatic content of these fuels. The association of low

aromatic content with reduced combustion temperature and low NO<sub>x</sub> emissions has been described in the literature.<sup>2</sup>

### 3.2.2 Engine-Out Emissions from SIDI and PFI Engines Using Indolene

Figure 7 compares engine-out emissions of the SIDI engine with those of the PFI engine. Both engines ran on Indolene. Weighted-average total hydrocarbon emissions from the SIDI vehicle are 294% more than those of the PFI vehicle. The SIDI engine operates in the stratified-charge mode for a significant part of the test. The stratified region has gradients of fuel/air mixture, ranging from much richer than stoichiometric to much leaner than stoichiometric. These rich and lean regions can be expected to contribute to the hydrocarbon emissions. In contrast, the PFI engine has a homogeneous mixture that is optimized by the oxygen sensor to minimize emissions.

Weighted-average NO<sub>x</sub> emissions from the SIDI vehicle are 41% more than those from the PFI vehicle. The SIDI engine operates at significantly higher combustion pressure than the PFI engine for two reasons: (1) The SIDI engine has a 12.0:1 compression ratio vs. 9.8:1 for the PFI engine, and (2) the SIDI engine operates at a higher intake-manifold pressure than does the PFI engine. The higher combustion pressure leads to higher combustion temperature and higher NO<sub>x</sub> emissions. In addition, the stratified-charge combustion of the SIDI engine is fundamentally different from the homogeneous-charge combustion of the PFI engine. The gradient of fuel mixture in the stratified charge ranging from very lean to very rich implies that portions of the mixture are nearly stoichiometric. These nearly stoichiometric regions will have a high combustion temperature, leading to NO<sub>x</sub> formation. The homogeneous mixture of the PFI engine is optimized sufficiently lean of the stoichiometric condition that little NO<sub>x</sub> forms. Differences in ignition timing may also account for some of the differences in engine-out NO<sub>x</sub> emissions.

Weighted-average engine-out CO emissions from the SIDI engine are about 4% less than those of the PFI engine. Most of this difference is accounted for in bag 1, where the SIDI CO emissions are 16% less than those of the PFI engine. In the cold start, the PFI engine requires an enriched fuel/air mixture until the engine warms up enough to vaporize the fuel that impinges on the intake ports. In contrast, all of the fuel goes directly into the cylinder in the SIDI engine, so variations in mixture during the cold start are not as significant.

### 3.2.3 Tailpipe Emissions from SIDI Engine for Five Fuels

Figure 8 compares the tailpipe emissions of the SIDI engine for the five fuels. Hydrocarbon emissions with Indolene (B) were 13% less than those with Indolene (A). Since the fuels are similar to each other, most of the difference can be attributed to differences between the test laboratories. Hydrocarbon emissions for Ultimate were 20% less, for low-sulfur fuel they were 12% more, and for RFG they were 27% less than those for Indolene (A). This is similar to

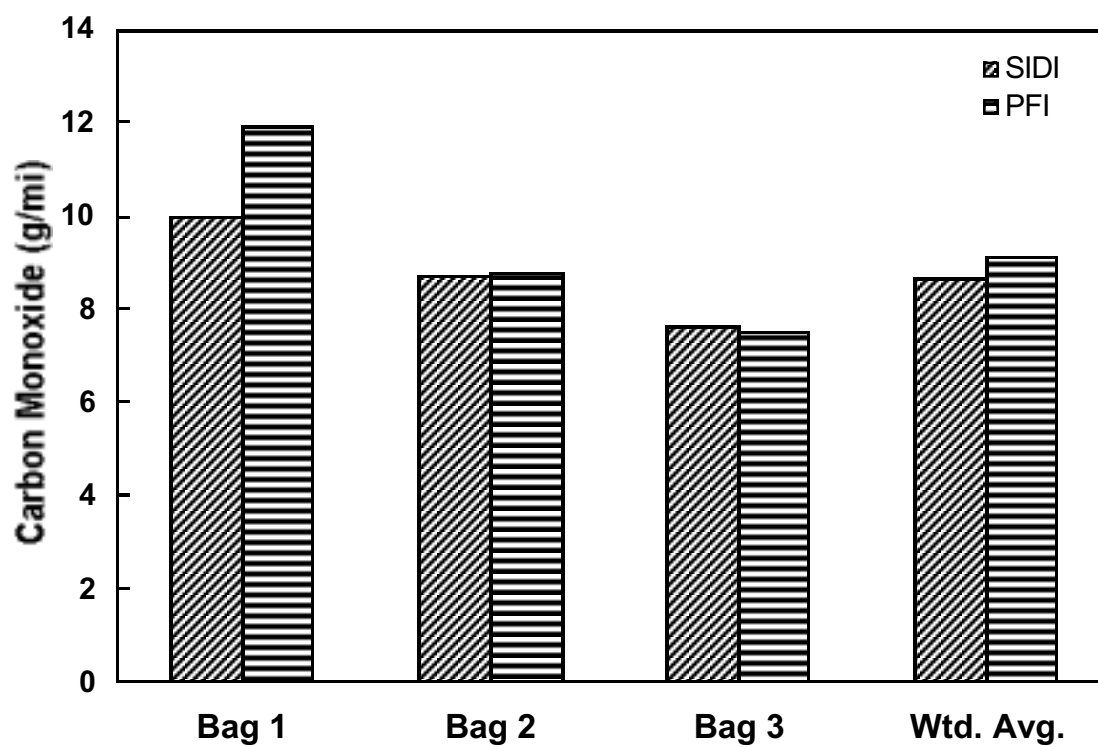
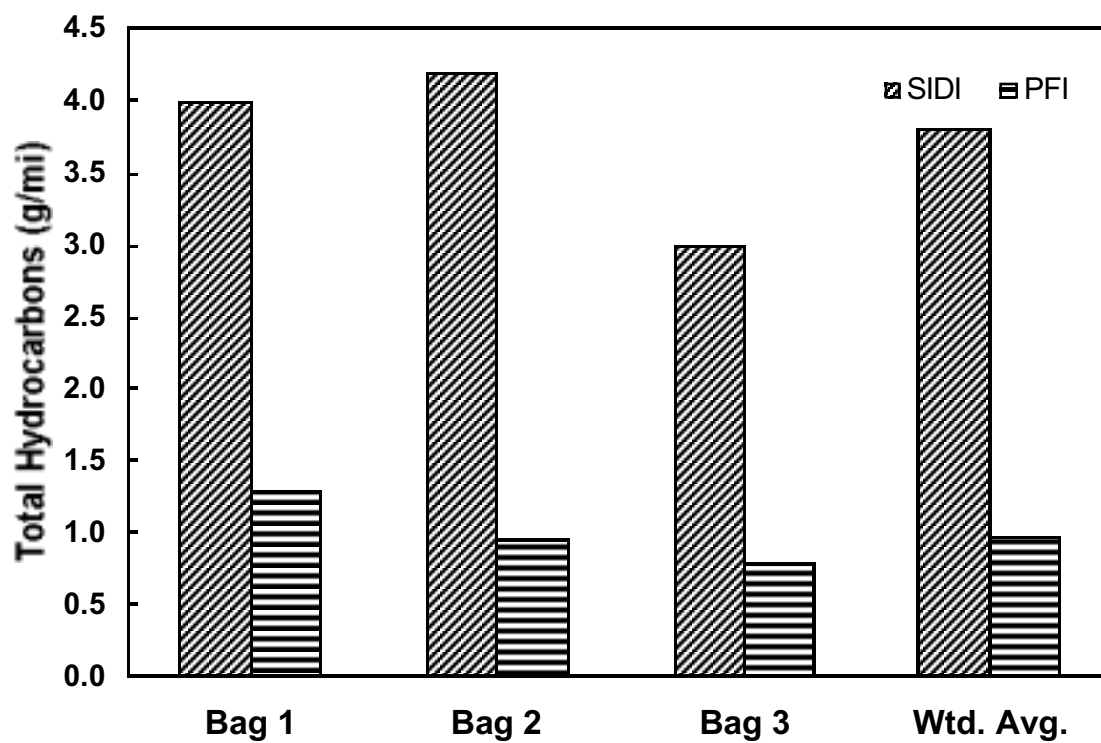


FIGURE 7 Comparison of Engine-Out Emissions for Mitsubishi-SIDI and Neon-PFI Vehicles during FTP-75 Cycle

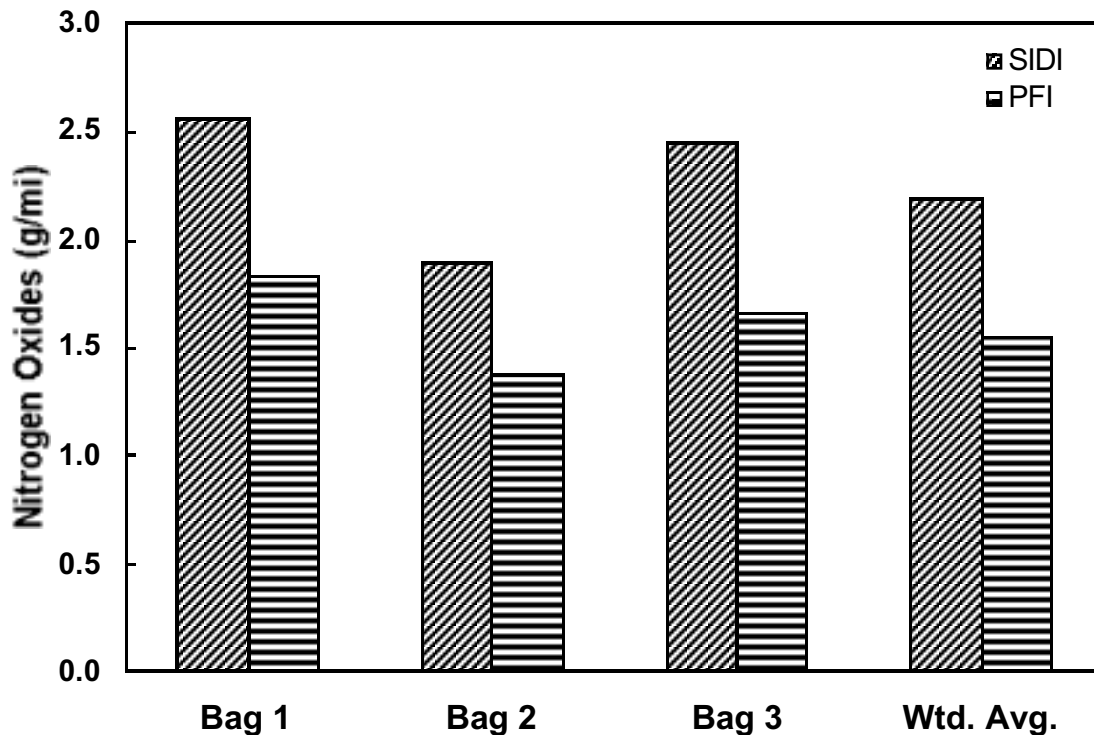


Figure 7 (Cont.)

the trend seen in Figure 6 for engine-out hydrocarbon emissions. The effect of cold-start emissions is shown by comparing bag 1 to bag 3. Hydrocarbon emissions of bag 1 are 7-12 times more than those of bag 3. This is much more than the 1.25 to 1.33 multiples for engine-out emissions. Therefore, the effect of the cold engine is smaller than that of the cold catalyst.

Weighted average  $\text{NO}_x$  for Indolene (B) was 24% more than that of Indolene (A). Ultimate produced 17% more and RFG produced 1.1% less  $\text{NO}_x$  than did Indolene (A). The most noteworthy trend is that weighted-average  $\text{NO}_x$  emissions from low-sulfur fuel are 40% less than those from Indolene (A). The same trend is seen in the bag emissions, with the low-sulfur  $\text{NO}_x$  emissions being 30%, 58%, and 36% less than those with Indolene for bags 1, 2, and 3, respectively. Weighted-average  $\text{NO}_x$  emissions with Ultimate were 17% more than those with Indolene. The same trend is not seen in the engine-out emissions of Figure 6, so the effect occurs in the catalytic converter.

Pentikäinen et al. have observed the same effect with three-way catalysts.<sup>2</sup> If the fuel contains a high percentage of aromatics, a large fraction of the engine-out hydrocarbons consists of aromatics. But if the fuel contains a low percentage of aromatics, then short-chain paraffins, such as methane and ethane, dominate the engine-out hydrocarbon content. The short-chain paraffins have a lower reactivity in the catalyst than the aromatics do and are, thus, less effective at reducing  $\text{NO}_x$ .



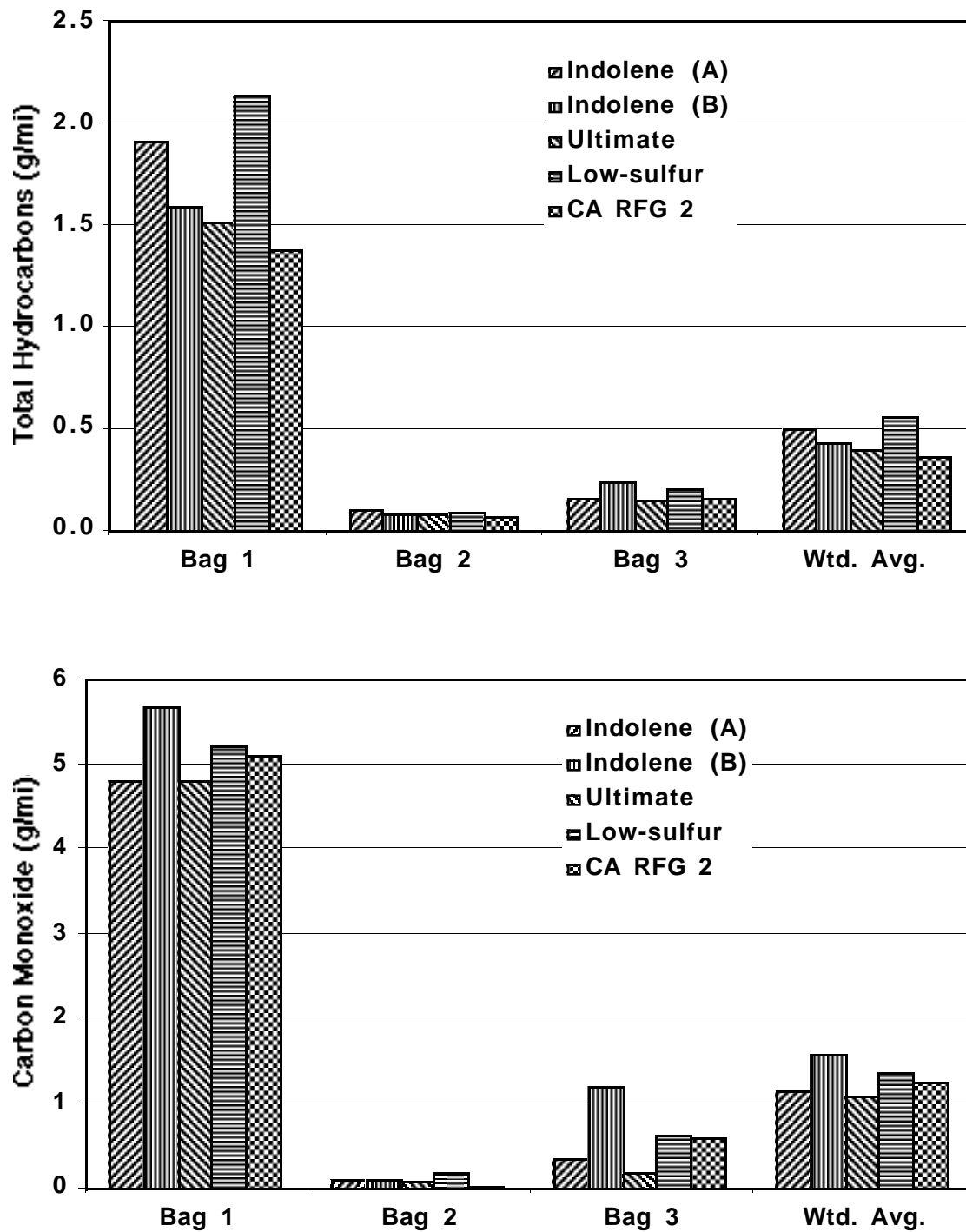


**FIGURE 8 Comparison of Tailpipe Emissions from Mitsubishi-SIDI with Five Different Fuels during FTP-75 Cycle**

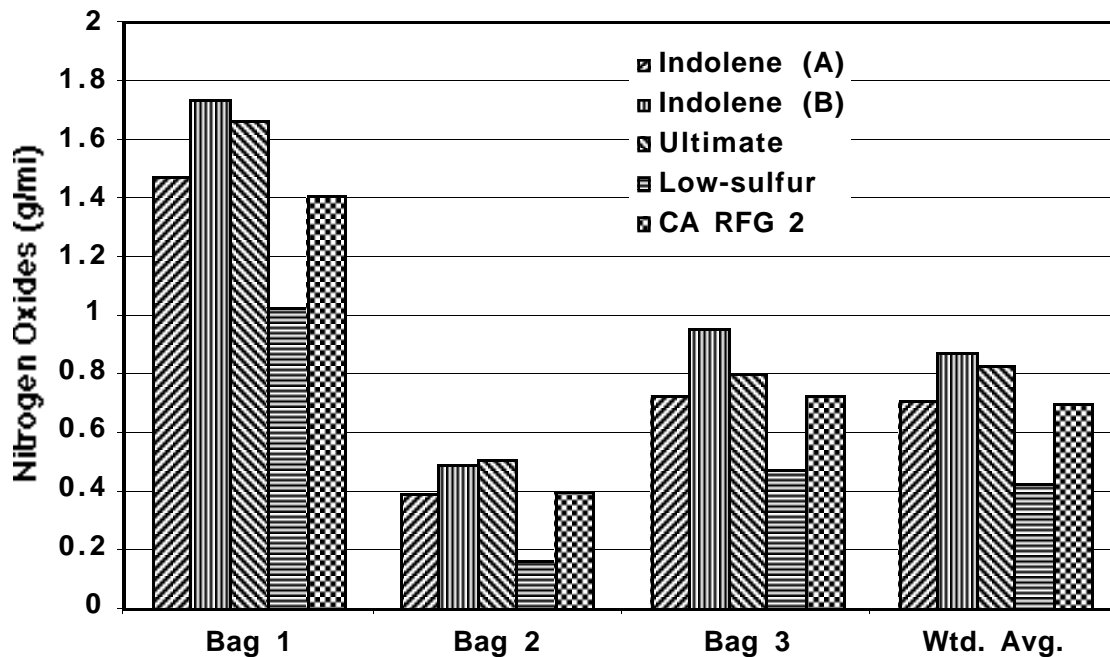


**FIGURE 8 (Cont.)**

Weighted-average CO for Indolene (B) was 36% more than that for Indolene (A). Weighted-average CO emissions with Ultimate were 6% less, those with low-sulfur fuel were 18% more, and those with RFG were 8.6% more than those with Indolene (A). The effect of the cold start on CO emissions was similar to the effect of the cold start on hydrocarbon emissions. CO emissions from bag 1 are 4.7-25 times higher than those from bag 3. This is more than the 1.30-1.55 multiples for engine-out CO emissions. Therefore, the cold catalyst has a greater effect on CO emissions than does the cold engine.

### 3.2.4 Particulate Emissions from SIDI Engine

Particulate emissions for the Mitsubishi SIDI are shown in Figure 9 for three conditions: RFG with catalyst, RFG without catalyst, and Indolene (B) with catalyst. The weighted-average particulate emissions for RFG with the catalyst total 0.007 g/mi, which is less than the PNGV goal of 0.010 g/mi. However, the cases of RFG without the catalyst and Indolene (B) with the catalyst exceed the goal.

Particles are known to adsorb unburned hydrocarbons, which adds to their mass. Comparison of the cases of RFG with and without the catalyst shows that the weighted-average particulate mass is 68% less with the catalyst than without the catalyst. Oxidation of the hydrocarbons removes them from the exhaust stream and prevents their adsorption by the particulate matter.

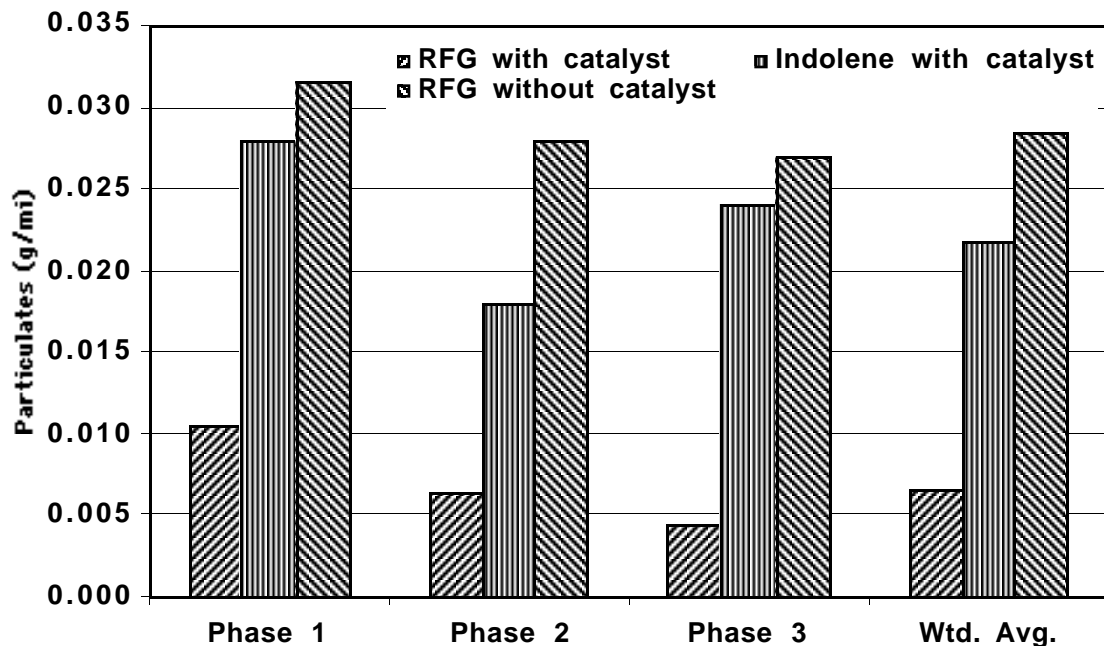


**FIGURE 9 Particulate Emissions from Mitsubishi SIDI during FTP-75 Cycle**

Comparison of Indolene (B) with the catalyst to RFG with the catalyst shows that 75% less particulate mass is emitted for RFG than for Indolene (B) in the weighted average. RFG has 30.2 ppm sulfur, but Indolene (B) has 161 ppm sulfur. Sulfur is known to condense on particulate matter as sulfuric acid and increase the particulate mass. Thus, both an oxidation catalyst and a low-sulfur fuel may be necessary to meet the PNGV goal for particulate emissions.

### 3.2.5 Tailpipe Emissions from SIDI and PFI Vehicles on Indolene (A)

Figure 10 compares the tailpipe emissions of the SIDI engine with those of the PFI engine, both running on Indolene (A). It should be noted that the SIDI engine was designed for Japanese emissions standards, which are less strict than U.S. standards. The tailpipe emissions from the SIDI engine do not meet the U.S. Tier I emissions standards for total hydrocarbons (0.25 g/mi) or  $\text{NO}_x$  (0.40 g/mi). Weighted-average THC emissions from the SIDI vehicle were almost three times more than those from the PFI vehicle. Weighted-average  $\text{NO}_x$  emissions from the SIDI vehicle were almost ten times more than those from the PFI vehicle. Weighted-average CO emissions from the SIDI vehicle were 19% less than those from the PFI vehicle. Bag emissions of CO from the SIDI vehicle were 7% more, 80% less, and 56% less than those of the PFI vehicle for bags 1, 2, and 3, respectively.

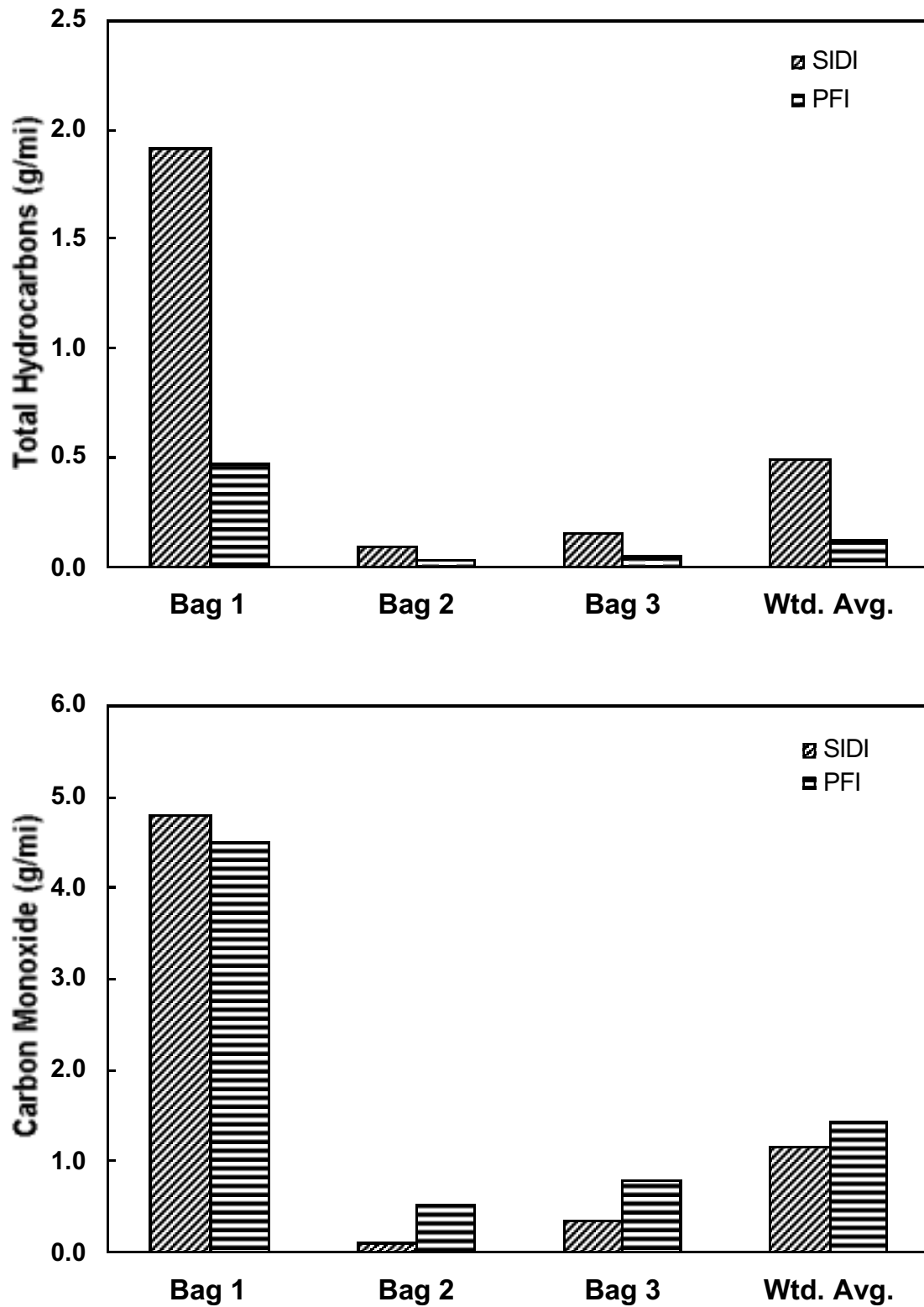


FIGURE 10 Comparison of Tailpipe Emissions from Mitsubishi-SIDI and Neon-PFI during FTP-75 Cycle

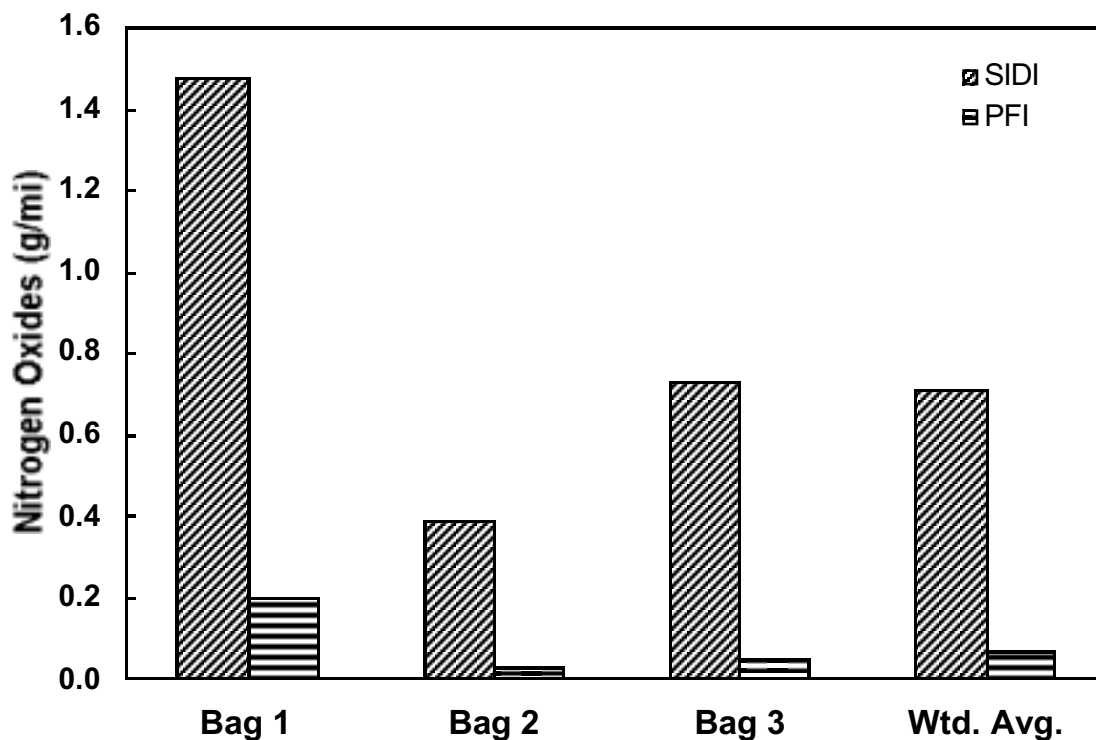


FIGURE 10 (Cont.)

### 3.2.6 Catalyst Efficiencies for SIDI and PFI Vehicles

Overall catalyst efficiencies for total hydrocarbons and carbon monoxide for the SIDI engine are comparable with those for the PFI engine, as indicated in Table 7. Because the engine-out hydrocarbon emissions are nearly three times higher for the SIDI engine than for the PFI engine, the tailpipe emissions are also nearly three times higher. Similarly, the engine-out CO emissions from the SIDI vehicle are 4% less than those of the PFI vehicle, and tailpipe CO emissions for the SIDI vehicle are 19% less than those of the PFI vehicle. The overall CO catalyst efficiency for the SIDI vehicle is 87%, compared to 84% for the PFI vehicle.

**TABLE 7 Comparison of Catalyst Efficiencies on the Basis of Weighted-Average Emissions**

Efficiency	SIDI	PFI
$\eta_{\text{THC}}$	87%	87%
$\eta_{\text{CO}}$	87%	84%
$\eta_{\text{NO}_x}$	68%	96%

As shown in Figure 10, tailpipe  $\text{NO}_x$  emissions are nearly ten times higher for the SIDI engine than for the PFI engine. In part, this is due to the 41% higher engine-out  $\text{NO}_x$  emissions of the SIDI engine, shown in Figure 7. The 68% overall  $\text{NO}_x$  catalyst efficiency of the SIDI engine, being lower than the 96%  $\text{NO}_x$  catalyst efficiency of the PFI engine, accounts for the remainder of the difference in tailpipe  $\text{NO}_x$ . The task of the  $\text{NO}_x$  catalyst is more difficult for the SIDI engine than it is for the PFI engine because the SIDI engine leaves more oxygen in the exhaust; exhaust oxygen works against the chemical reduction of  $\text{NO}_x$ .

### 3.2.7 FTP Emissions from SIDI and PFI Vehicles Compared with PNGV Goals

FTP emissions from both vehicles are compared with the PNGV goals in Figure 11. The PNGV goals ( $\text{CO}$ , 1.7 g/mi; NMHC, 0.125 g/mi;  $\text{NO}_x$ , 0.2 g/mi; and PM, 0.01 g/mi) are shown as horizontal lines in Figure 11. The PFI engine meets the standards for  $\text{CO}$ , NMHC, and  $\text{NO}_x$ , but the SIDI engine meets only the  $\text{CO}$  standard. Although the SIDI engine was not designed to meet U.S. standards, the figure demonstrates the challenge facing the SIDI engine, particularly in meeting the NMHC and  $\text{NO}_x$  standards. The PFI vehicle was not tested for PM, but it is expected to meet the goal. Whether the SIDI vehicle can meet the PM goal depends on the type of fuel used. With RFG, the SIDI vehicle meets the PM goal, but with Indolene (B), it does not. Condensation of sulfur-bearing compounds on particulate nuclei is the likely reason for failure to meet the PM goal with Indolene (B); RFG contains 30.2 ppm sulfur, but Indolene (B) contains 161 ppm.

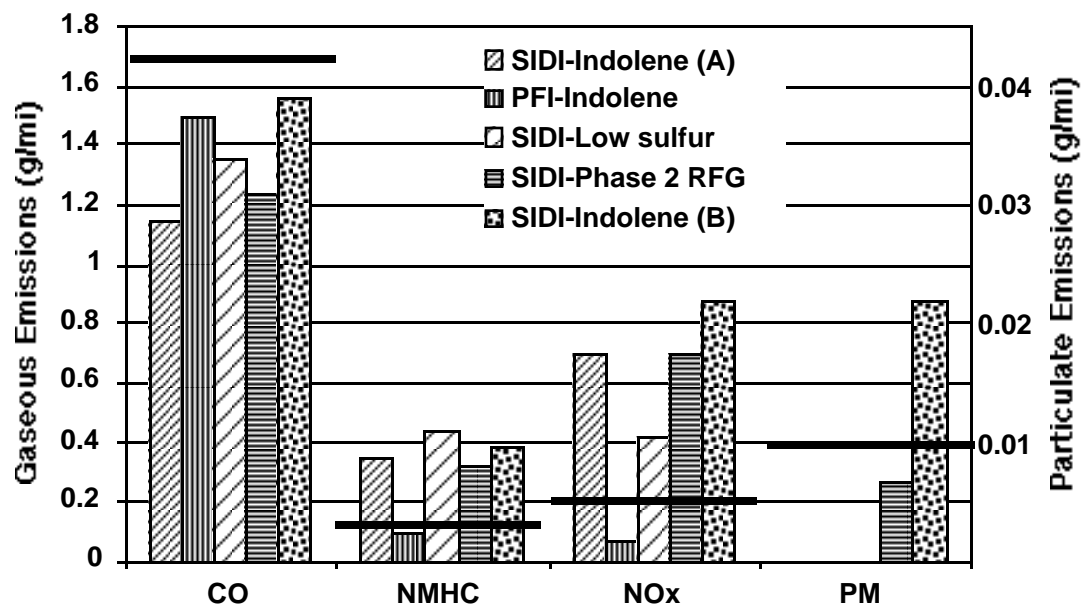


FIGURE 11 Mitsubishi-SIDI's Challenge in Meeting PNGV Goals

### 3.3 Second-by-Second Emissions

#### 3.3.1 Engine-Out Emissions from SIDI Engine for Three Fuels

Engine-out emissions from the SIDI engine tested at Amoco are shown in Figures 12, 13, and 14, for Phases 1, 2, and 3 of the FPT-75 test procedure, respectively. Each figure is a composite of four variables versus time. The variables are speed, total hydrocarbons, carbon monoxide, and nitrogen oxides. Each emissions instrument has a delay that is due to the transit time needed for the sample to move from the engine to the instrument. These delays are THC, 6.6 s; CO, 9.3 s; NO<sub>x</sub>, 19.0 s; and CH<sub>4</sub>, 17.3 s. Data shown in the figures are corrected for the delays. Peaks in emissions correspond to accelerations of the vehicle. Changes in scale of the emissions variables from one bag to another reflect cold-start vs. warm-engine operation and acceleration rates. Phases 1 and 3, which share the same speed vs. time relationships, have higher speeds and accelerations than Phase 2. Thus, Phases 1 and 3 have higher emissions peaks than does Phase 2.

The highest hydrocarbon peaks and troughs occur with the low-sulfur gasoline, and the lowest occur with Ultimate. This is the same trend seen in Figure 6. In Phase 1, the highest hydrocarbon peaks are Indolene, 1236 ppm; Ultimate, 979.5 ppm; and low-sulfur fuel, 1406 ppm. All of these peaks occurred at 35 s, which corresponds to the first acceleration after the cold start when the instrument delay is taken into account. The highest peaks in Phase 2 are Indolene, 489.5 ppm; Ultimate, 450.7 ppm; and low-sulfur fuel, 593.3 ppm. The highest peaks in Phase 3 are Indolene, 588 ppm; Ultimate, 578.3 ppm; and low-sulfur fuel, 751.9 ppm. The highest peaks in Phases 2 and 3 did not all occur at the same times. Comparison of Phase 1 with Phase 3, which had the same speeds and accelerations, shows the effect of the cold start (Phase 1) relative to a warm engine (Phase 3). Peaks in Phase 1 are roughly twice as great as those of Phase 3. Comparison of Phase 2, which has lower speeds and milder accelerations than Phase 3, with Phase 3 shows the effect of acceleration. Peaks in Phase 3 are 20-30% higher than those in Phase 2.

The highest CO peaks in Phase 1 correspond to the first acceleration after the cold start. They are Indolene, 2001 ppm; Ultimate, 2104 ppm; and low-sulfur fuel, 2163 ppm. The highest CO peaks in Phase 2 are Indolene, 895 ppm; Ultimate, 848 ppm; and low-sulfur fuel, 858 ppm. These peaks do not all correspond to the same accelerations. The highest CO peaks in Phase 3 are Indolene, 1445 ppm; Ultimate, 1554 ppm; and low-sulfur fuel, 1582 ppm. All of these peaks occurred during the acceleration to 56.7 mph.

The highest NO<sub>x</sub> peaks in Phase 1 do not correspond to the first acceleration after the cold start. Instead, they correspond to the acceleration to 56.7 mph. The Phase 1 peaks are Indolene, 494.2 ppm; Ultimate, 498.0 ppm; and low-sulfur fuel, 495.1 ppm. With the cold engine during the first acceleration, combustion temperatures would be lower than they are during the acceleration to 56.7 mph, when the engine has begun to warm up. The Phase 3 peaks, which correspond to the

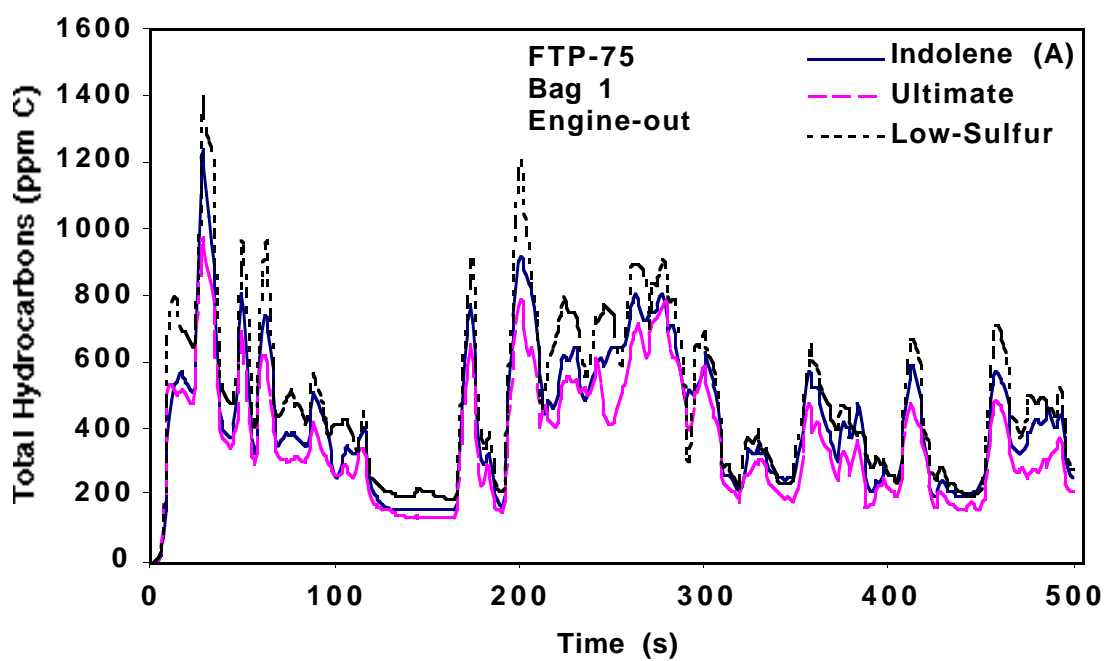
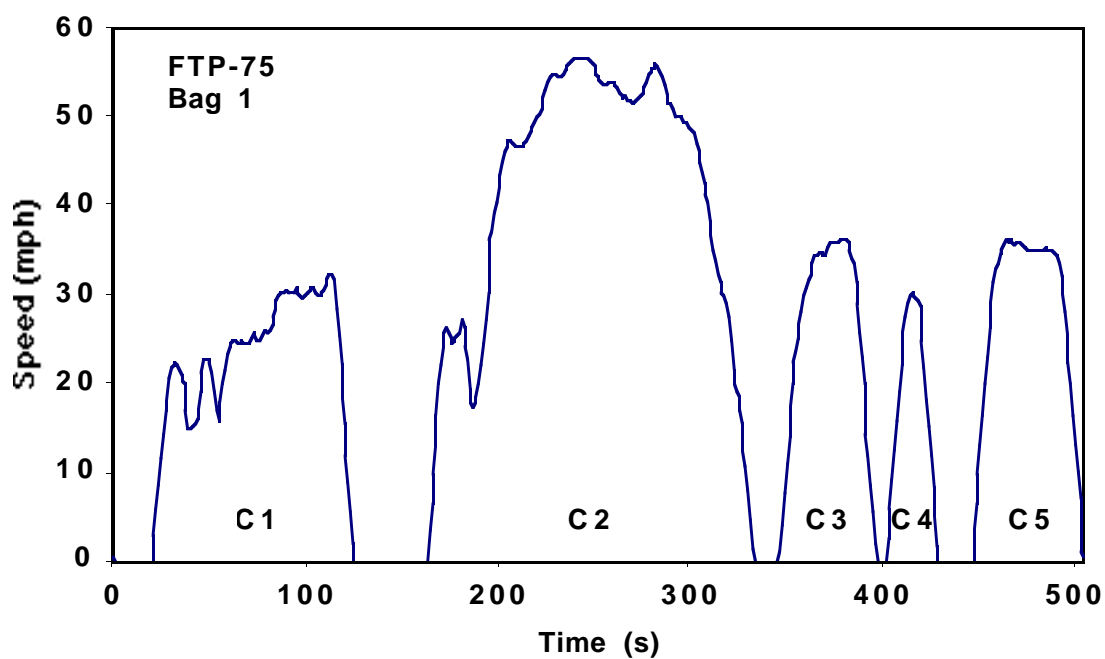


FIGURE 12 Comparison of Engine-Out Emissions for Three Gasolines during FTP Cold Phase (Bag 1)



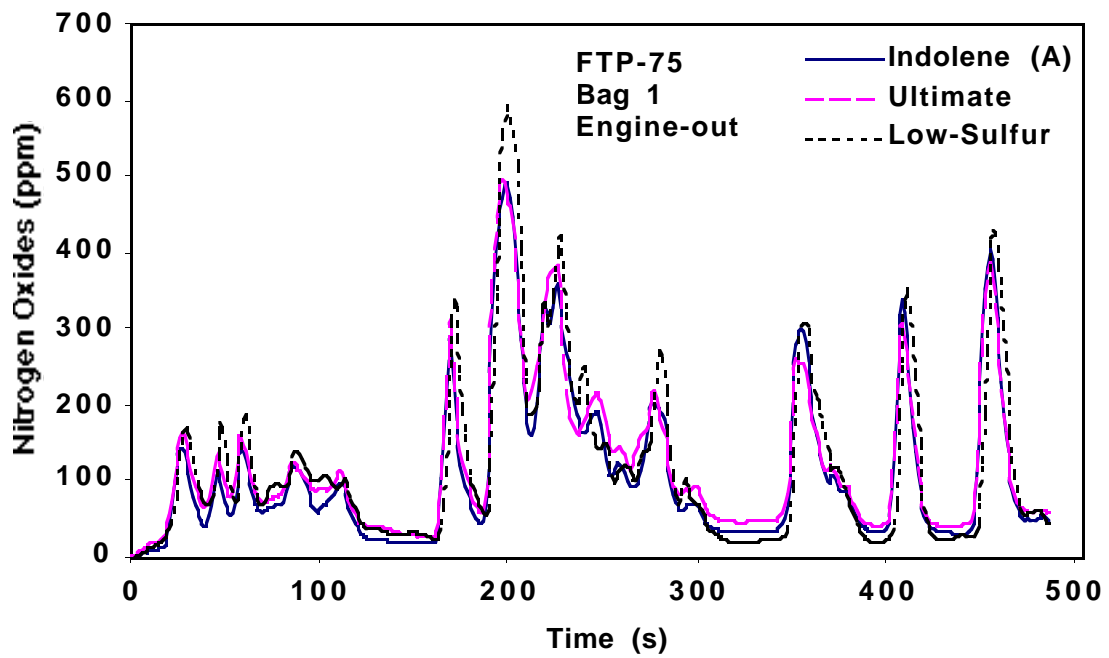
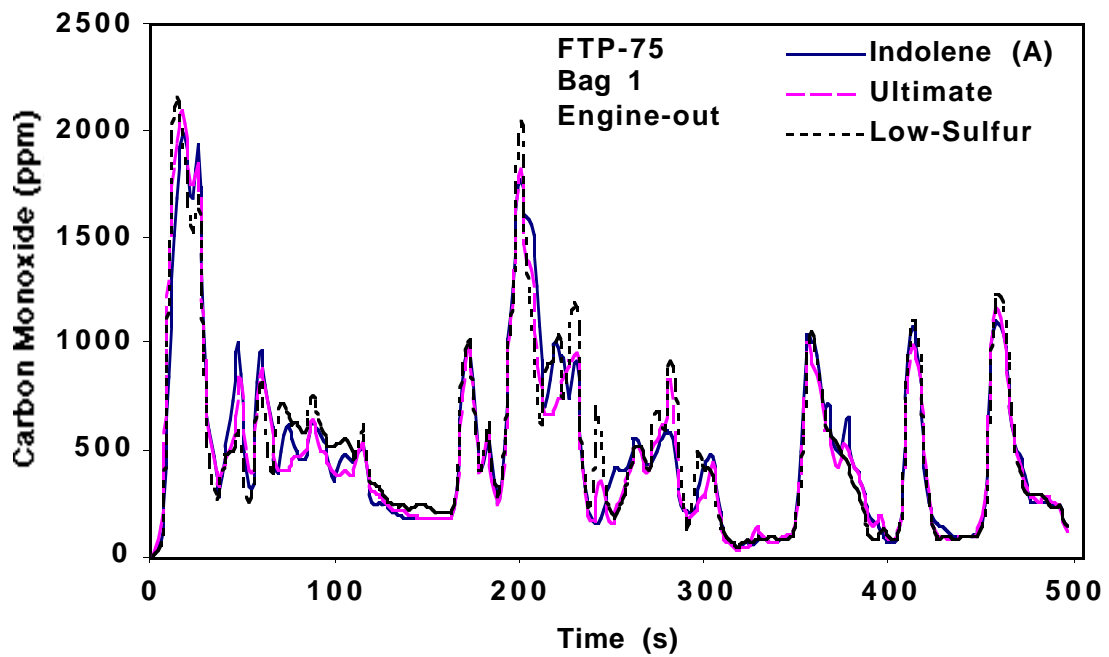
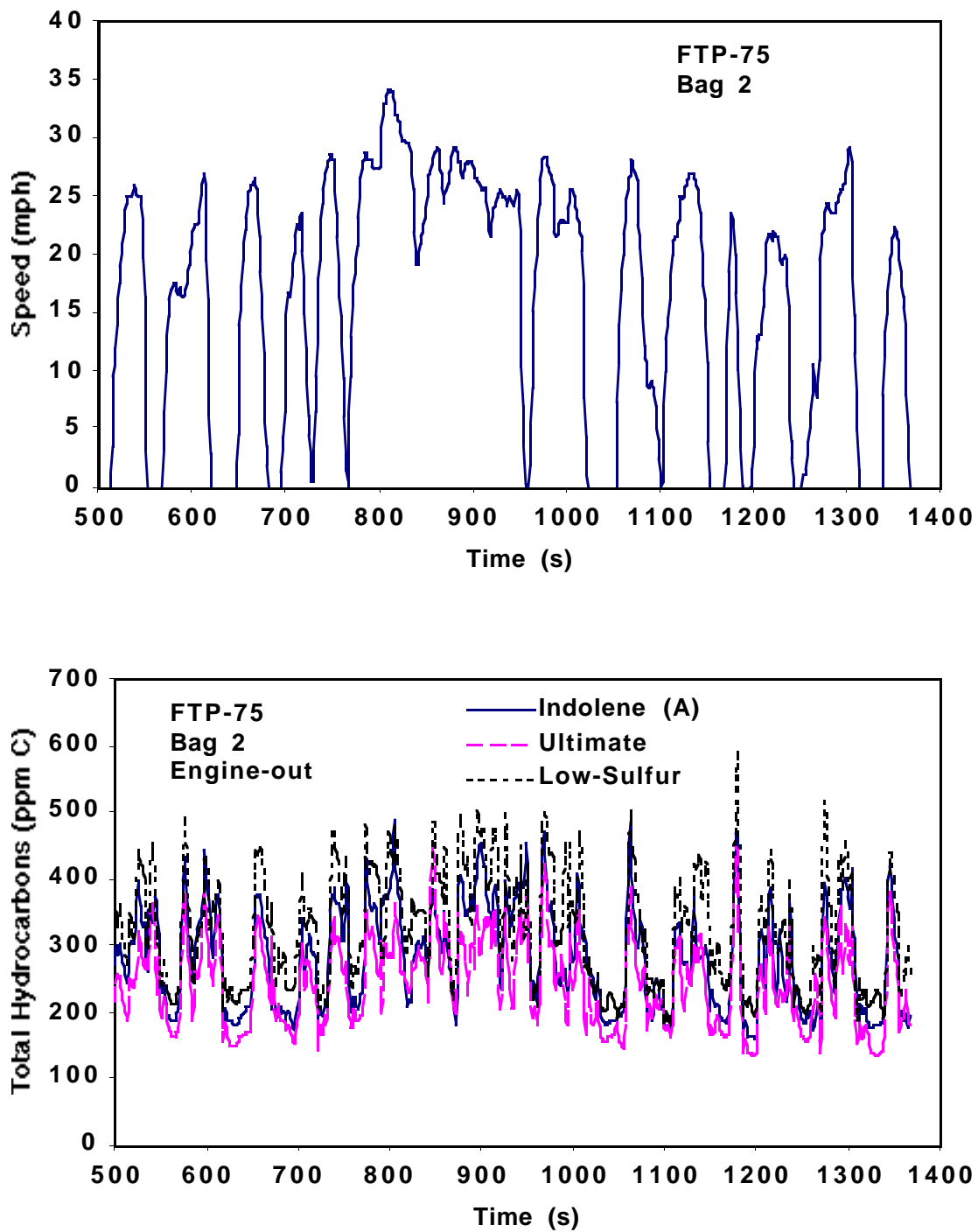


FIGURE 12 (Cont.)



**FIGURE 13 Comparison of Engine-Out Emissions from Three Gasolines during Second Phase of FTP (Bag 2)**

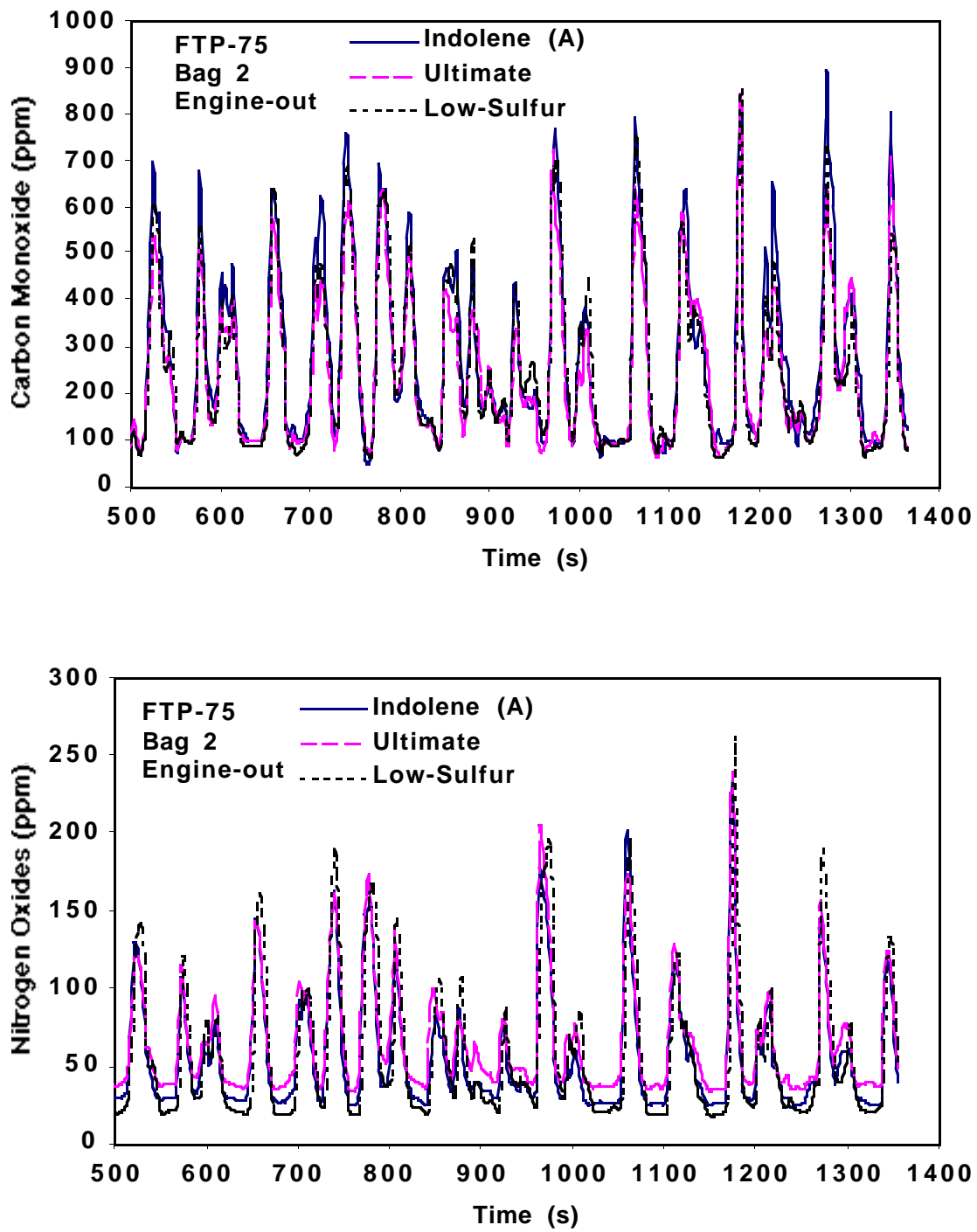


FIGURE 13 (Cont.)

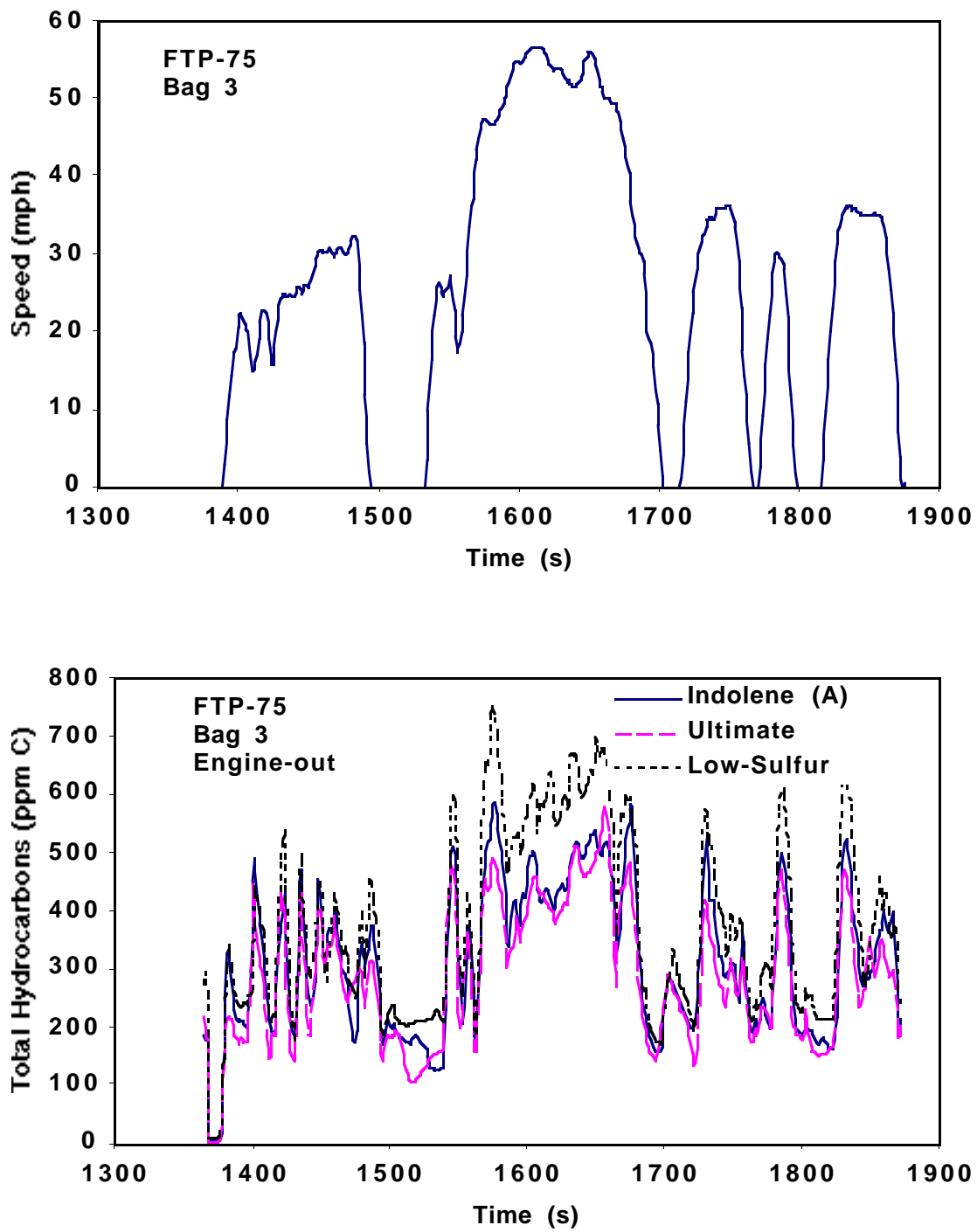


FIGURE 14 Comparison of Engine-Out Emissions from Three Gasolines during Third Phase of FTP (Bag 3)

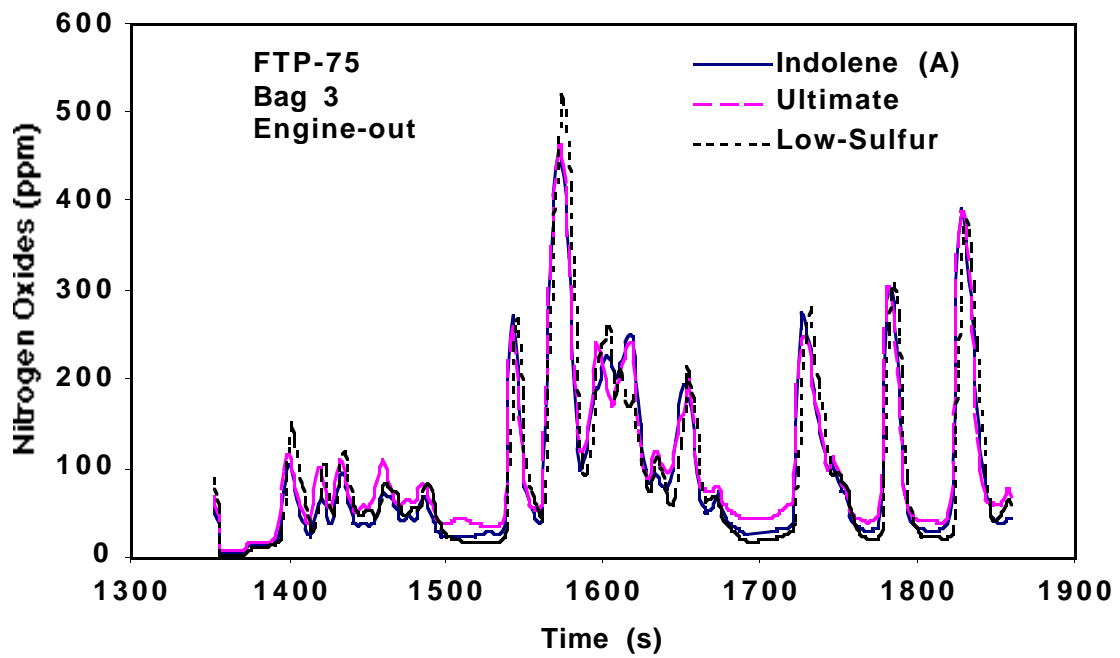
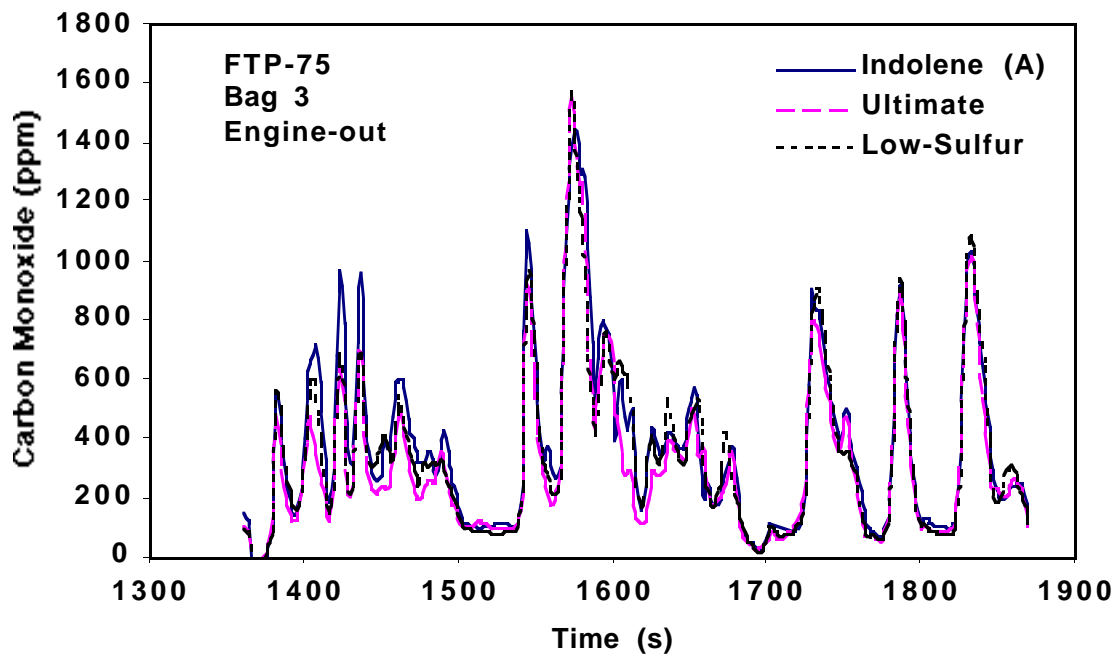


FIGURE 14 (Cont.)

acceleration to 56.7 mph, are Indolene, 464.3 ppm; Ultimate, 465.3 ppm; and low-sulfur fuel, 520.9 ppm. The NO<sub>x</sub> peaks of Phase 2 are Indolene, 236.1 ppm; Ultimate, 240.1 ppm; and low-sulfur fuel, 263.3 ppm. These peaks are about 50% smaller than the Phase 1 and Phase 3 peaks because the accelerations in Phase 2 are less severe.

### 3.3.2 Engine-Out Emissions from SIDI and PFI Engines on Indolene

Figures 15, 16, and 17 show the Phase 1, Phase 2, and Phase 3 engine-out emissions, respectively, for the two vehicles, both running on Indolene. Phase 1 engine-out hydrocarbon emissions are 210% higher for the SIDI engine than for the PFI engine. The difference is larger after the first 120 s, which reflects the cold-engine enrichment of the PFI engine. The highest hydrocarbon peaks are SIDI, 1236.0 ppm; PFI, 672.8 ppm. Both peaks occur 35 s after startup during the first acceleration. The Phase 1 peak with the SIDI engine is about 80% higher than the peak with the PFI engine. In Phase 2, the hydrocarbon peaks with the PFI engine are all lower than the lowest trough with the SIDI engine. The highest peaks with the two engines are SIDI, 489.5 ppm; PFI, 150.7 ppm. The highest peak with the SIDI engine is more than three times the highest peak with the PFI engine. The same trend continues in Phase 3, where the highest peaks are SIDI, 588.0 ppm; PFI, 202.0 ppm. Both peaks occur during the acceleration to 56.7 mph.

The higher hydrocarbon emissions from the SIDI engine in Phases 2 and 3 appear to be a consequence of the stratified-charge mode of combustion. In the stratified-charge mode, the air/fuel ratio varies continuously from very lean to very rich. In the leanest and richest regions, combustion is incomplete and unburned hydrocarbons are left in the cylinder. The PFI engine, in contrast, has a homogeneous mixture that is optimally controlled by the oxygen sensor and the computer. Regions that are too lean or too rich to burn completely are minimal.

Phase 1 CO emissions are 16% less with the SIDI engine than with the PFI engine. The PFI engine has a large CO spike of 3569 ppm at about 40 s, which is probably a result of the cold-engine enrichment and the first acceleration. That spike is about 80% higher than the highest peak of 2001 ppm with the SIDI engine.

After the engine has warmed up, Phases 2 and 3 show that both the base levels and peaks of CO emissions are lower for the SIDI engine than for the PFI engine. In the rich regions of the stratified charge, considerable CO is produced initially.<sup>3</sup> Only a small amount of CO is produced in the lean regions. The overall air/fuel ratio in the SIDI engine can be as high as 30:1. Therefore, the CO that is initially produced in the rich regions must be burned when those regions mix with regions containing excess oxygen. The PFI engine typically operates slightly leaner than stoichiometric ( $\lambda > 1$ ), so its CO level is slightly elevated compared to that of the SIDI engine.

Phase 1 engine-out NO<sub>x</sub> emissions are 41% more with the SIDI engine than with the PFI engine. NO<sub>x</sub> emissions with the PFI engine show three spikes that are higher than those of the

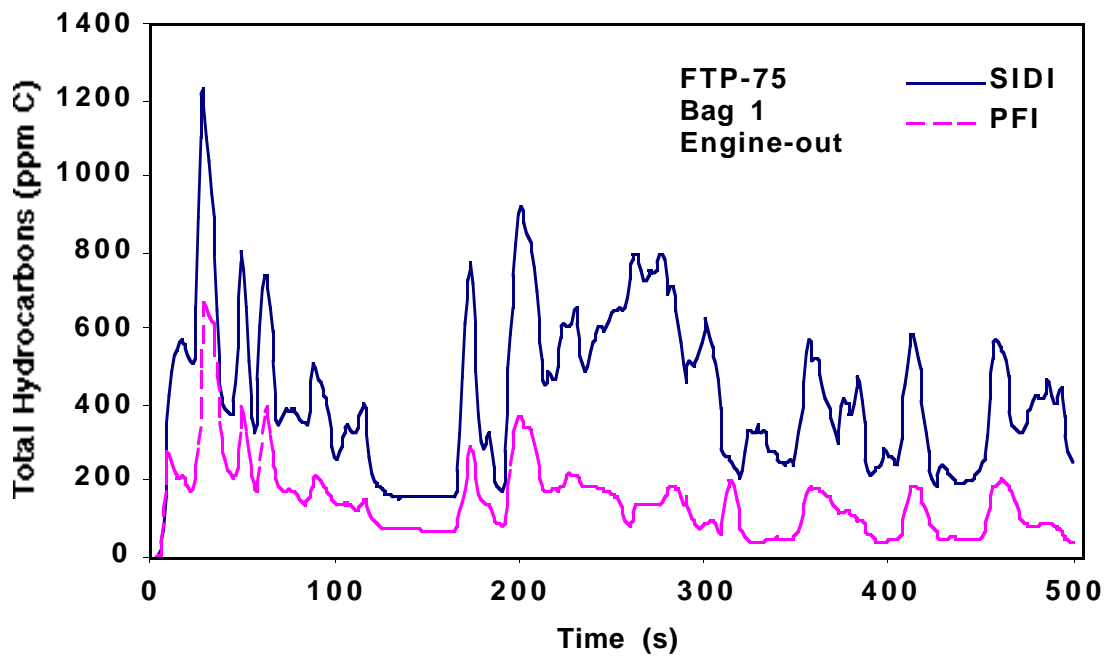
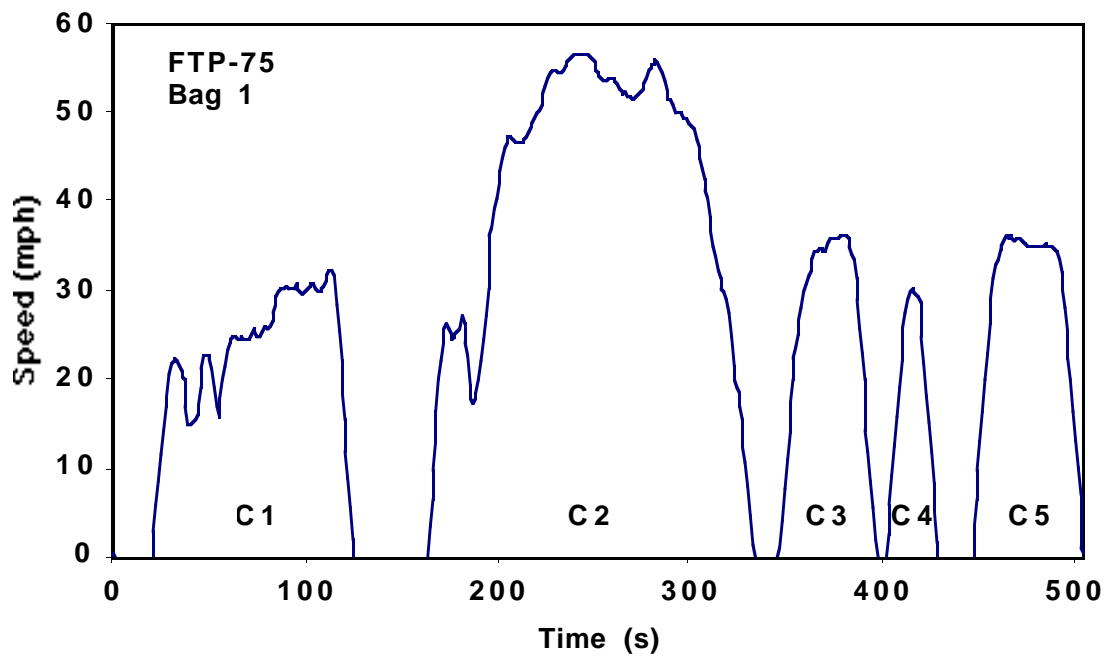


FIGURE 15 Comparison of Engine-Out Emissions from Mitsubishi-SIDI and Neon-PFI Vehicles during FTP Cold Phase (Bag 1)

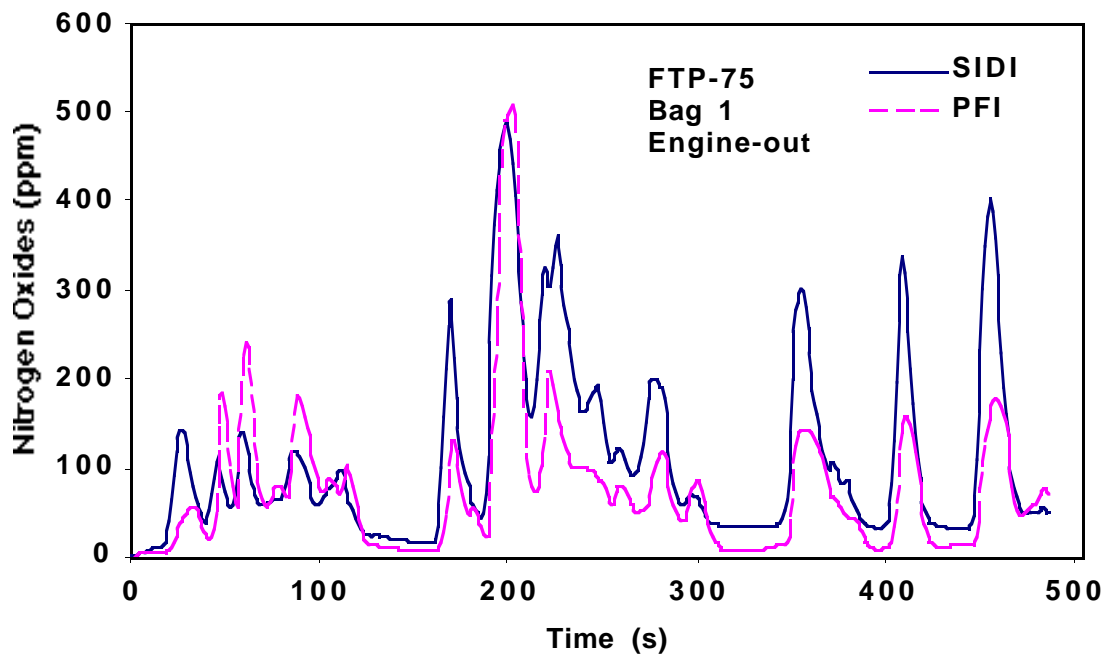
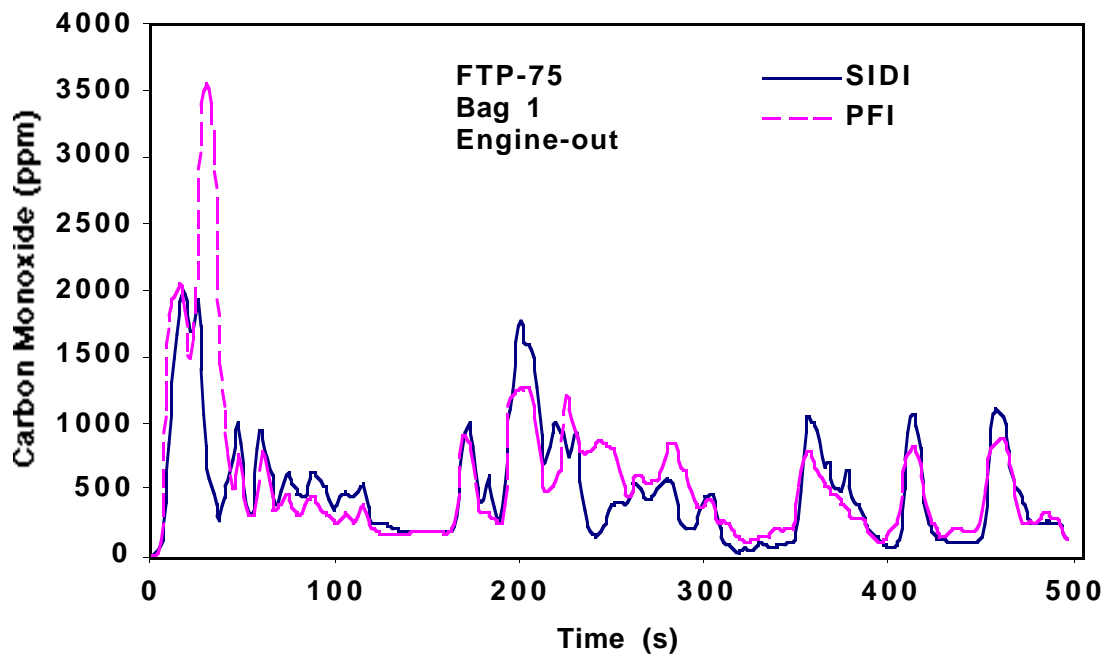
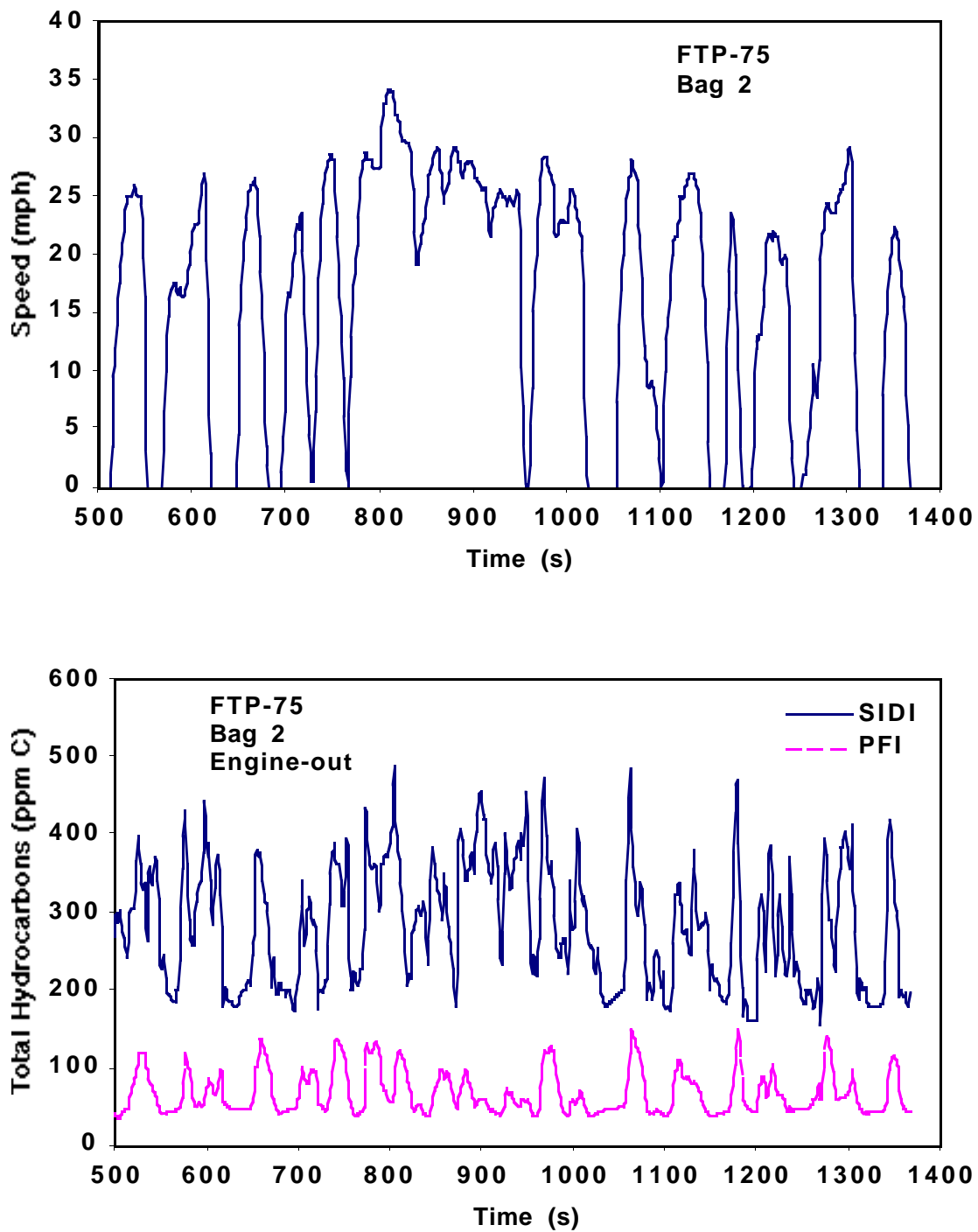


FIGURE 15 (Cont.)





**FIGURE 16 Comparison of Engine-Out Emissions from Mitsubishi-SIDI and Neon-PFI Vehicles during Second Phase of FTP (Bag 2)**

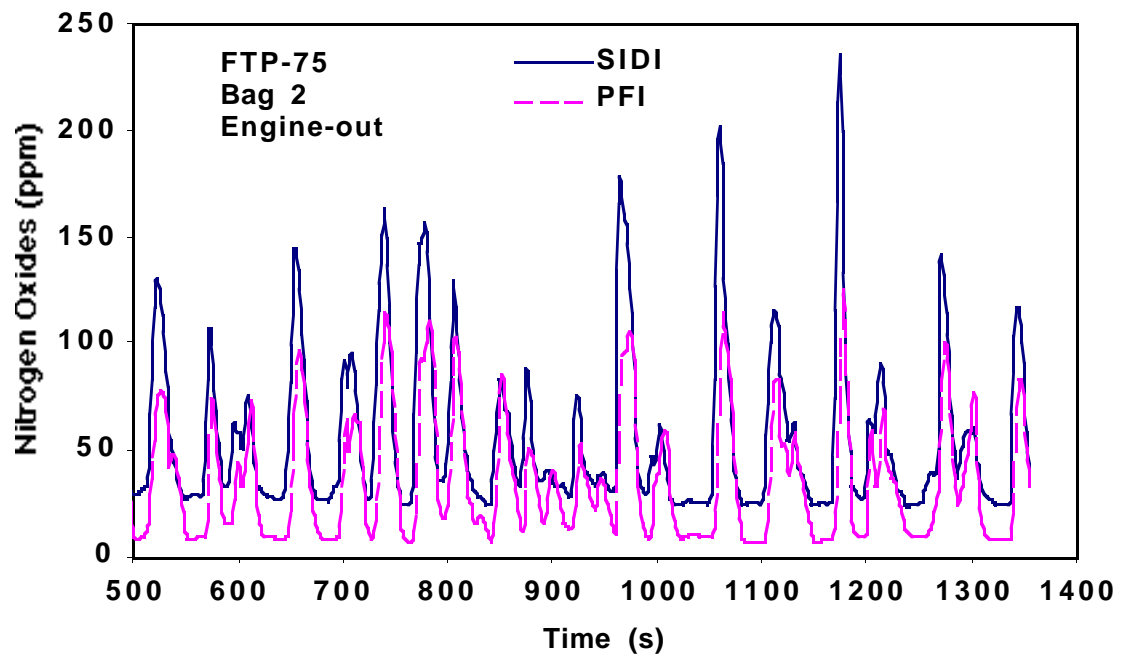
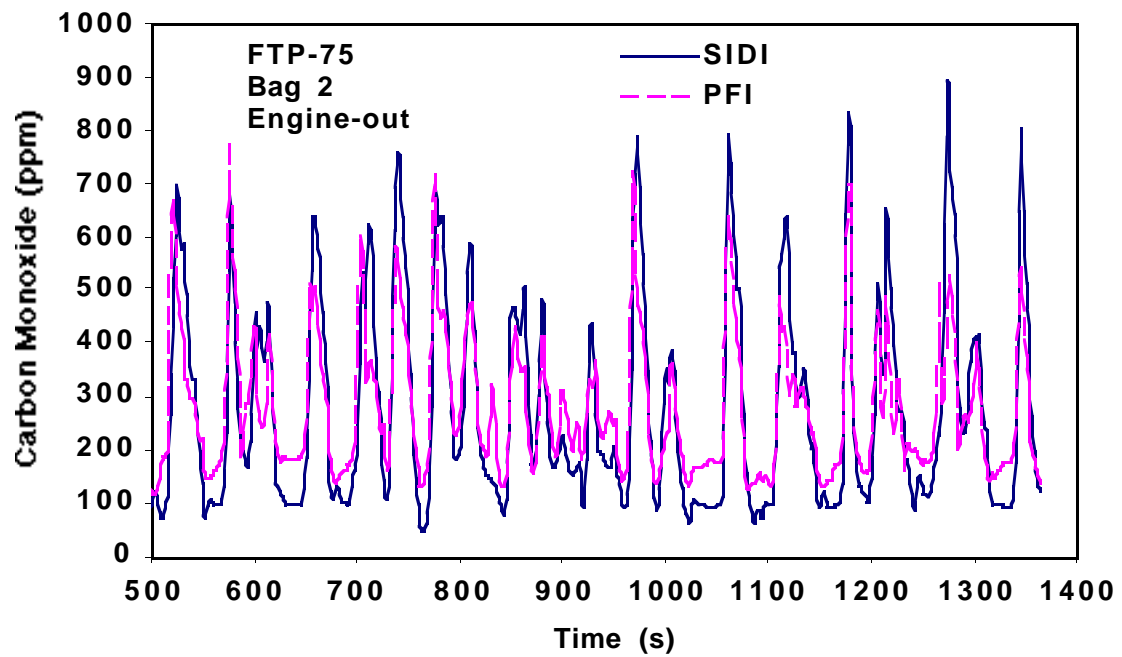
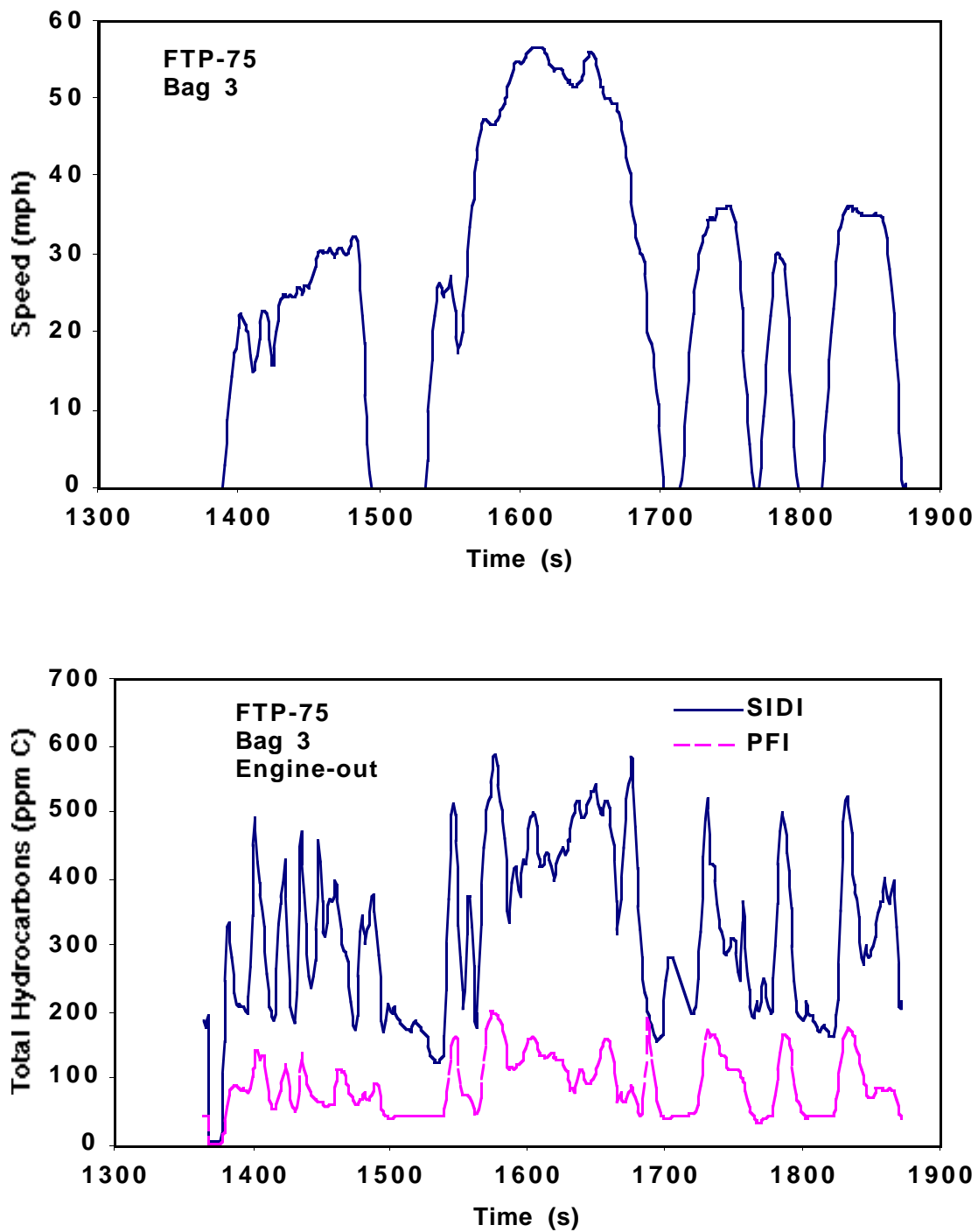


FIGURE 16 (Cont.)



**FIGURE 17 Comparison of Engine-Out Emissions from Mitsubishi-SIDI and Neon-PFI Vehicles during Third Phase of FTP (Bag 3)**

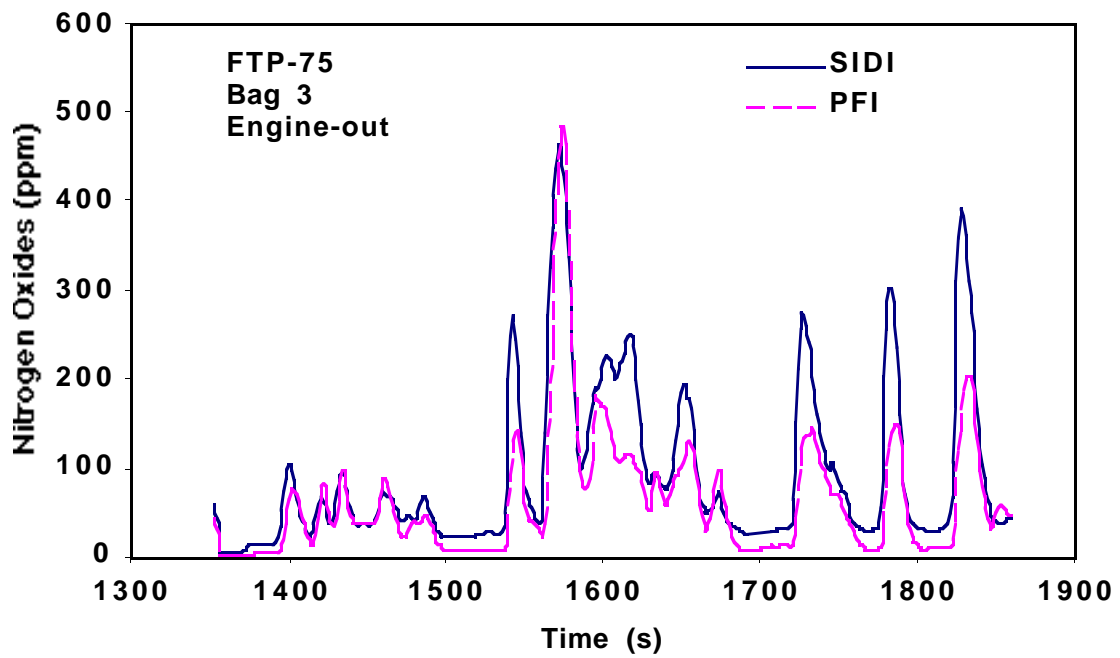
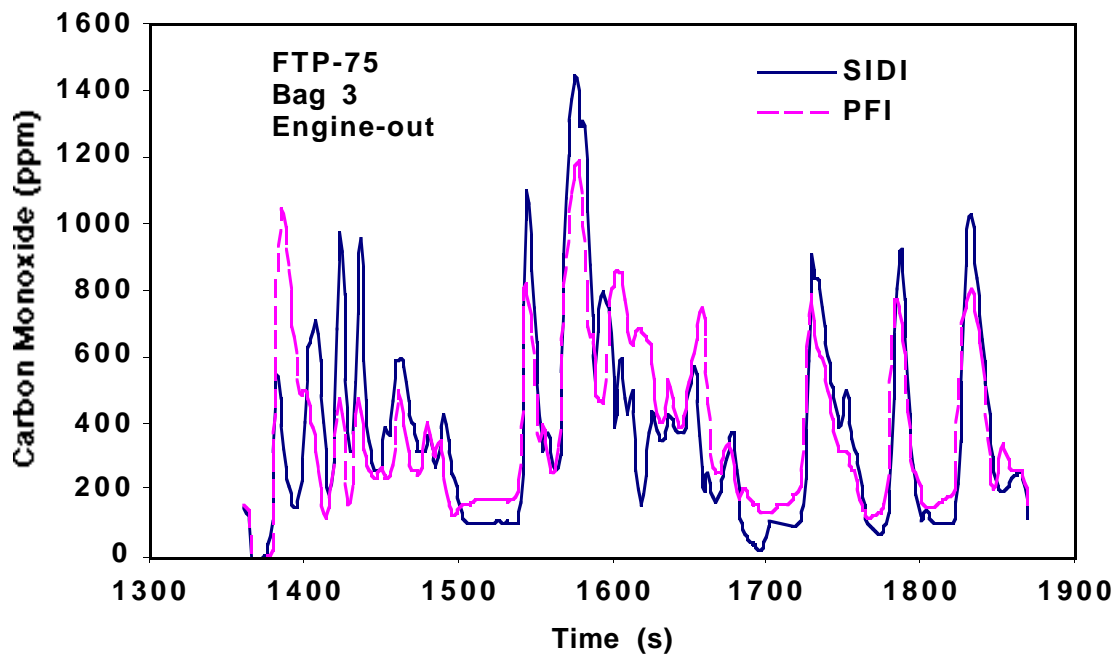


FIGURE 17 (Cont.)

SIDI engine in the first 120 s of operation. This is probably a result of cold-engine enrichment in the PFI engine. After the first 120 s of operation, the PFI engine produces less  $\text{NO}_x$  than the SIDI engine.

In warm-engine operation, Phases 2 and 3, the higher levels of  $\text{NO}_x$  emissions exhibited by the SIDI engine are probably due to (1) the high 12.0:1 compression ratio, (2) the relatively high intake-manifold pressure, and (3) the stratified-charge mode of operation. The high compression ratio and high intake-manifold pressure combine to give a high in-cylinder pressure, which implies a high in-cylinder temperature. Combustion temperature is highest with an air/fuel ratio slightly leaner than stoichiometric, and high combustion temperature favors formation of  $\text{NO}_x$ .<sup>4</sup> Since the gradient of air/fuel mixtures in the stratified charge covers the range from very lean to very rich, some parts of the mixture will achieve temperatures where a large amount of  $\text{NO}_x$  will be formed. The PFI engine has a 9.8:1 compression ratio and a throttled intake manifold; the air/fuel ratio is optimized by the exhaust oxygen sensor and the computer to control  $\text{NO}_x$  formation.

Both engines use exhaust-gas recirculation (EGR) to control  $\text{NO}_x$  formation, but the amounts of EGR and control algorithms are unknown. Differences in EGR amount and control could be partly responsible for the higher engine-out  $\text{NO}_x$  emissions of the SIDI engine compared with that of the PFI engine.

During the hard acceleration to 57.6 mph (1590 s in Phase 3), a peak in  $\text{NO}_x$  emissions occurs in which the emissions are higher for the PFI engine than for the SIDI engine. The peak for the SIDI engine is 464 ppm, and the peak for the PFI engine is 486 ppm. Since this is a hard acceleration, the SIDI engine probably reverts to its homogeneous-charge mode and the air/fuel ratio for the PFI engine is enriched for the acceleration. In this situation, the in-cylinder conditions would be similar for both engines. Both engines would have a homogeneous charge that was close to stoichiometric, both engines would have a high intake-manifold pressure, and EGR would be cut off in both engines to achieve high power output.

### 3.3.3 Tailpipe Emissions from SIDI Vehicle for Three Fuels

Tailpipe emissions from the SIDI vehicle are compared for the three gasolines in Figures 18, 19, and 20, corresponding to Phases 1, 2, and 3 of the FTP, respectively. Responses to acceleration transients are similar for all three fuels in all phases of the tests. Figure 18 shows that the catalytic converter requires about 210 s to warm up and react the hydrocarbons and CO.  $\text{NO}_x$  control requires about 300 s to take effect, but some peaks are evident even after 300 s.

The highest peaks for THC in Phase 1 are Indolene, 1379.6 ppm C; Ultimate, 1349.4 ppm C; and low-sulfur fuel, 1666.9 ppm C. These peaks occurred during the first acceleration after the cold start. As with the bag emissions (Figure 8), the low-sulfur gasoline has the highest peak, and Ultimate has the lowest peak.

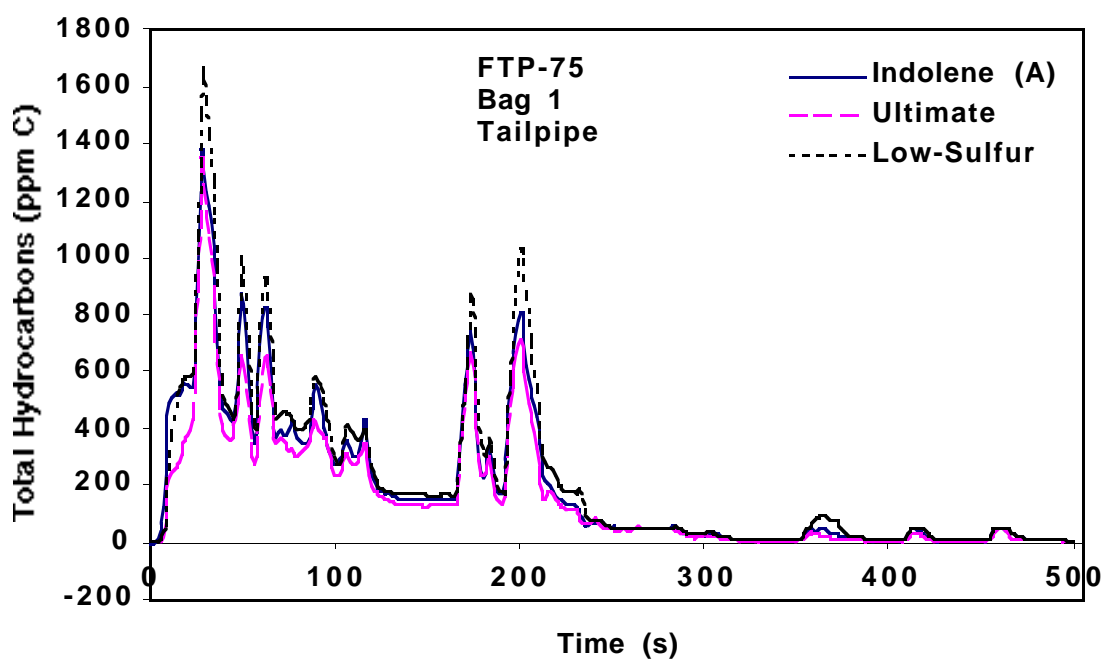
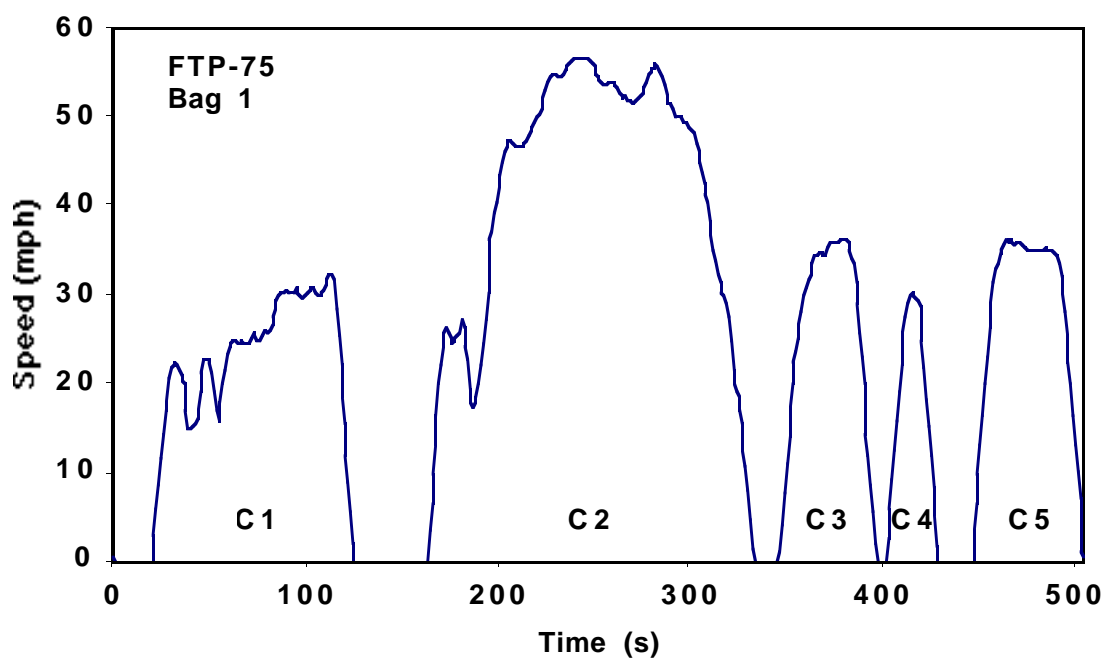


FIGURE 18 Comparison of Tailpipe Emissions for Three Gasolines during FTP Cold Phase (Bag 1)

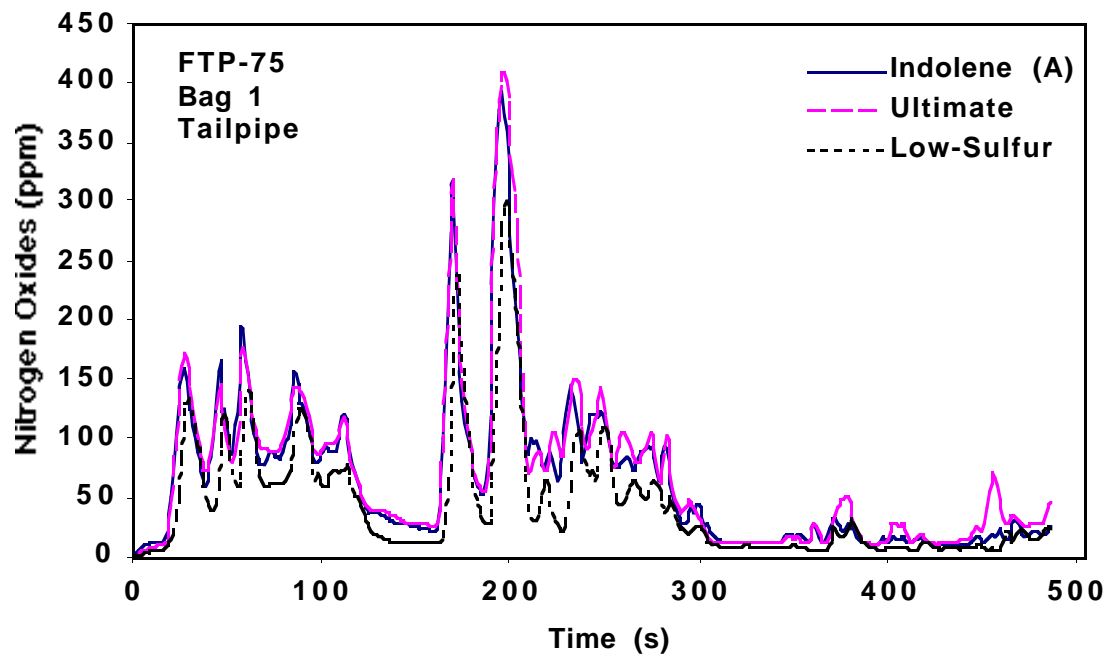
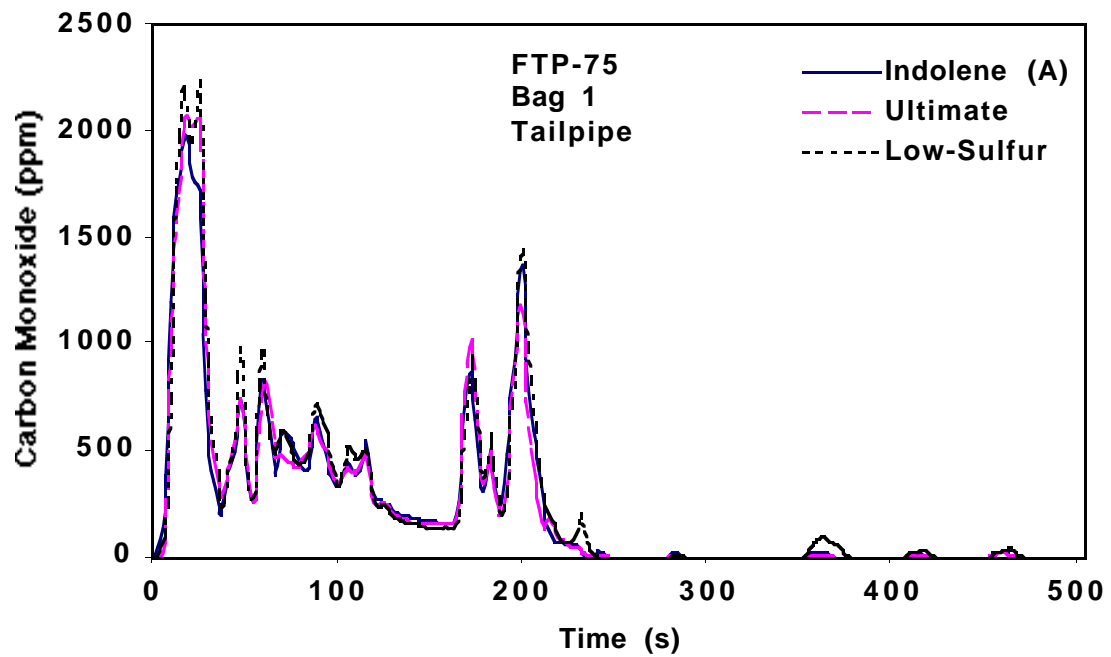


FIGURE 18 (Cont.)

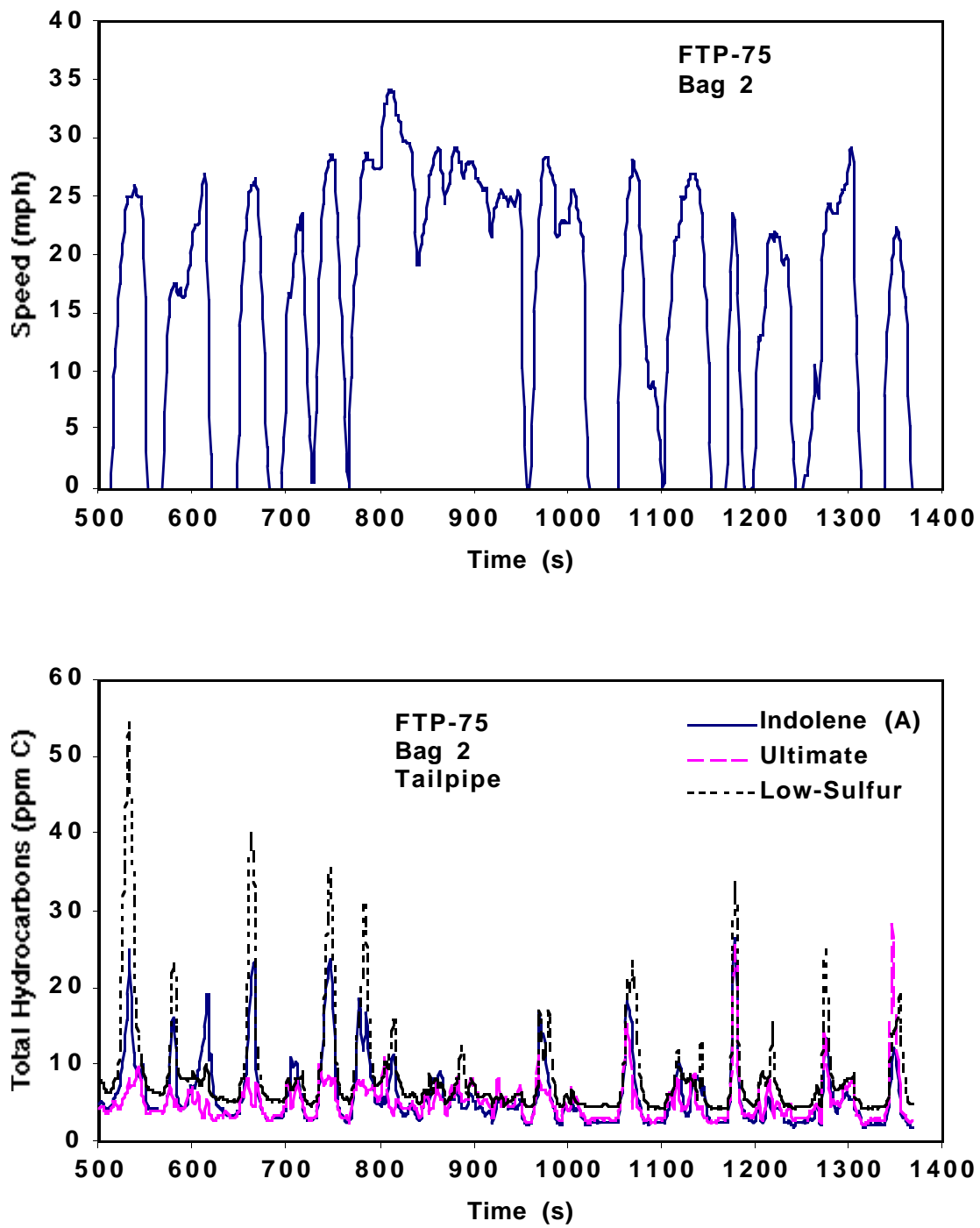


FIGURE 19 Comparison of Tailpipe Emissions from Three Gasolines during Second Phase of FTP (Bag 2)



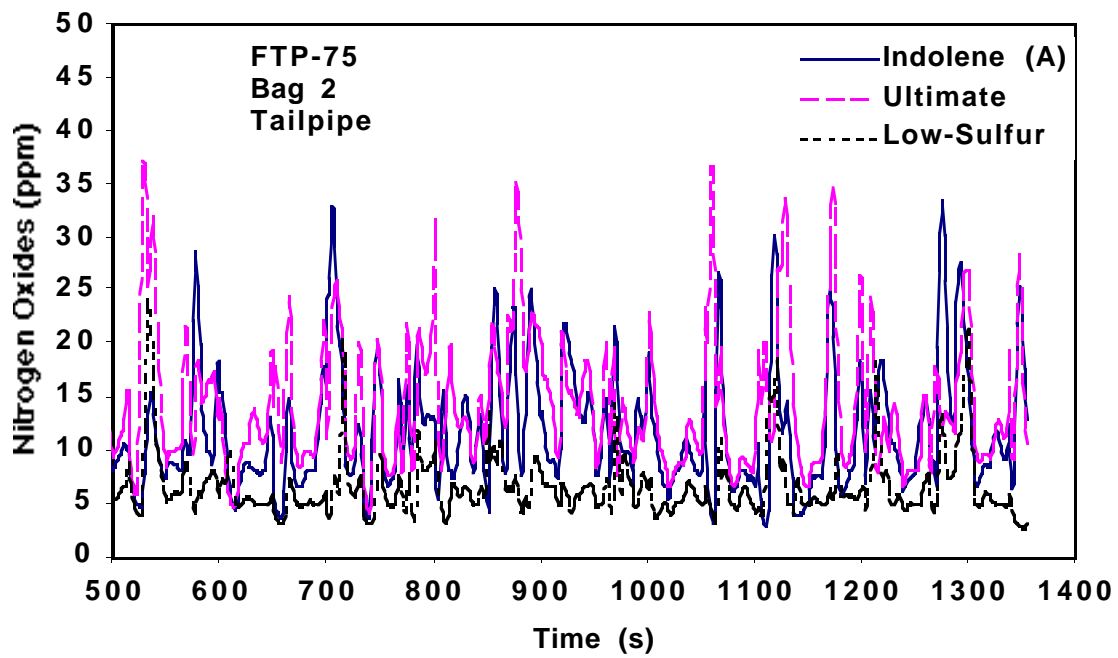
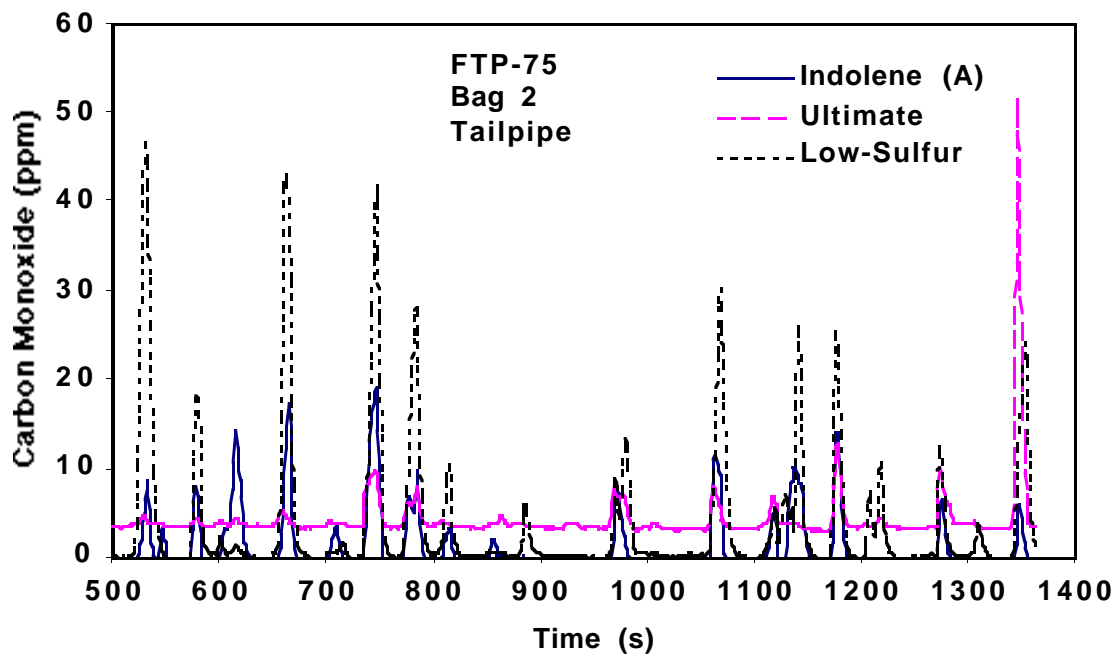


FIGURE 19 (Cont.)

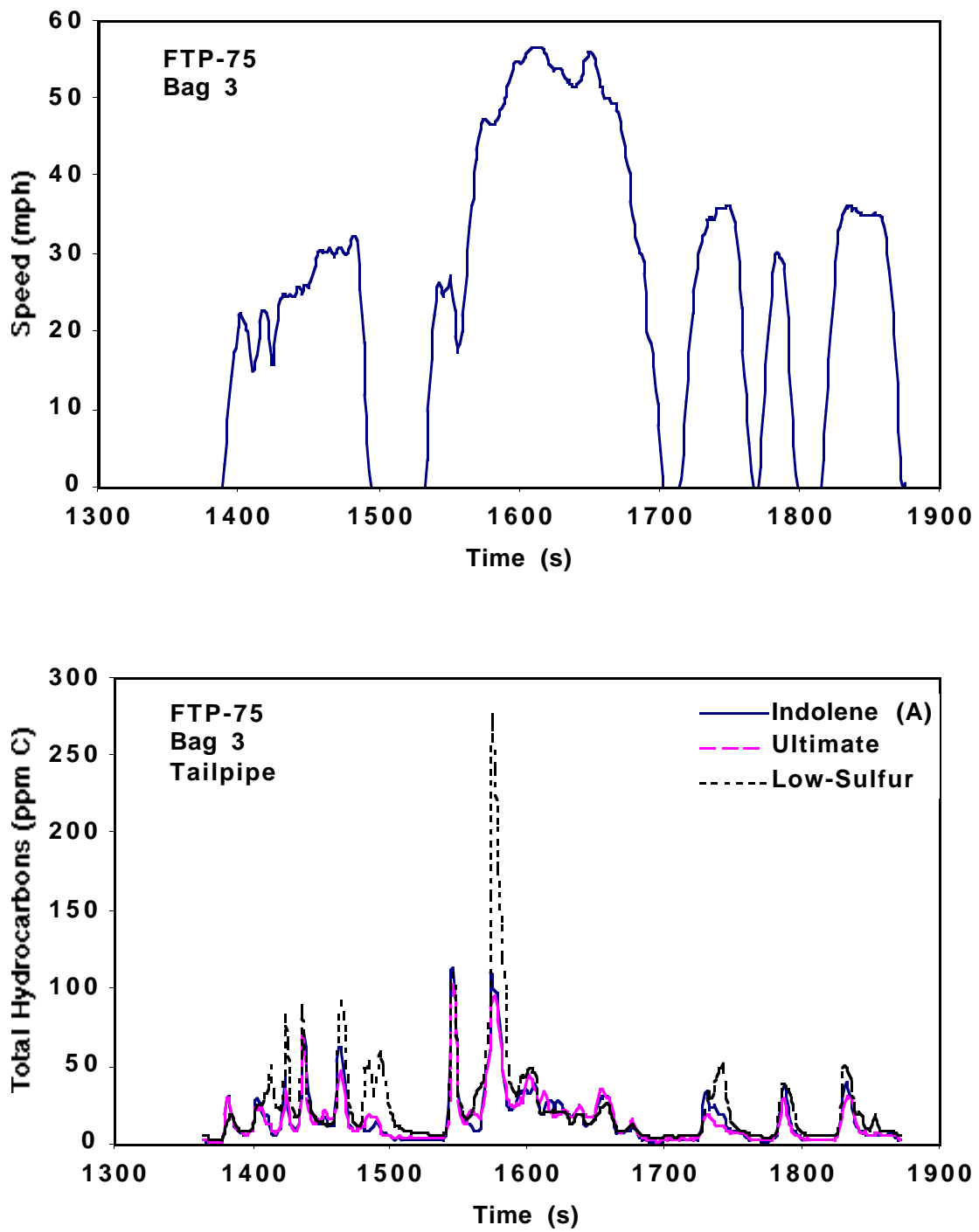


FIGURE 20 Comparison of Tailpipe Emissions from Three Gasolines during Third Phase of FTP (Bag 3)

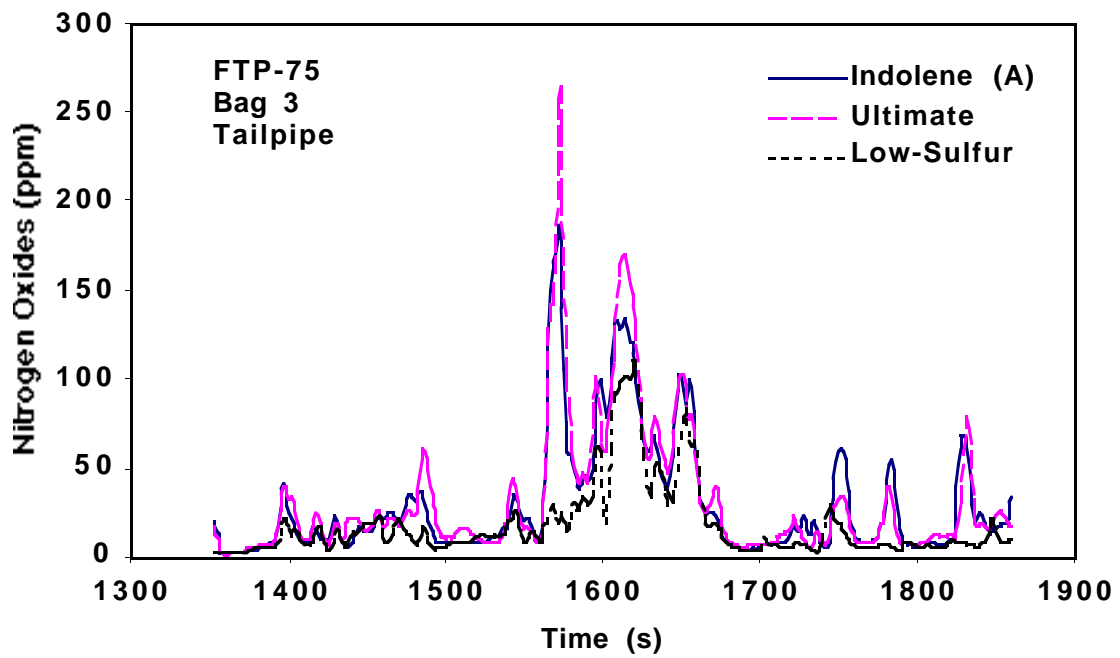
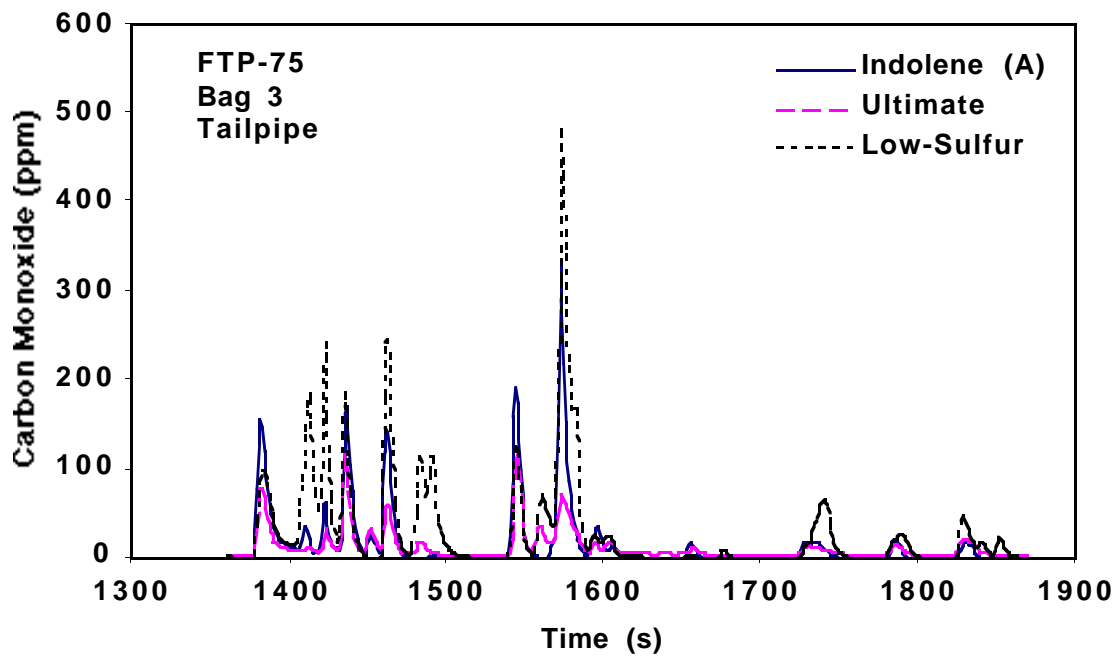


FIGURE 20 (Cont.)

The highest peaks for CO in Phase 1 are Indolene, 1982.9 ppm; Ultimate, 2074.1 ppm; and low-sulfur fuel, 2234.7 ppm. These peaks also occurred during the first acceleration after the cold start. As with the bag emissions (Figure 8), the low-sulfur gasoline has the highest peak.

The highest peaks for NO<sub>x</sub> in Phase 1 are Indolene, 393.9 ppm; Ultimate, 409.1 ppm; and low-sulfur fuel, 300.0 ppm. These peaks occurred during the acceleration to 56.7 mph, which is the longest and most aggressive acceleration in Phase 1. As with the bag emissions (Figure 8), Ultimate has the highest peak, and the low-sulfur gasoline has the lowest peak.

Phase 2 tailpipe measurements of THC, CO, and NO<sub>x</sub> for the three gasolines are shown in Figure 19. The highest THC peaks in Phase 2 are Indolene, 26.4 ppm C; Ultimate, 28.4 ppm C; and low-sulfur fuel, 54.6 ppm C. These peaks occurred at different accelerations, which suggests that variations in driver technique played a role in determining the highest peaks and their locations.

The highest CO peaks in Phase 2 are Indolene, 19.0 ppm; Ultimate, 51.5 ppm; and low-sulfur fuel, 47.0 ppm. These peaks also occurred at different accelerations, which suggests that variations in driver technique played a role in determining the highest peaks and their locations.

The highest NO<sub>x</sub> peaks in Phase 2 are Indolene, 33.5 ppm; Ultimate, 44.9 ppm; and low-sulfur fuel, 24.3 ppm. These peaks occurred at different times. The NO<sub>x</sub> graph does not show clearly identifiable accelerations, as the THC and CO graphs do and as the engine-out NO<sub>x</sub> graph of Figure 13 does. This lack of identifiable accelerations may have been due to opening and closing of the EGR valve and to the driver's manipulation of the accelerator pedal.

Phase 3 tailpipe measurements of THC, CO, and NO<sub>x</sub> for the three gasolines are shown in Figure 20. The highest THC peaks in Phase 3 are Indolene, 114.5 ppm C; Ultimate, 103.7 ppm C; and low-sulfur fuel, 278.3 ppm C. Unlike the Phase 1 peaks, which occurred during the first acceleration, these peaks occurred during the acceleration to 56.7 mph. The peaks are only 8-17% as high as the Phase 1 peaks because the catalytic converter has warmed up in Phase 3.

The highest CO peaks in Phase 3 are Indolene, 330.4 ppm; Ultimate, 116.0 ppm; low-sulfur fuel, 482.8 ppm. These peaks are 6-22% as high as the Phase 1 peaks, which occurred during the first acceleration before the catalytic converter warmed up. In Phase 3, only the peak for Ultimate occurred during the first acceleration; the peaks for Indolene and the low-sulfur fuel occurred during the acceleration to 56.7 mph.

The highest NO<sub>x</sub> peaks in Phase 3 are Indolene, 187.8 ppm; Ultimate, 265.4 ppm; and low-sulfur fuel, 110.6 ppm. These peaks occurred at 1590 s during the acceleration to 56.7 mph, but the peak for the low-sulfur fuel occurred 48 s after the peaks for the other fuels. As was the case for Phase 2, opening and closing of the EGR valve and the driver's manipulation of the accelerator pedal may have affected NO<sub>x</sub> emissions.

### 3.3.4 Tailpipe Emissions from SIDI and PFI Vehicles on Indolene

Figures 21, 22, and 23 show the Phase 1, 2, and 3 tailpipe emissions, respectively, for the two vehicles, both running on Indolene. The highest THC peaks in Phase 1 are SIDI, 1379.6 ppm C; PFI, 820.1 ppm C. Both peaks occur during the first acceleration after startup, before the catalyst has warmed up. The highest THC peaks for engine-out emissions occur at the same time (see Figure 15).

The highest CO peaks in Phase 1 are SIDI, 1982.9 ppm; PFI, 3062.4 ppm. The time relationship of the two peaks is the same as for the engine-out CO peaks. (See Figure 15.) In particular, the PFI engine peak occurs about 40 s after startup and is 54% higher than the SIDI engine peak, which occurs 27 s after startup. At those times, the catalytic converter has not warmed up enough to become effective. The high peak for the PFI engine is probably due to cold-start enrichment.

The highest NO<sub>x</sub> peaks in Phase 1 are SIDI, 393.9 ppm at 214 s after startup; PFI, 127.6 ppm at 66 s after startup. The SIDI peak occurs during the acceleration to 56.7 mph, but the PFI peak occurs during the first acceleration after the cold start. The SIDI catalyst has not warmed up enough to become effective until after the second acceleration, while the PFI catalyst is effective before the second acceleration. The NO<sub>x</sub> emissions for the two vehicles were integrated under the curve for the first acceleration (0-163 s), the second acceleration (163-346 s), and the remainder of the cycle (346-505 s) to determine the effect of the slow catalyst warm-up on the SIDI vehicle. The contributions to total NO<sub>x</sub> emissions from the first acceleration are SIDI, 37%; PFI, 74%. Contributions from the second acceleration are SIDI, 54%; PFI, 16%. Contributions from the remainder of Phase 1 are SIDI, 8.5%; PFI, 9.4%. The effect of faster catalyst warm-up on SIDI NO<sub>x</sub> emissions was estimated as follows: The contribution from the first acceleration was unchanged, but the contributions from the second acceleration and the remainder of Phase 1 were reduced by the same proportions as those of the PFI vehicle. This yielded a Phase 1 NO<sub>x</sub>-emission reduction of 50% for the SIDI vehicle. Phase 1 NO<sub>x</sub> emissions would be decreased from 1.472 g/mi to 0.736 g/mi. The weighted-average NO<sub>x</sub> emissions would decrease from 0.705 g/mi to 0.56 g/mi, a 21% reduction. Other modifications would be necessary to meet the PNGV goal of 0.2 g/mi.

Phase 2 tailpipe measurements of THC, CO, and NO<sub>x</sub> for the two vehicles running on Indolene are shown in Figure 22. The highest THC peaks in Phase 2 are SIDI, 26.4 ppm C; PFI, 11.9 ppm C. These peaks occurred at different times, which suggests that driver technique played a role in determining the highest peaks and their locations.

The highest CO peaks in Phase 2 are SIDI, 19.0 ppm; PFI, 245.0 ppm. Both peaks occurred at 754 s. CO peaks correspond to the accelerations of the cycle. PFI peaks are consistently higher than those of the SIDI vehicle.

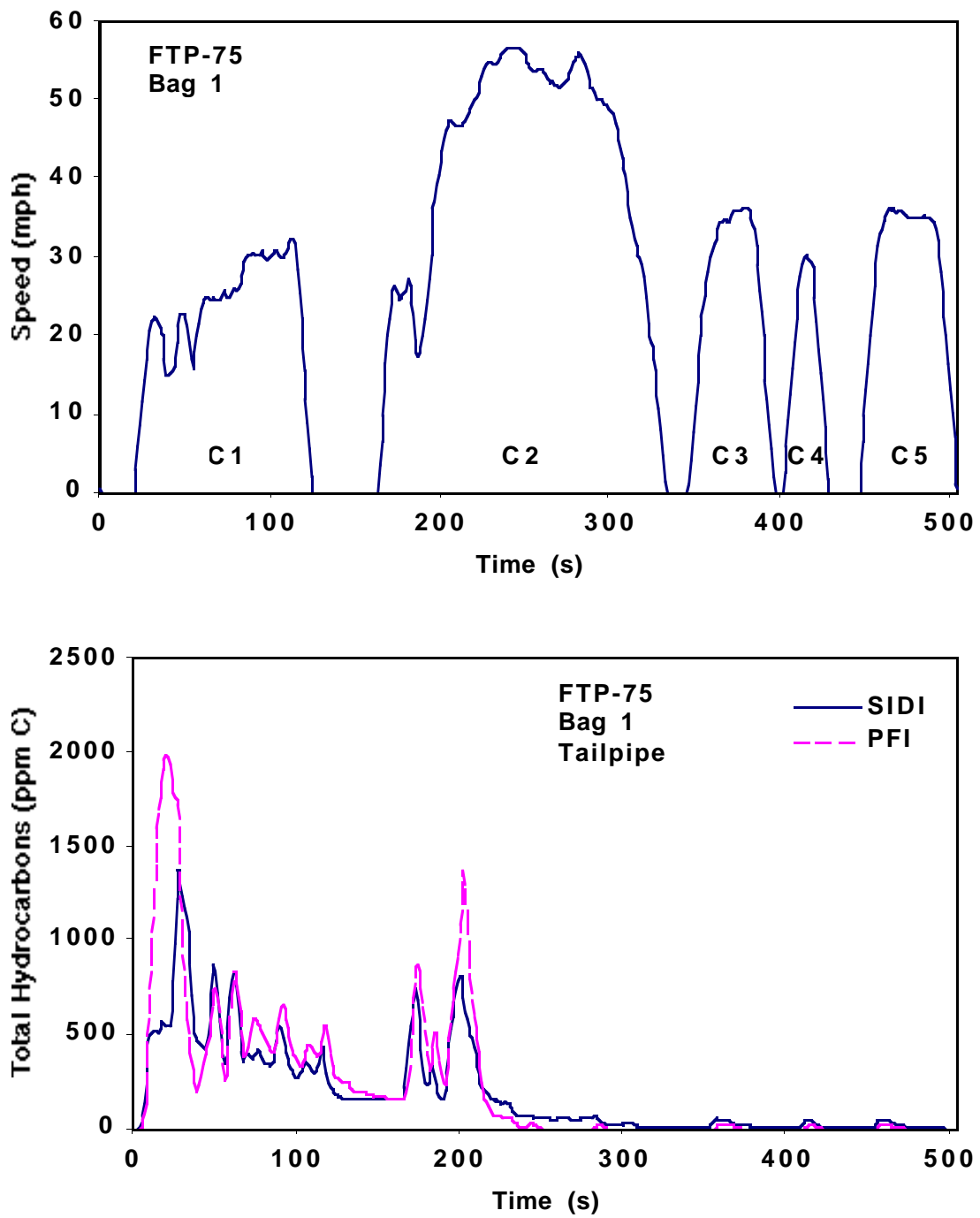


FIGURE 21 Comparison of Tailpipe Emissions from Mitsubishi-SIDI and Neon-PFI Vehicles during FTP Cold Phase (Bag 1)

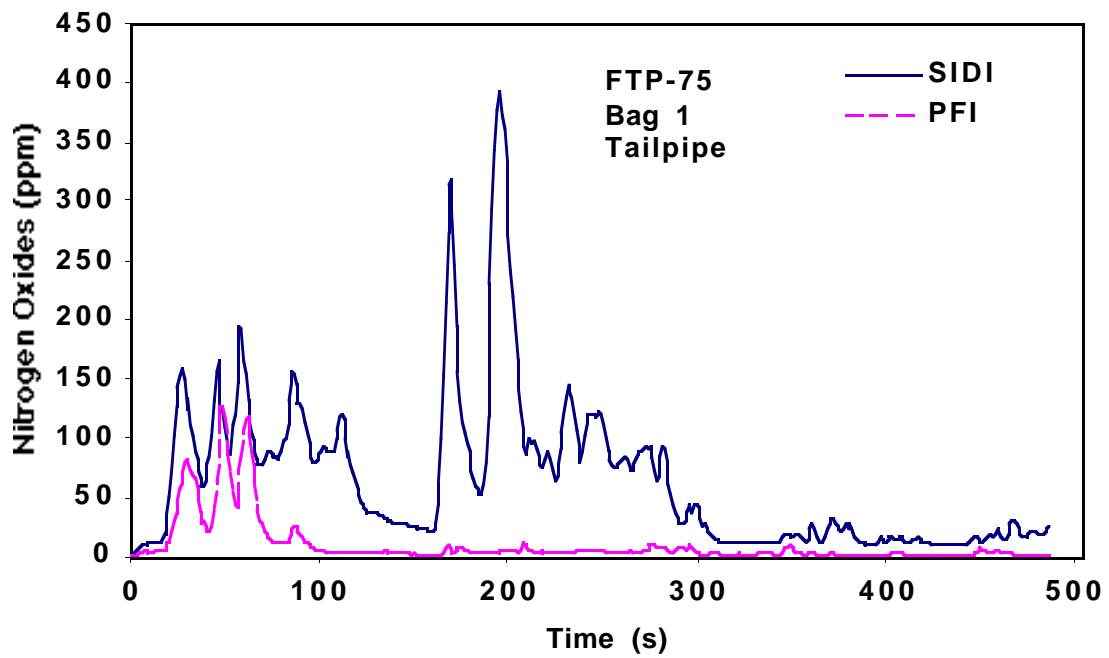
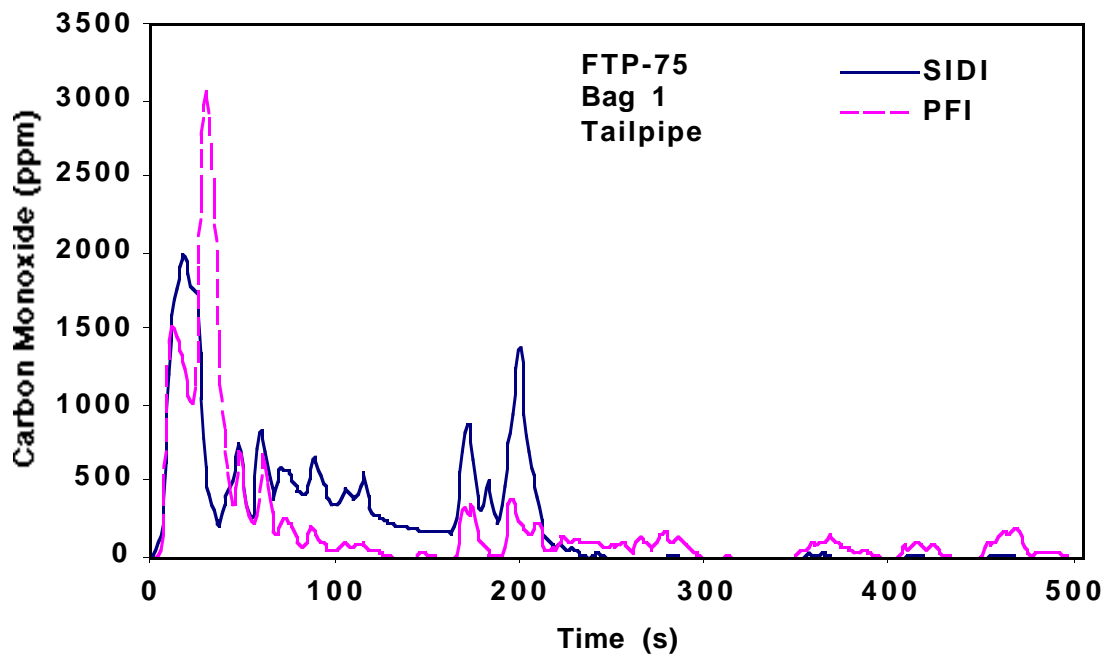
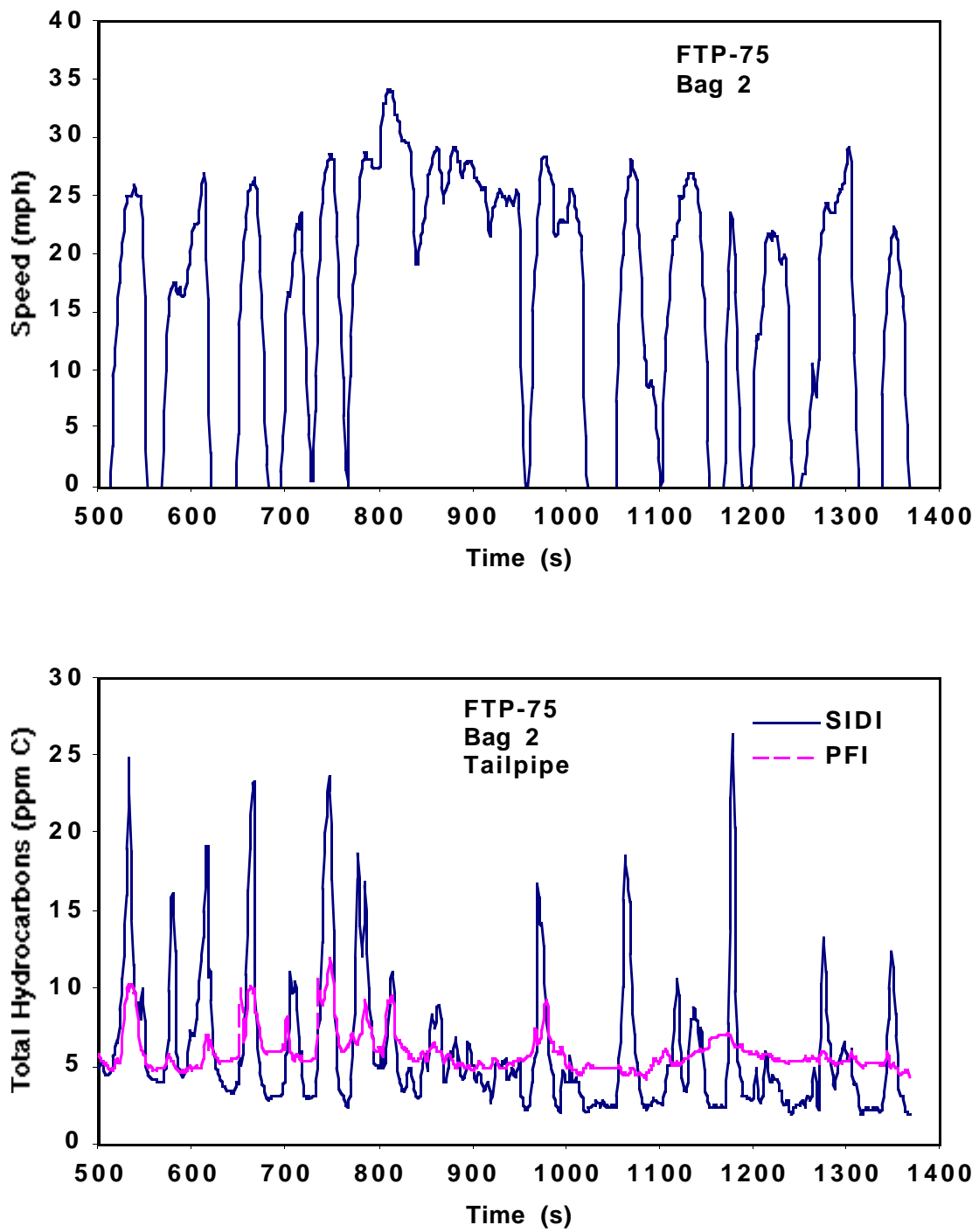


FIGURE 21 (Cont.)



**FIGURE 22 Comparison of Tailpipe Emissions from Mitsubishi-SIDI and Neon-PFI during Second Phase of FTP (Bag 2)**



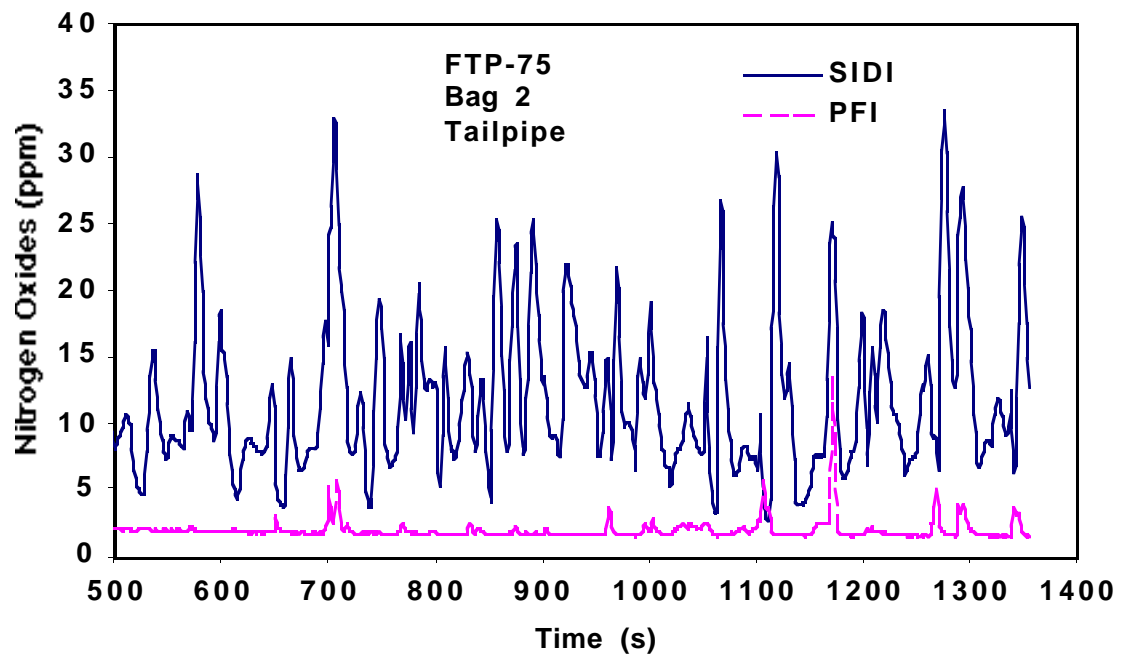
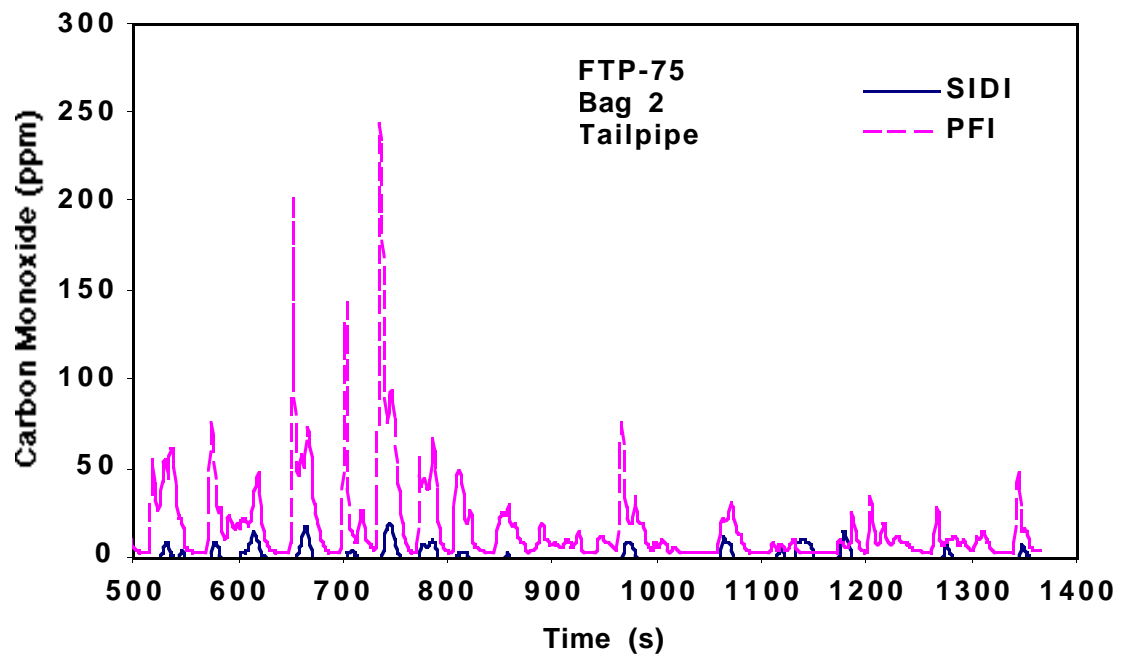


FIGURE 22 (Cont.)

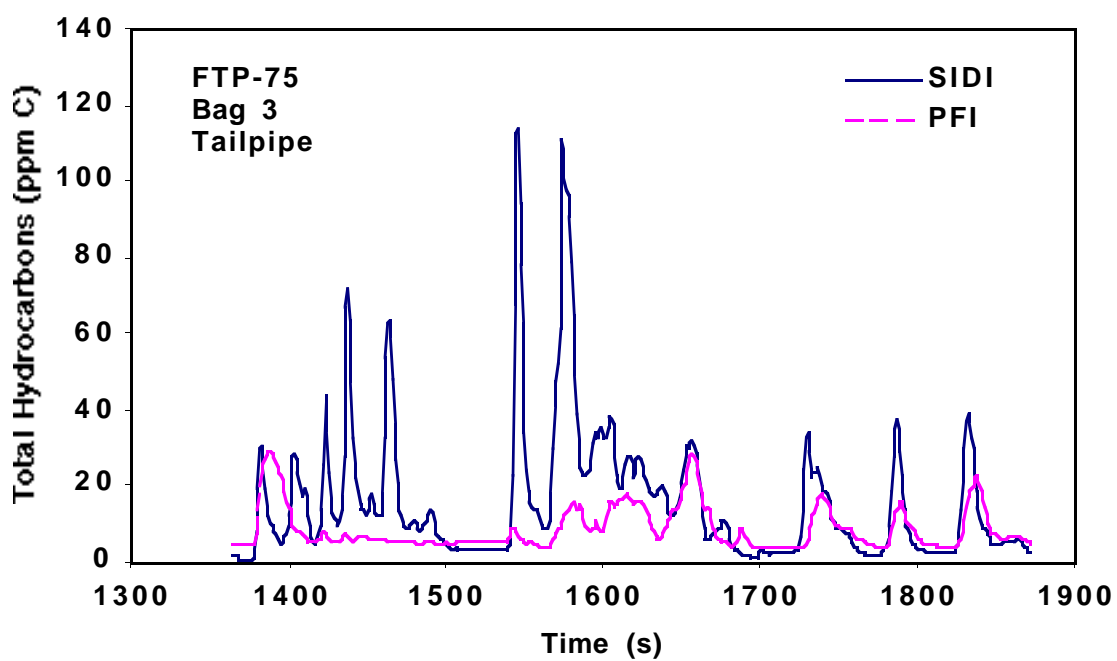
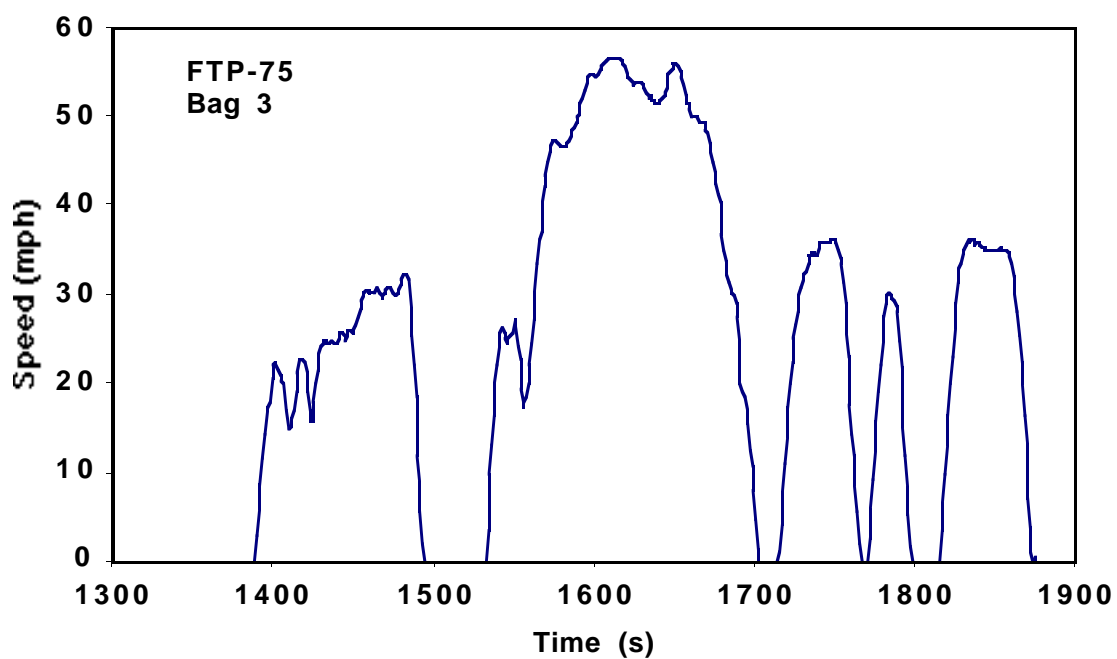


FIGURE 23 Comparison of Tailpipe Emissions from Mitsubishi-SIDI and Neon-PFI during Third Phase of FTP (Bag 3)

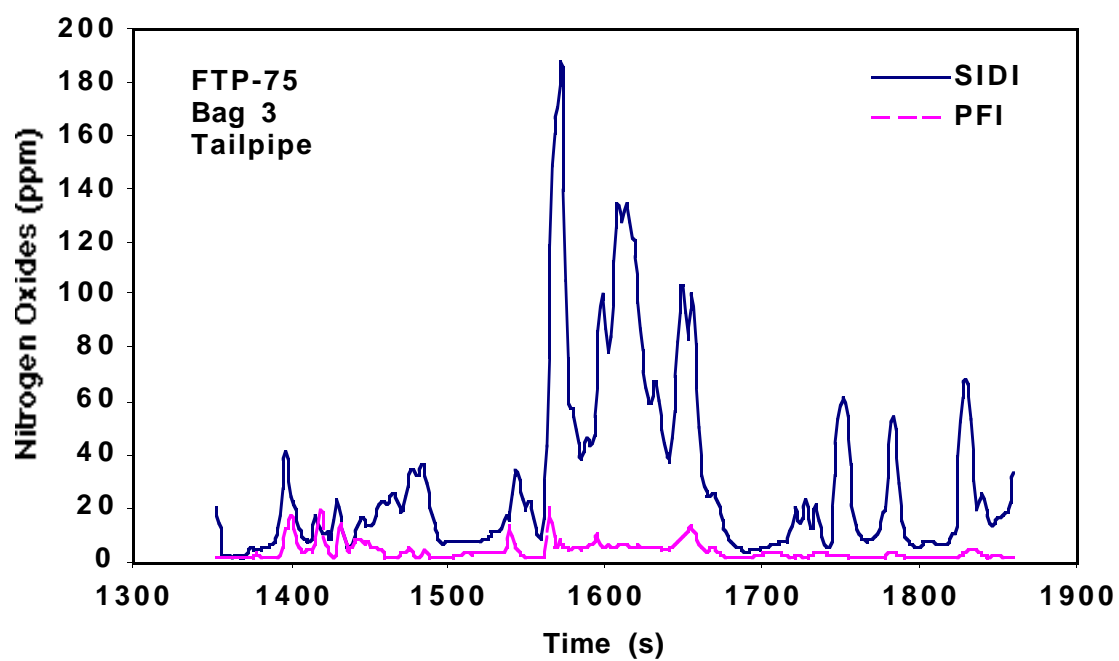
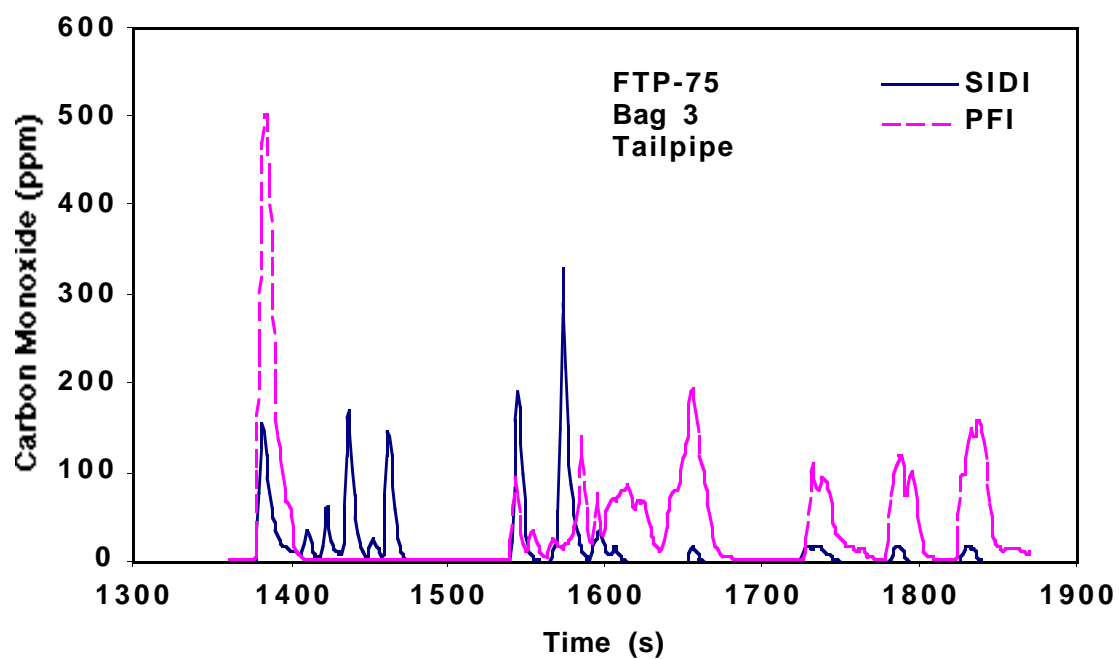


FIGURE 23 (Cont.)

The highest NO<sub>x</sub> peaks are SIDI, 33.5 ppm; PFI, 13.7 ppm. The PFI curve consists of well-defined low peaks above a low baseline. The SIDI curve has no well-defined baseline and has many more peaks than the PFI curve has. Differences in EGR-control algorithms and vehicle response to accelerator-pedal inputs may account for this.

Phase 3 tailpipe measurements of THC, CO, and NO<sub>x</sub> for the two vehicles running on Indolene are shown in Figure 23. The highest THC peaks in Phase 3 are SIDI, 114.5 ppm C; PFI, 29.6 ppm C. These peaks occurred at different times, which suggests that driver technique played a role in determining the highest peaks and their locations.

The highest CO peaks in Phase 3 are SIDI, 330.4 ppm; PFI, 506.5 ppm. CO peaks correspond to the accelerations of the cycle. PFI peaks are consistently higher than those of the SIDI vehicle.

The highest NO<sub>x</sub> peaks are SIDI, 187.8 ppm; PFI, 20.7 ppm. The PFI curve consists of well-defined low peaks above a low baseline. These peaks occurred at about the same time during the acceleration to 56.7 mph.

### **3.3.5 FTP Emissions from SIDI Vehicle, Measured at ATL**

Additional information was obtained in the second-by-second measurements conducted at ATL. Second-by-second measurements of speed, acceleration, total hydrocarbons, carbon monoxide, nitrogen oxides, exhaust oxygen, and exhaust-gas temperature for Phase 1 of the FTP are shown in Figure 24. Fuels used were RFG, both with and without the catalytic converter, and Indolene (B) with the catalytic converter. The data were corrected for instrument delay by shifting the time axis as follows: total hydrocarbons, 11.2 s; carbon monoxide, 15.9 s; and nitrogen oxides, 10.9 s.

With RFG, the traces of engine-out and tailpipe emissions for hydrocarbons, carbon monoxide, and nitrogen oxides follow nearly the same paths for the first 200 s. After the 200-s mark, the paths for the RFG engine-out emissions are higher than the paths for the tailpipe emissions.

The exhaust-gas temperature before the converter is less than 270°C prior to the 200-s mark and more than 270°C after the 200-s mark. The 200-s mark clearly identifies the catalyst warm-up time. The exhaust-gas temperature for the Indolene (B) is typically about 20°C less than that of the RFG. This partly accounts for the higher emissions of THC, CO, and NO<sub>x</sub> with Indolene (B) compared with those emissions with RFG. The higher content of oxygenated compounds of RFG compared to Indolene (B) also accounts for the higher THC and CO emissions with Indolene (B).

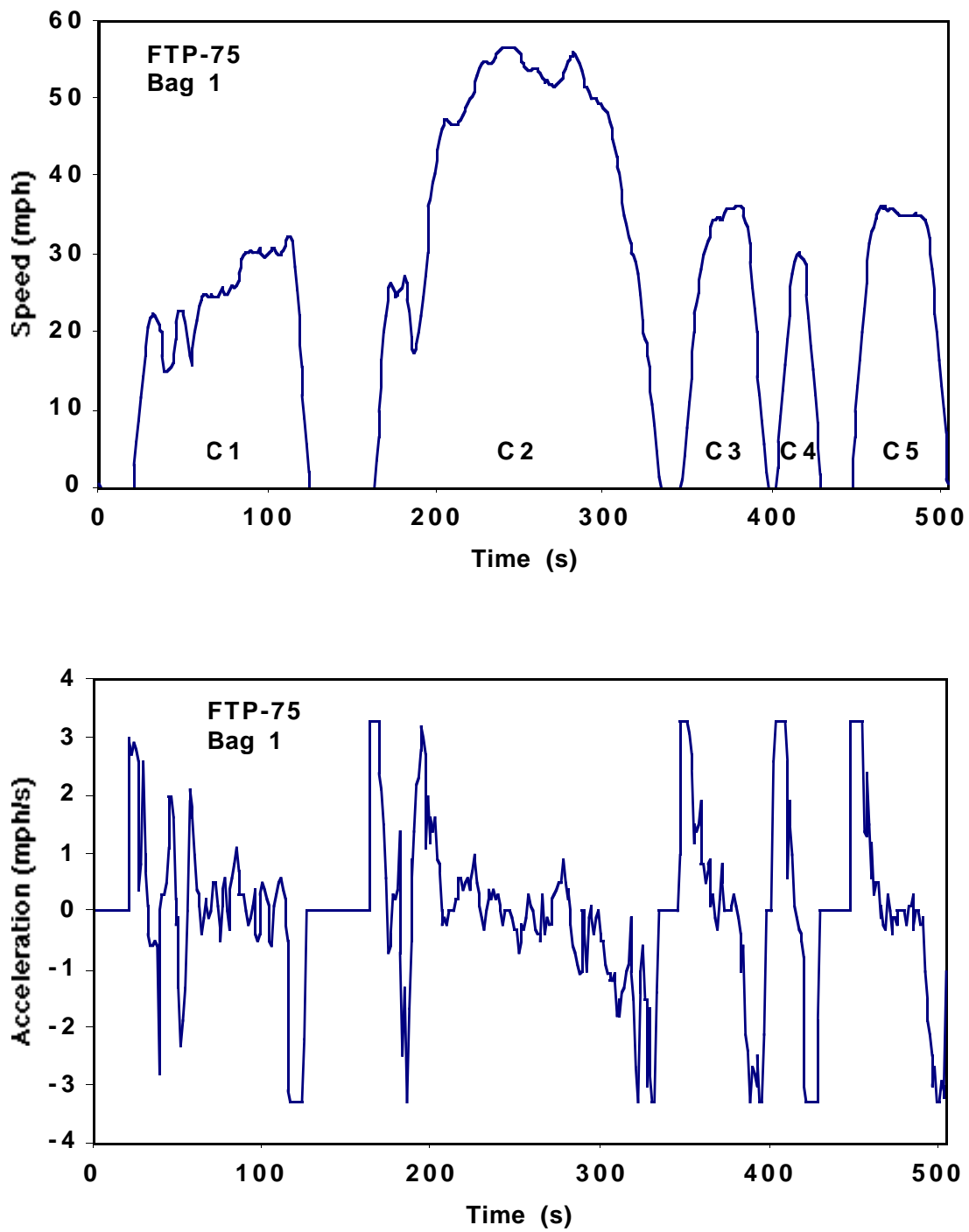


**FIGURE 24 Comparison of Tailpipe and Engine-Out Emissions for Two Gasolines during the First Phase of the FTP (Bag 1)**

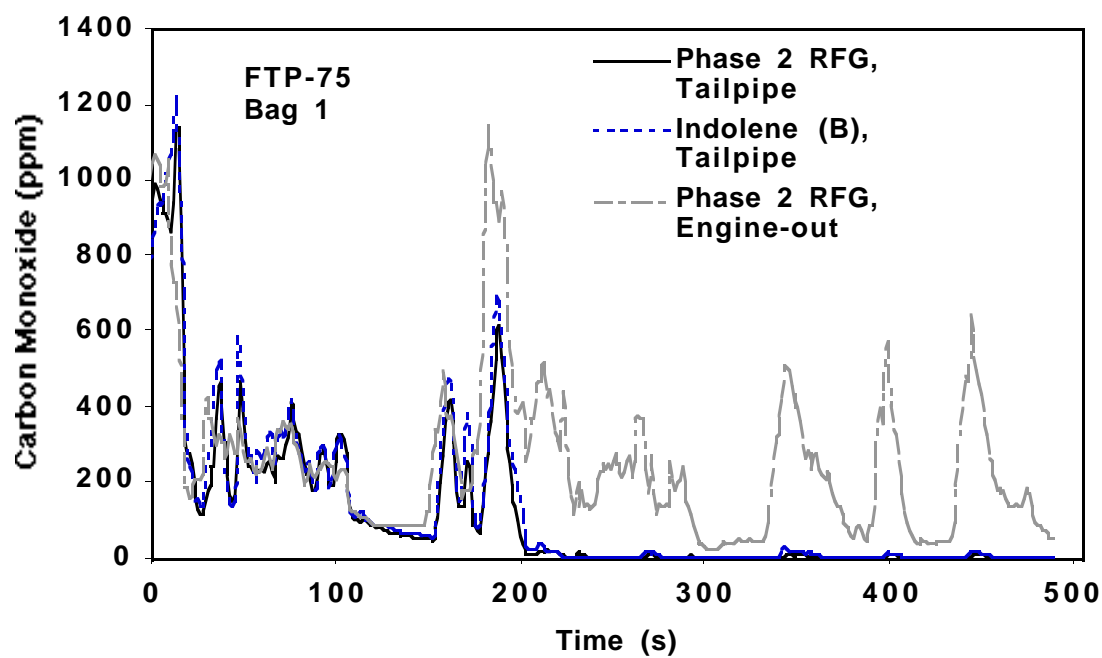
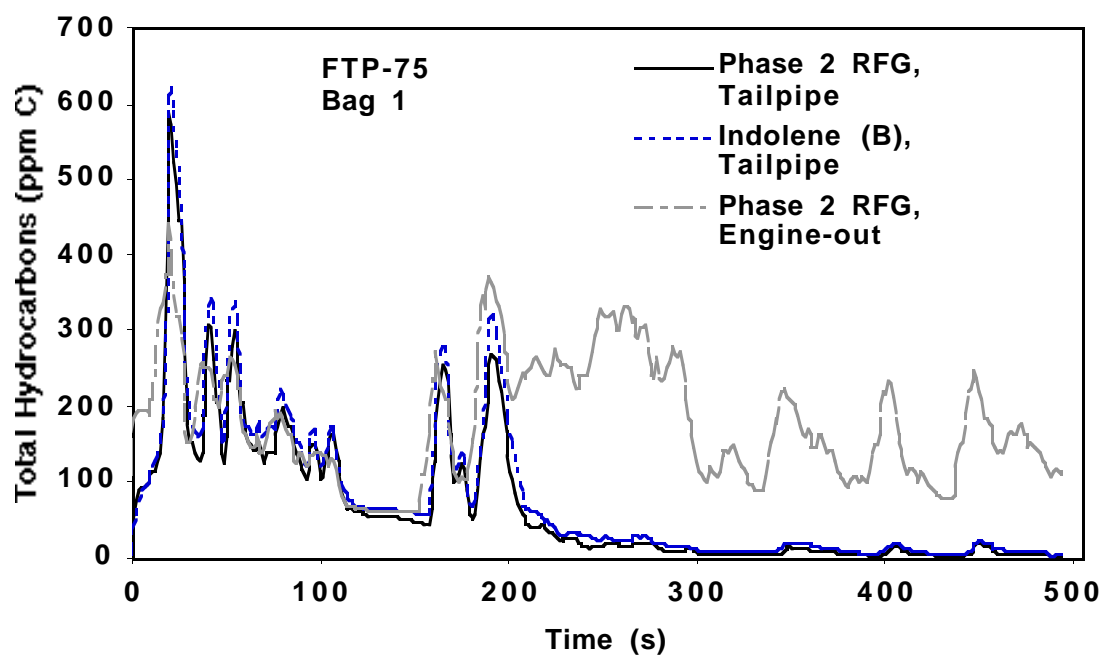


FIGURE 24 (Cont.)

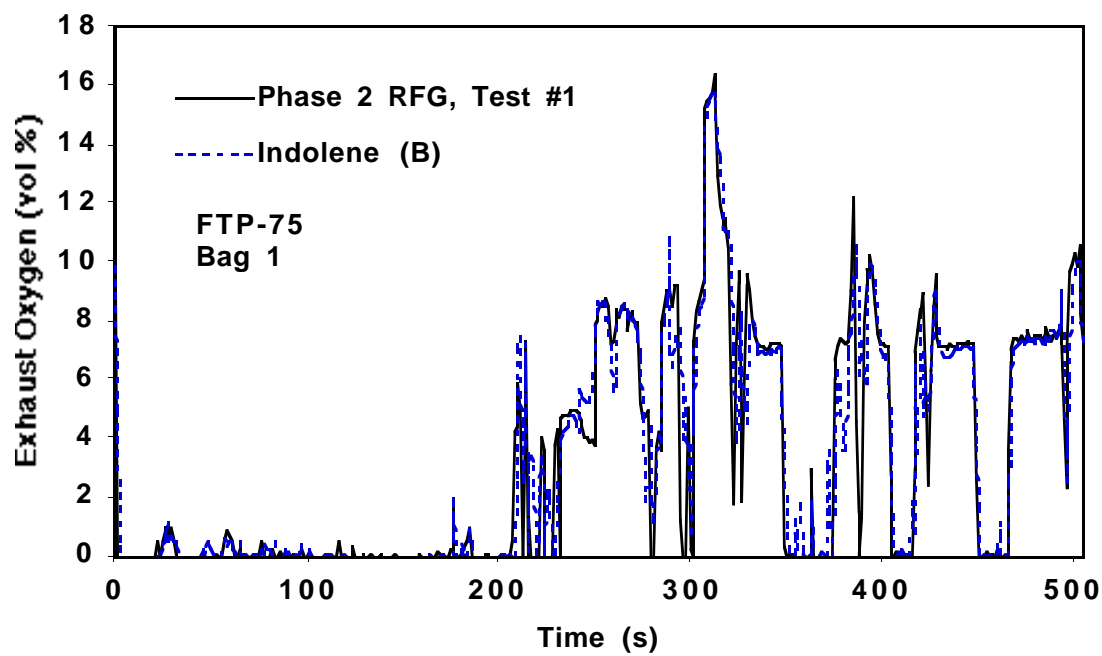
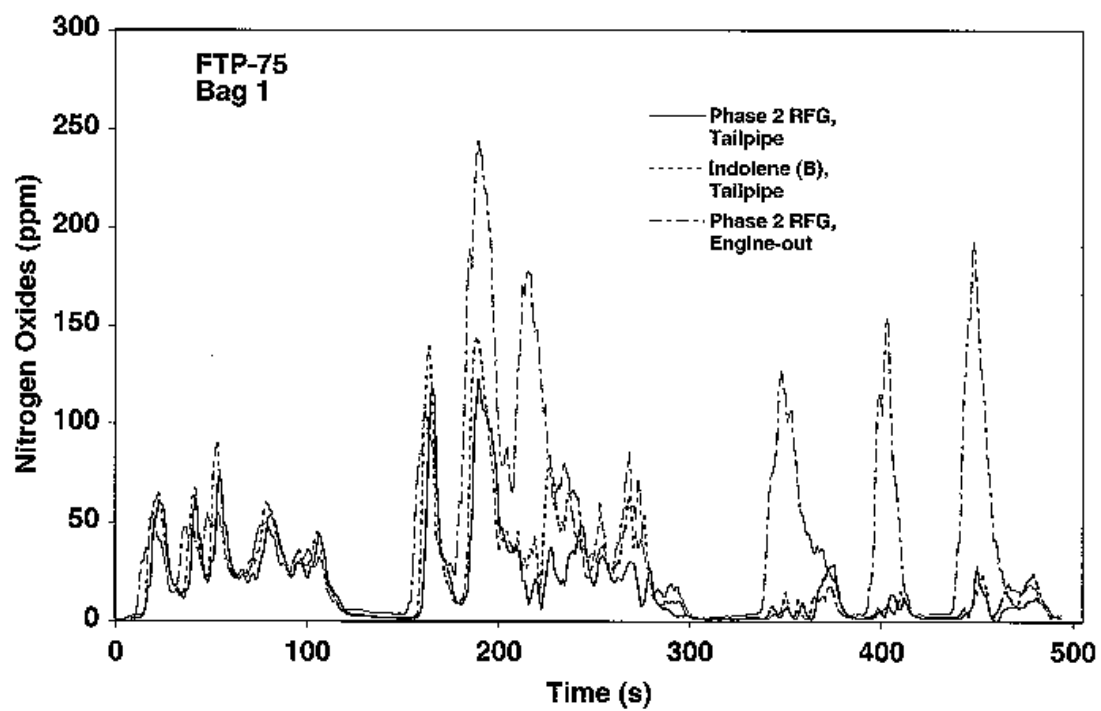
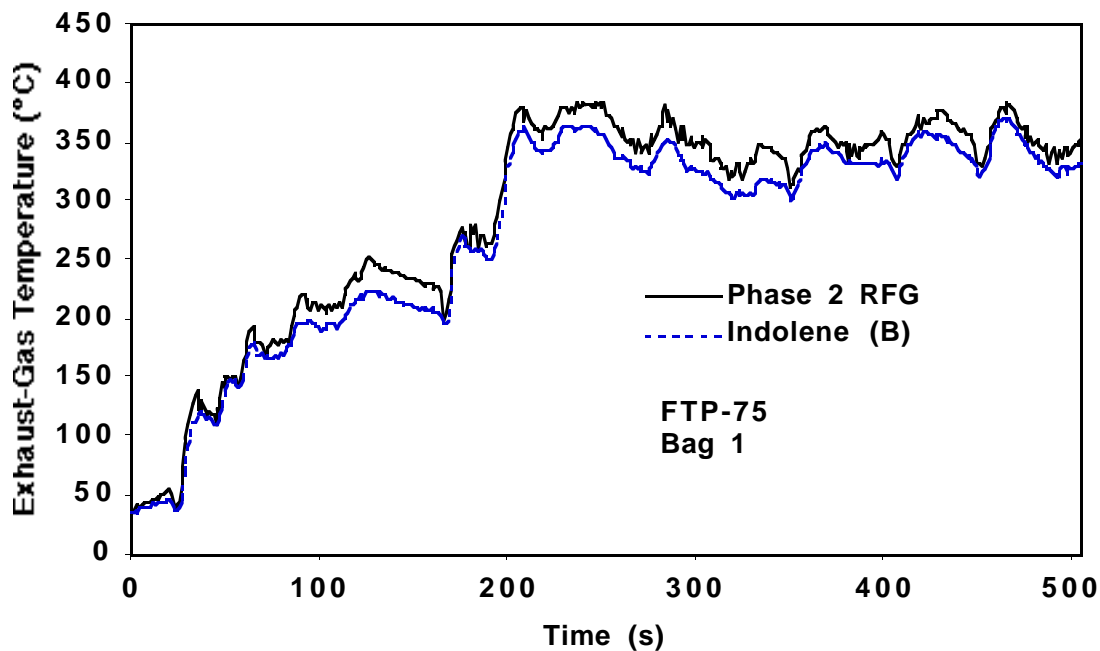


FIGURE 24 (Cont.)



**FIGURE 24 (Cont.)**

The exhaust-oxygen traces show that oxygen is less than 2% for the first 200 s, but it increases to roughly 8% (with numerous peaks and troughs) after the 200-s mark. The engine operates in the throttled, homogeneous-charge mode for the first 200 s. After 200 s, the engine switches between stratified-charge mode and homogeneous-charge mode. During intervals of stratified-charge mode, the control system attempts to maintain about 8% oxygen in the exhaust. Peaks above 8% oxygen correspond to decelerations. Troughs below 5% oxygen generally correspond to accelerations, but one trough at the 300-s mark and another at the 495-s mark occur during decelerations. During the troughs, the engine operates in the homogeneous-charge mode. In the case of the accelerations, the engine operates in the homogeneous-charge mode to provide more power than would otherwise be available in the stratified-charge mode. The troughs at the 300- and 495-s marks may be brief excursions into the homogeneous-charge mode as the driver manipulates the accelerator pedal.

Figure 25 shows the second-by-second measurements of speed, acceleration, total hydrocarbons, carbon monoxide, nitrogen oxides, exhaust oxygen, and exhaust-gas temperature at the catalyst inlet during Phase 2. The engine-out measurements for RFG are not shown because they are on a different scale. The exhaust-gas temperature is above 270°C throughout Phase 2, so the catalyst is at its operating temperature. As was the case in Phase 1, the exhaust-gas temperature for Indolene was about 20°C less than that of RFG. This may partly account for the lower tailpipe emissions of THC, CO, and NO<sub>x</sub> with RFG compared to Indolene. The higher oxygen content of RFG also accounts for its lower emissions of THC and CO compared to Indolene.



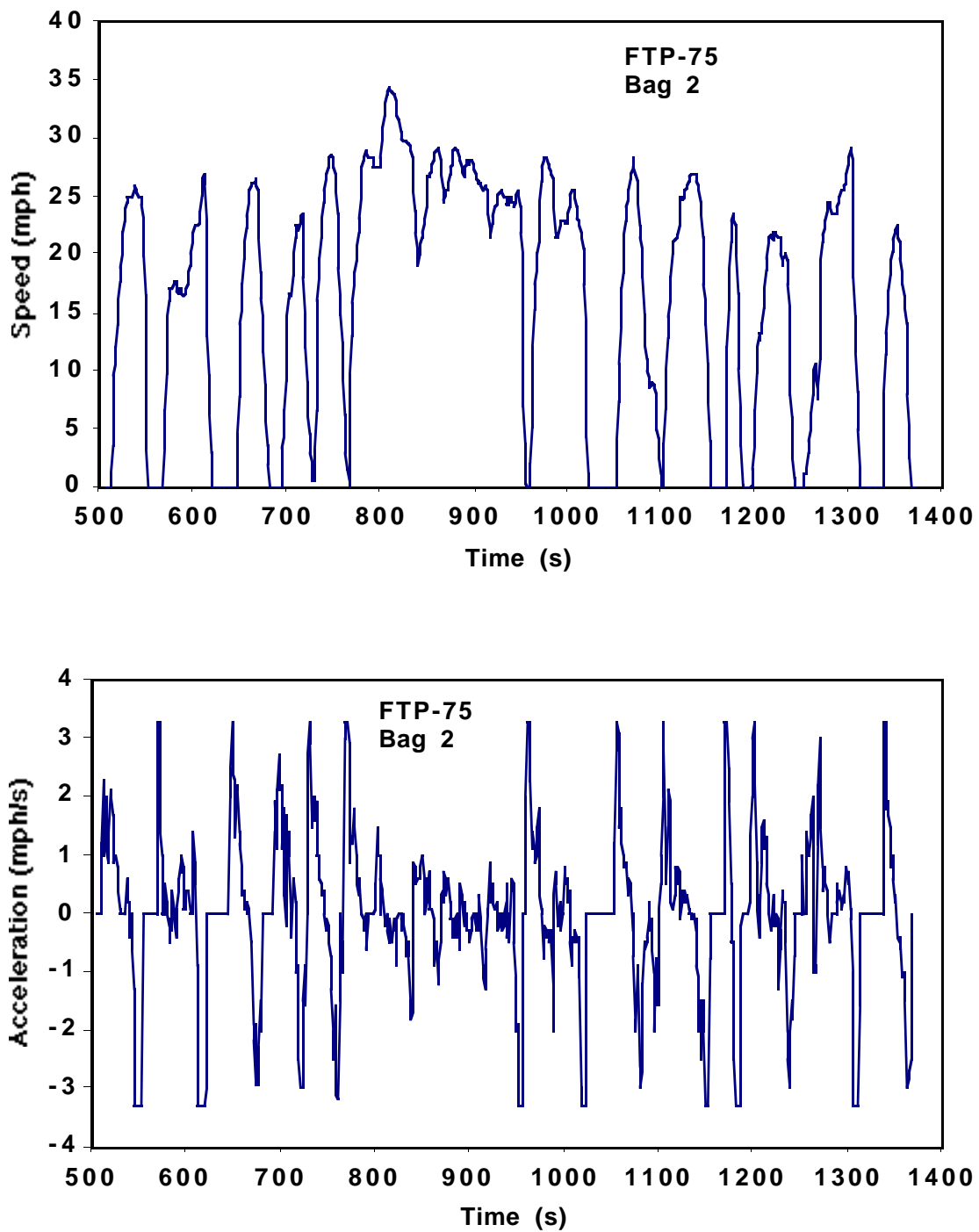


**FIGURE 25 Comparison of Emissions for Two Gasolines during the Second Phase of the FTP (Bag 2)**

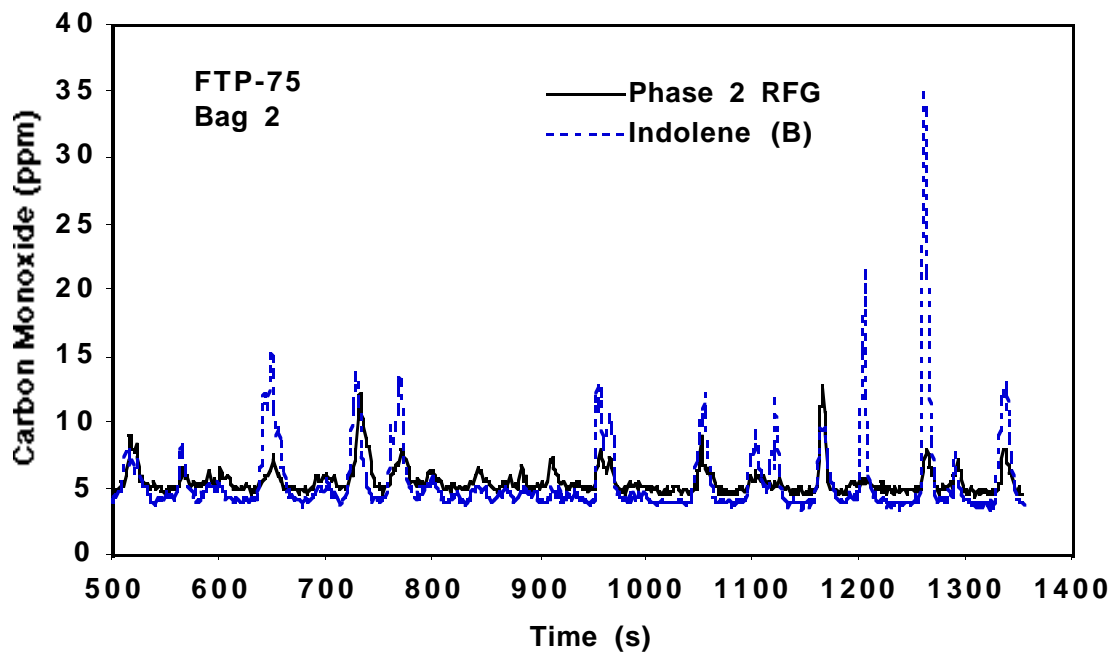
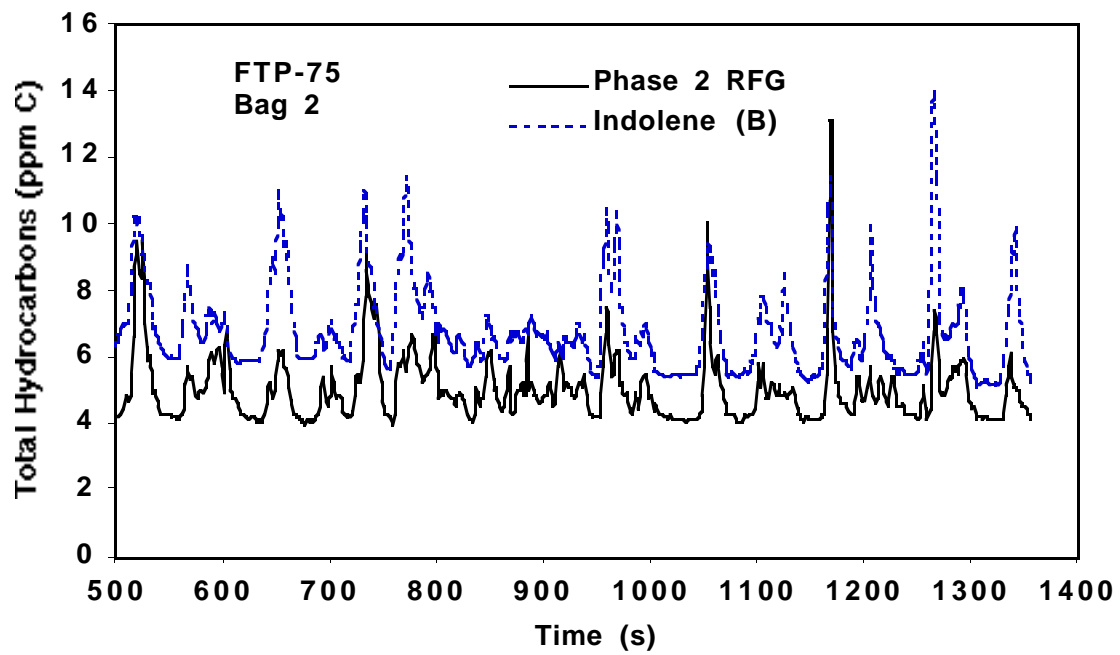


FIGURE 25 (Cont.)

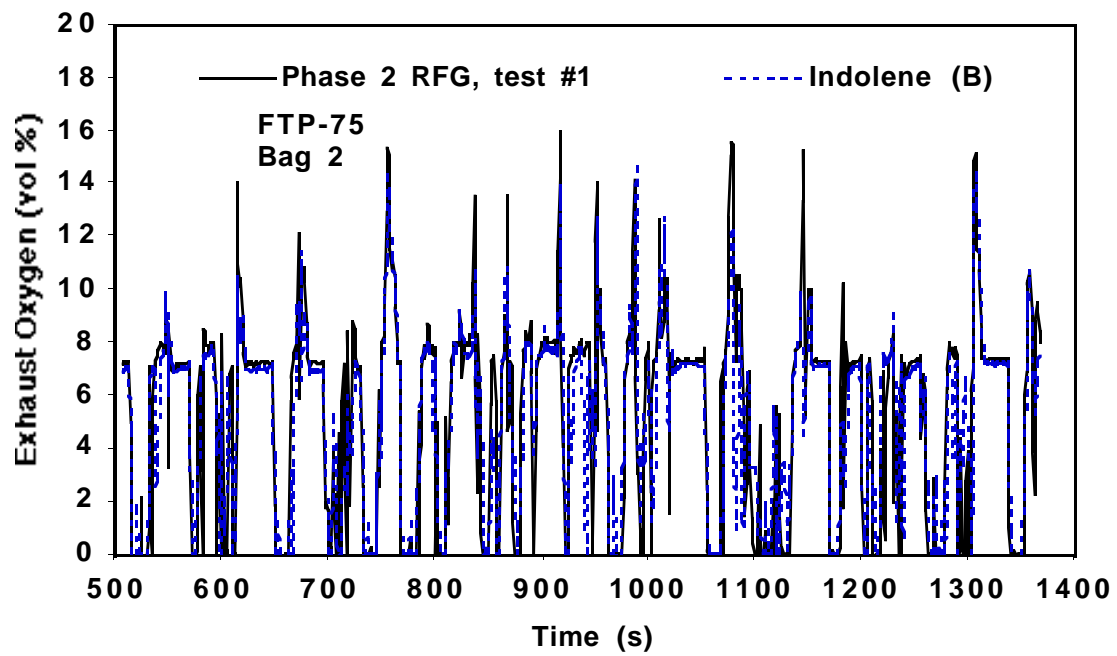
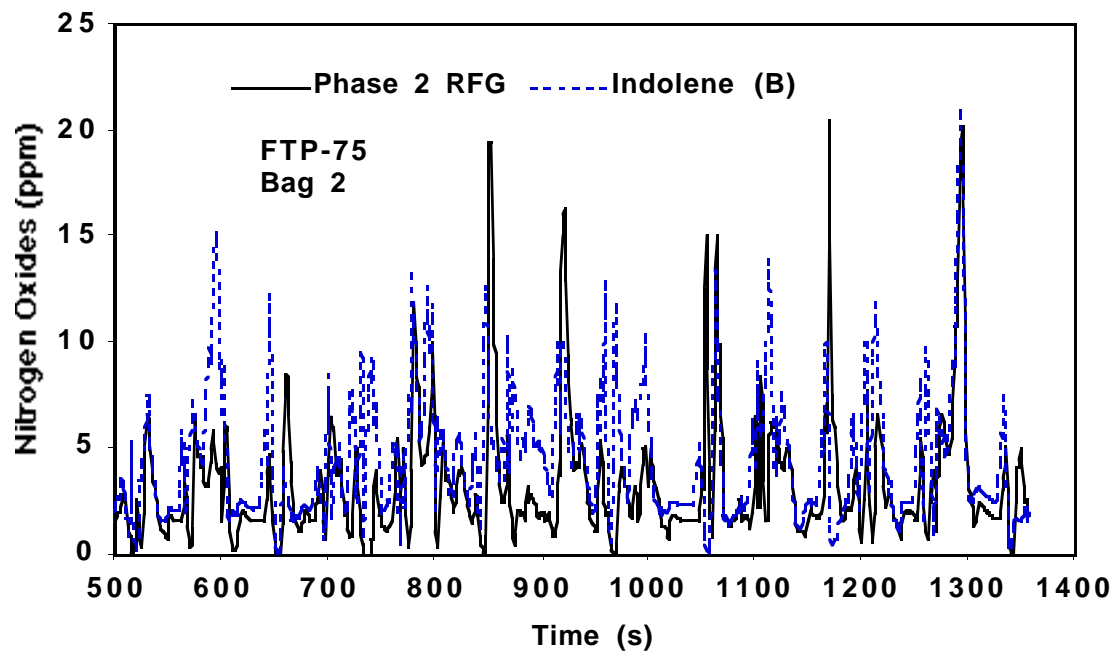
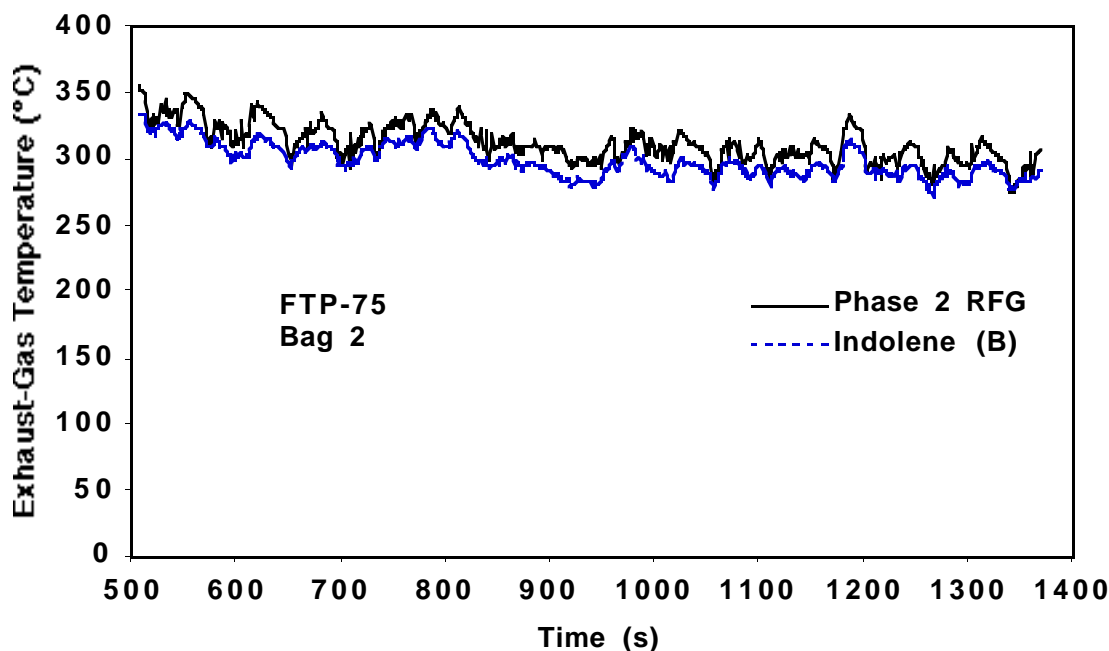


FIGURE 25 (Cont.)



**FIGURE 25 (Cont.)**

The oxygen traces show that the exhaust oxygen operates at about 7% when the engine is idling. This is particularly evident in the time periods 620-645 s, 1028-1052 s, and 1313-1337 s, but it can also be seen in the shorter idling periods. There are numerous peaks and troughs in the oxygen traces. The peaks coincide with decelerations. The troughs generally correspond to strong accelerations, but some narrow troughs correspond to decelerations or minor accelerations. Examples of the latter occur at 947, 1070, 1091, 1147, 1183, and 1238 s. These may be brief excursions into the homogeneous-charge mode as the driver manipulates the accelerator pedal.

Peaks in the THC and CO traces generally correspond to accelerations, and troughs in those traces generally correspond to decelerations. An attempt was made to correlate brief increases in THC or CO levels with the narrow troughs in exhaust oxygen at 947 s, 1070 s, etc., but no such increases were found. The lack of correlation is probably attributable to the response times of the instruments (10-15 s), which are too slow to capture the brief changes in THC or CO (2-3 s).

Peaks and troughs in the  $\text{NO}_x$  trace do not correlate well with accelerations and decelerations. Some peaks correspond to accelerations, and some troughs correspond to decelerations, but many counterexamples occur. Examples of peaks that do not correspond to accelerations are found at 520, 659, 797, 852, 922, 1064, and 1295 s. Examples of troughs that do not correspond to decelerations are found at 570, 649, 730, 966, 1211, and 1311 s. These anomalies may result from opening and closing of the EGR valve or the driver's manipulation of the accelerator pedal.

Figure 26 shows the second-by-second measurements of speed, total hydrocarbons, carbon monoxide, nitrogen oxides, exhaust oxygen, and catalyst-inlet temperature during Phase 3. The emissions plots include engine-out data as well as tailpipe data. The speed vs. time relationship is the same as that for Phase 1, but Phase 3 begins at the end of a 10-minute soak with a warm engine. At the beginning of Phase 3, the exhaust-gas temperature at the catalyst inlet is 175-190°C, compared to 35°C in Phase 1 (Figure 24). As in Phase 1, the exhaust-gas temperature does not exceed 275°C until 200 s has elapsed. After the first 200 s, the Phase 1 and Phase 3 exhaust-gas-temperature plots are similar.

The exhaust-oxygen plot for Phase 3 differs substantially from that of Phase 1. The oxygen measurement for RFG Test #2 was not used for this plot because of a bad connection to the oxygen meter. Phase 3 begins with the engine operating in the stratified-charge mode. In Phase 1, the engine operated in the homogeneous-charge mode for the first 200 s. In both phases, the engine operated in the homogeneous-charge mode during strong accelerations.

The THC plot shows that the catalyst is active during all of Phase 3. The plot shows that tailpipe THC emissions are relatively higher in the first 200 s than they are after the 200-s mark. Thus, the catalyst is more effective when the exhaust-gas temperature exceeds 275°C. Results shown in the CO plot are similar.

The NO<sub>x</sub> plot shows that the catalyst is effective in reducing the peaks that are due to accelerations, but it is less effective at reducing NO<sub>x</sub> that occurs in high-speed operation. NO<sub>x</sub> peaks due to acceleration at the 1401, 1419, 1431, 1542, 1571, 1650, 1725, 1781, and 1827-s marks are reduced by 70 to 92%. The catalyst reduced NO<sub>x</sub> by less than 50% during the high-speed operation from 1589 to 1639 s. The exhaust-oxygen plot shows that the engine operated with little or no excess oxygen during the accelerations. The NO<sub>x</sub> catalyst is effective because it can break down the hydrocarbons into NO<sub>x</sub> reductants, and the lack of oxygen favors NO<sub>x</sub> reduction. During cruise, the engine switched to stratified-charge mode, as shown by the oxygen plot. Even though the engine-out NO<sub>x</sub> during cruise is less than it is during acceleration, tailpipe NO<sub>x</sub> is greater because the exhaust oxygen inhibits NO<sub>x</sub> reduction.

### 3.4 Hydrocarbon Speciation

The hydrocarbon composition of tailpipe emissions is compared for the two vehicles, both running on Indolene (A), in Figure 27. The PFI exhaust contains a higher percentage of aromatics than does the SIDI exhaust, 38.4% vs. 24.3%. The SIDI's iridium-based catalyst destroys aromatics more effectively than the PFI's three-way catalyst does. Destruction of aromatics would tend to yield olefins because of the double bonds of the aromatics. The composition of the SIDI exhaust is 22.6% olefins, compared to 13.9% for the PFI exhaust. Even though the PFI exhaust has a higher percentage of aromatics than the SIDI exhaust, the absolute quantity is less in the former case.

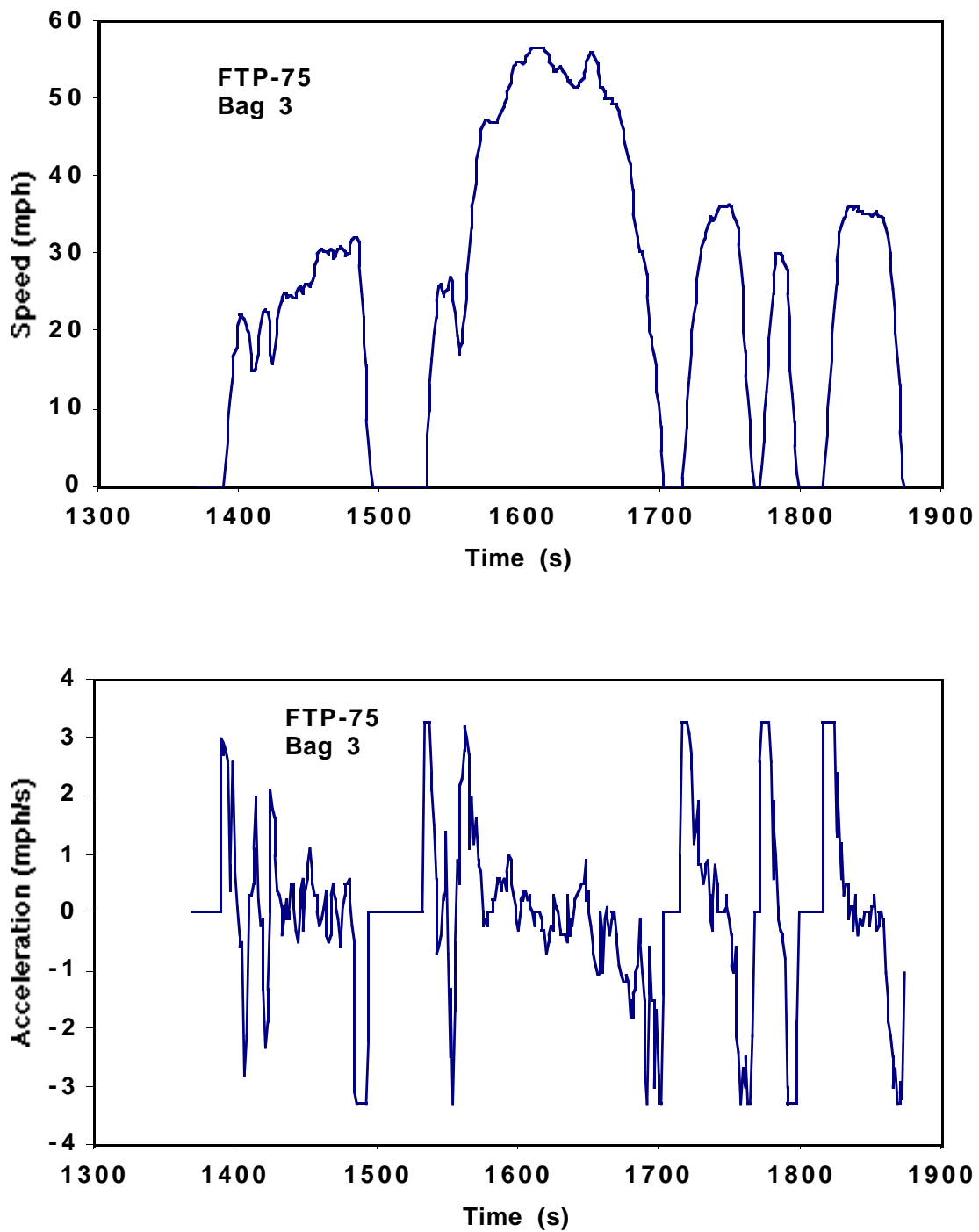


**FIGURE 26 Comparison of Tailpipe and Engine-Out Emissions for Two Gasolines during the Third Phase of the FTP (Bag 3)**

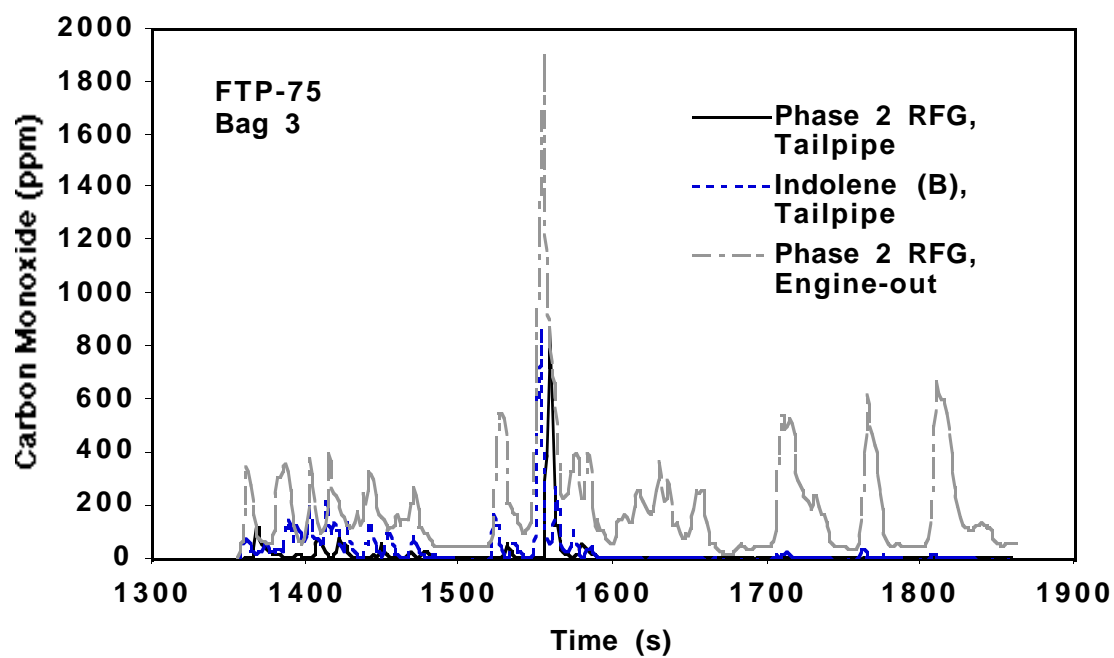
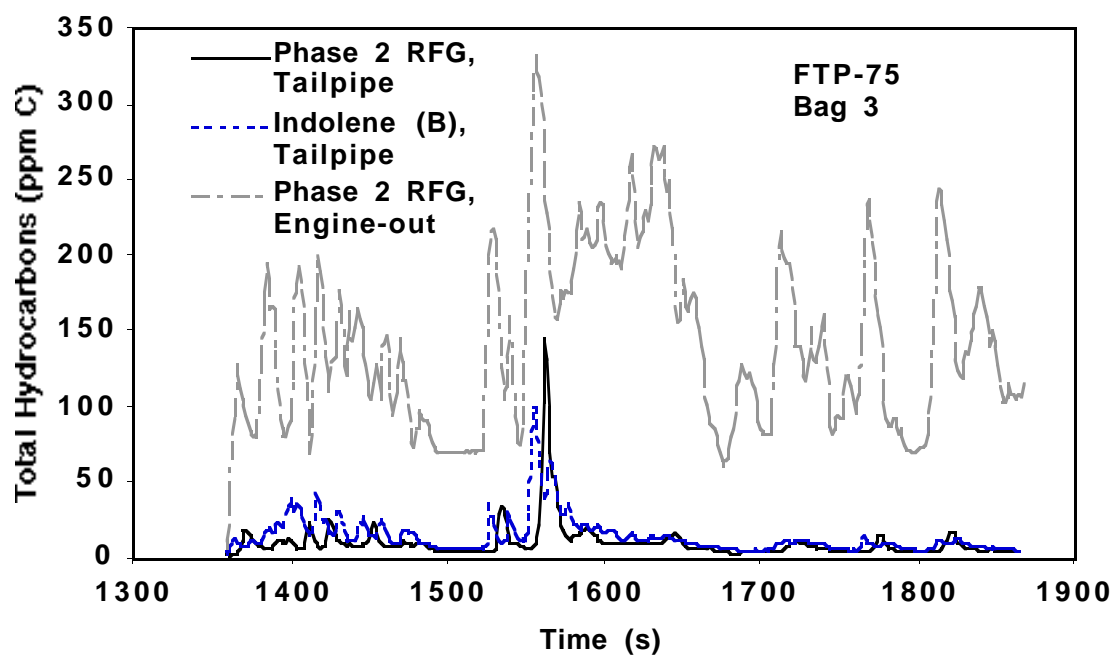


FIGURE 26 (Cont.)

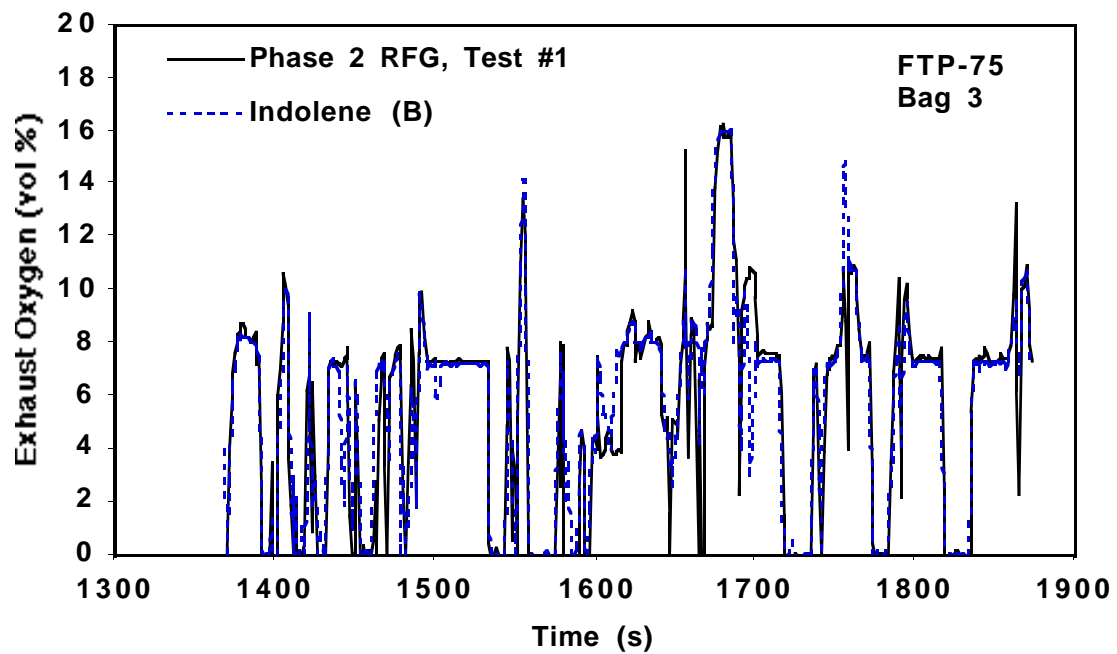
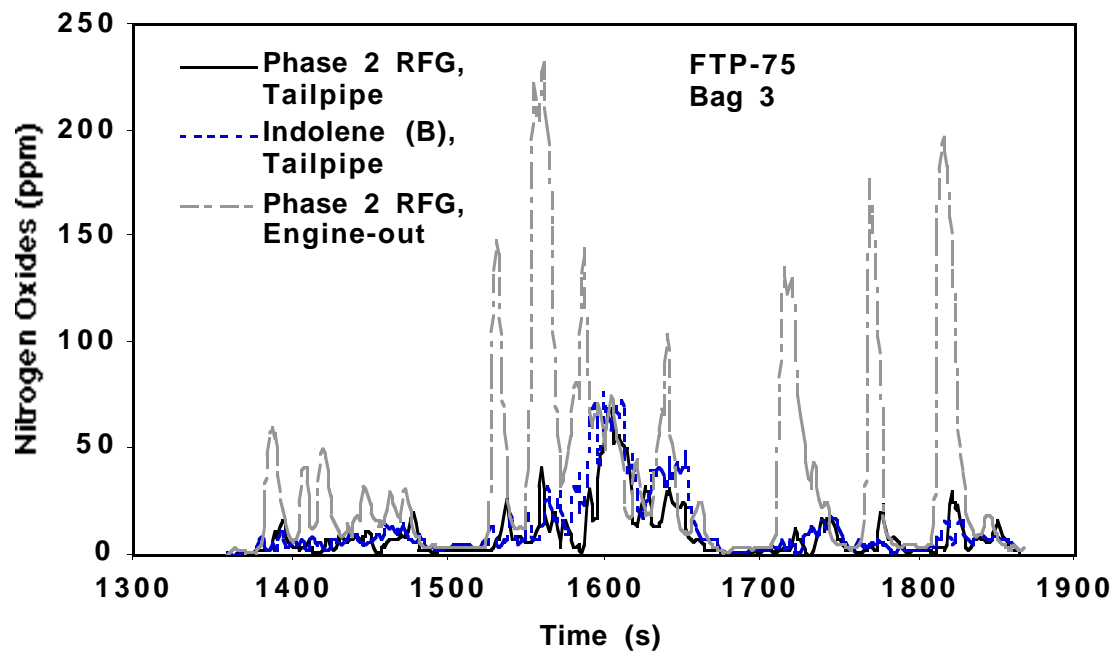


FIGURE 26 (Cont.)



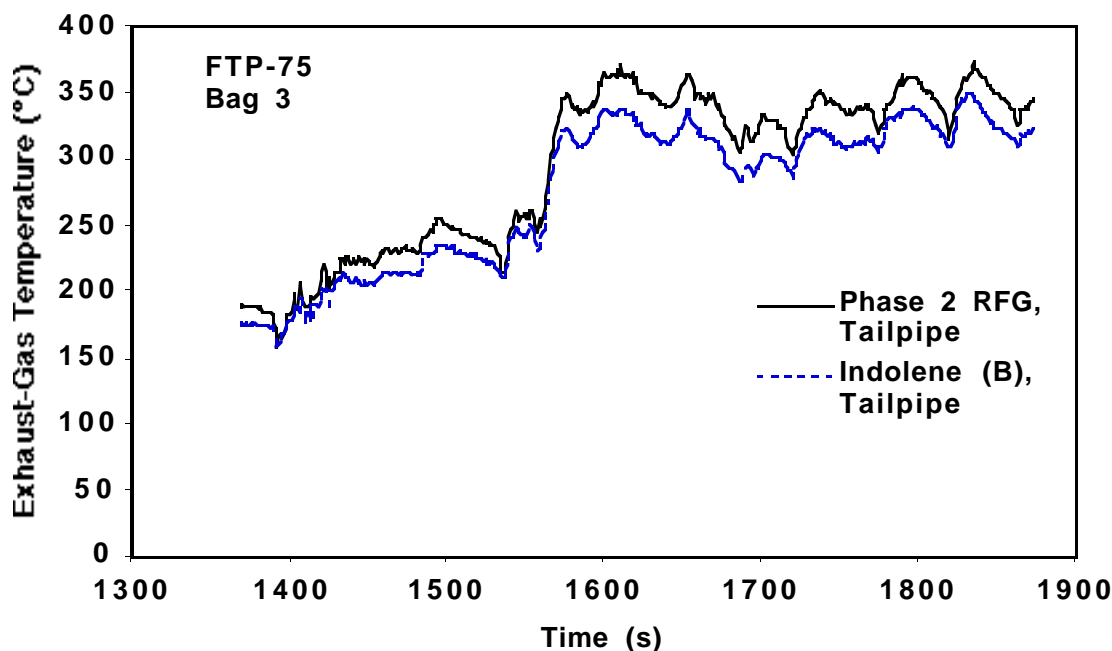
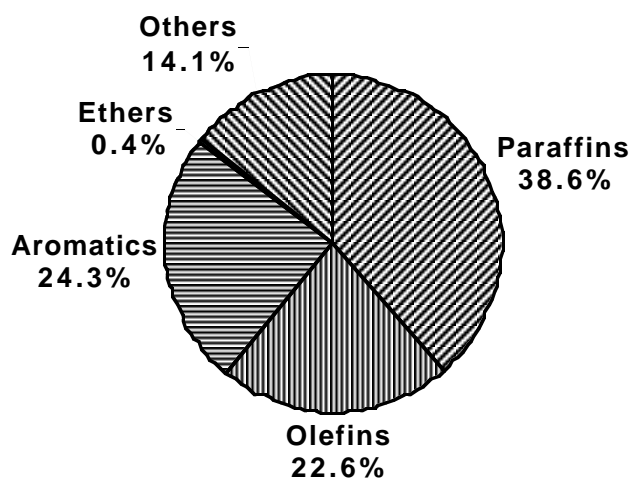
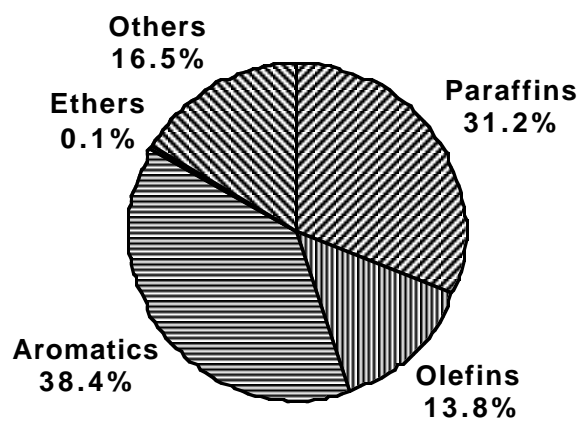


FIGURE 26 (Cont.)

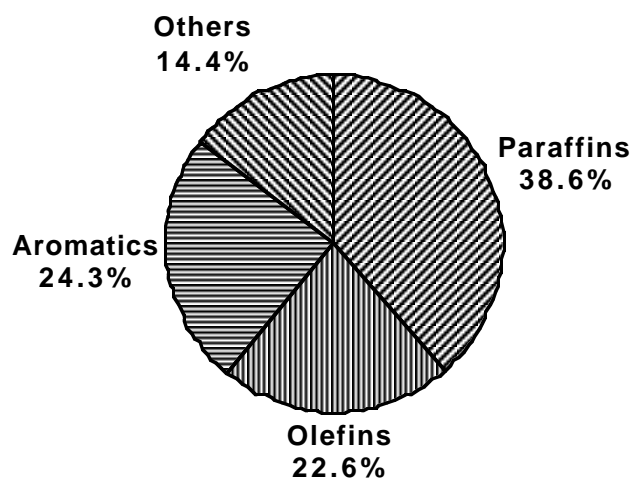
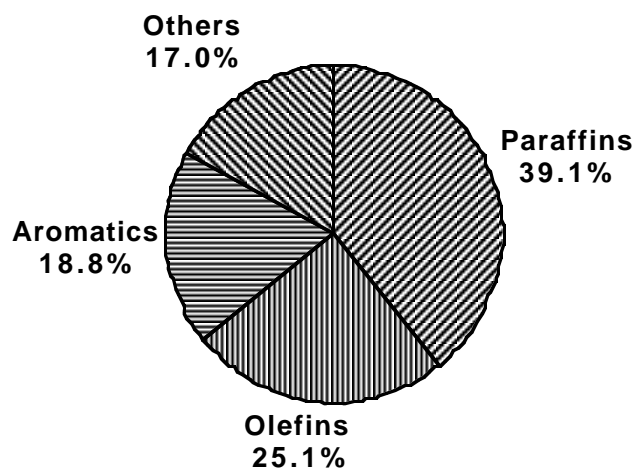
The tailpipe hydrocarbon composition for the SIDI vehicle is compared in Figure 28 for Indolene (A) and Ultimate. Although the Ultimate had more aromatics than the Indolene (A), 49.4% vs. 27.5%, its percentage of tailpipe aromatics was less, 18.8% vs. 24.3%. The reason is unknown. The low-sulfur fuel had the largest percentage of aromatics in its composition (63.9%), and its exhaust composition of 44.4% aromatics reflects this.

### 3.5 Ozone-Forming Potential

Ozone-forming potential, computed from the speciated emissions, is shown in Figure 29 for the SIDI vehicle running on three gasolines. Two effects dominate the results: (1) In Phase 1, the quantity of hydrocarbon emissions is inversely related to the Reid vapor pressure. The low-sulfur gasoline, which has a Reid vapor pressure of 7.92 psi, has the highest hydrocarbon emissions, and the Ultimate gasoline, which has a Reid vapor pressure of 12.62 psi, has relatively low hydrocarbon emissions. Reid vapor pressure is critical to hydrocarbon emissions during the cold-start period. The ozone-forming potential is closely related to the amount of hydrocarbons emitted. (2) In Phases 2 and 3, the ozone-forming potential is related to the amount of engine-out aromatics. The low-sulfur fuel, which has a high aromatic content, produces the highest quantity of engine-out aromatics. Indolene (A), with the lowest aromatic content, produces the lowest quantity of engine-out aromatics. Aromatics have high ozone-forming potentials.

**SIDI Tailpipe Weighted Average****PFI Tailpipe Weighted Average**

**FIGURE 27 Tailpipe Hydrocarbon Composition with Indolene (A)  
(SIDI, top; PFI, bottom)**

**SIDI, Indolene (A)****SIDI, Ultimate**

**FIGURE 28 Tailpipe Hydrocarbon Composition for Mitsubishi SIDI (Indolene (A), top; Ultimate, middle; low-sulfur, bottom)**

## SIDI, Low-Sulfur

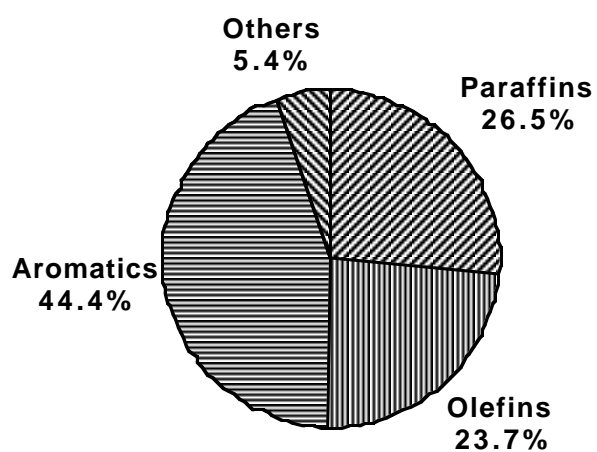


FIGURE 28 (Cont.)

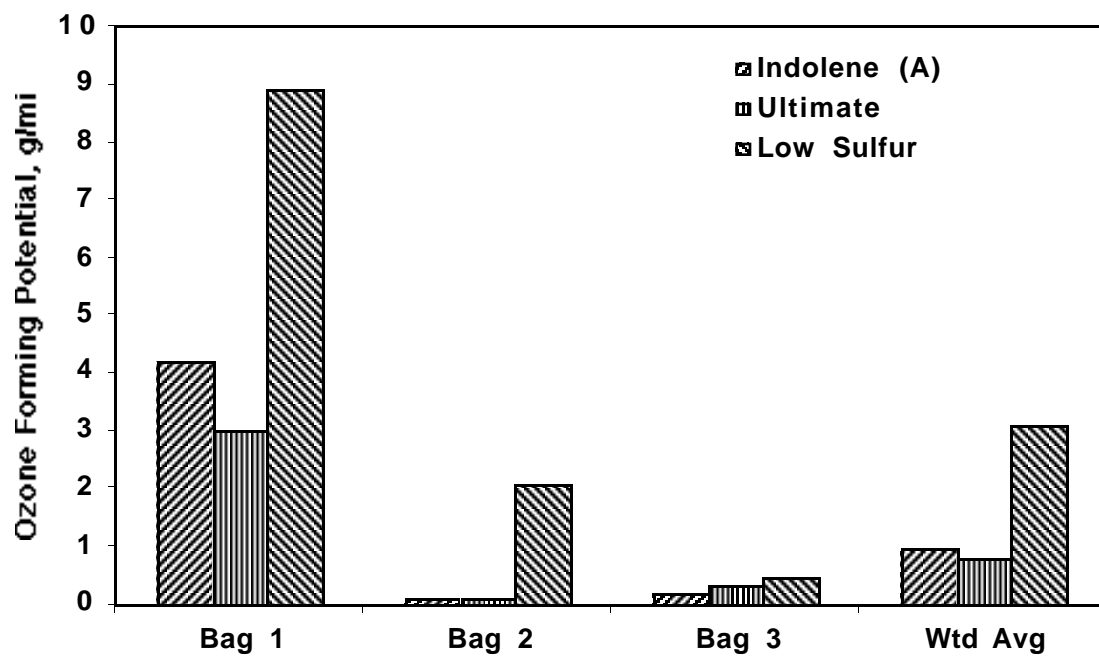
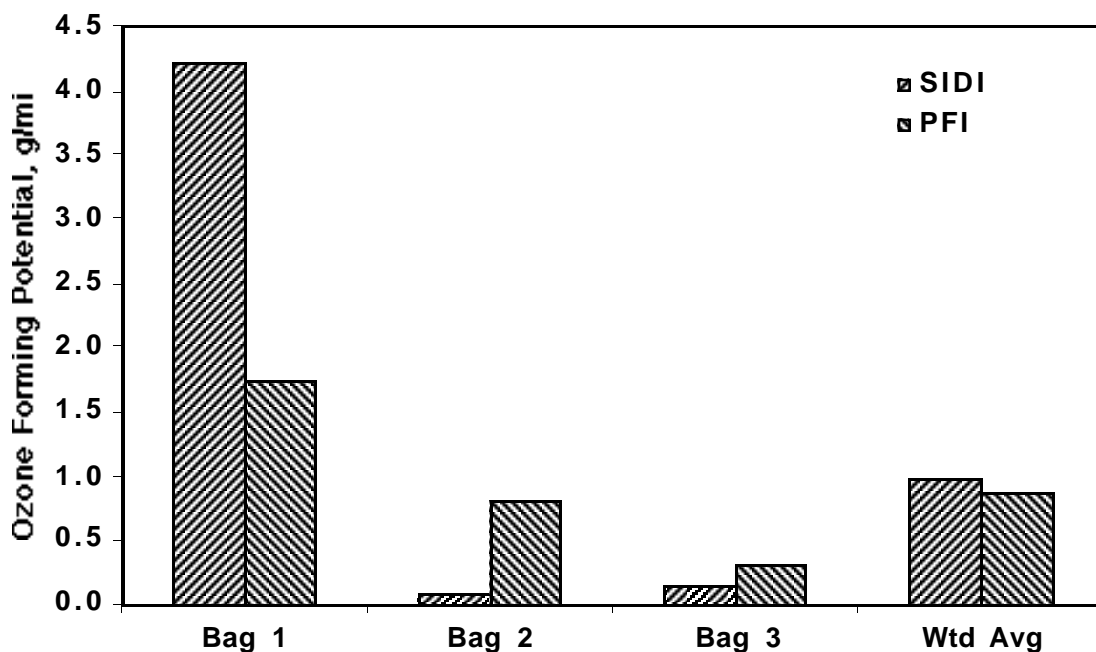


FIGURE 29 Comparison of Ozone-Forming Potential of Indolene (A), Ultimate, and Low-Sulfur Gasolines in SIDI Vehicle

Figure 30 compares the ozone-forming potential for the SIDI vehicle with that of the PFI vehicle. Both vehicles ran on Indolene (A). In Phase 1, the ozone-forming potential of the SIDI vehicle is 144% more than that of the PFI vehicle. The reasons are that (1) the SIDI engine emits more hydrocarbons than the PFI engine does and (2) the catalytic converter of the SIDI vehicle takes longer to warm up than the PFI catalytic converter does; thus, the SIDI vehicle emits more hydrocarbons at the tailpipe. (See Figure 10.) In Phases 2 and 3, both catalytic converters have warmed up. Although the SIDI vehicle emits more hydrocarbons in Phases 2 and 3 than the PFI vehicle does (see Figure 10), the tailpipe emissions of the PFI vehicle contain a higher percentage of aromatics than do those of the SIDI vehicle (see Figure 27). Because the aromatics have high ozone-forming potential, the ozone-forming potential for the PFI vehicle in Phases 2 and 3 is higher than that of the SIDI vehicle. Thus, the weighted-average ozone-forming potential for the SIDI vehicle is only 13% more than that of the PFI vehicle. If the SIDI catalytic converter had the same warm-up characteristics as the PFI catalytic converter, the SIDI vehicle's weighted-average ozone-forming potential would be reduced to 0.52 g/mi, which is 40% less than that of the PFI vehicle.



**FIGURE 30 Comparison of Ozone-Forming Potential of SIDI vs. PFI Vehicles**

### 3.6 Catalyst Efficiency

Catalytic converter efficiency for the three fuels in the SIDI vehicle is shown in Figures 31, 32, and 33 for Phases 1, 2, and 3, respectively. In Figure 31 (Phase 1), the THC and CO conversion efficiencies rise steeply at about 200 s. Before 200 s, there is considerable variation in the curves from one fuel to another, but after 200 s, all fuels follow similar curves. After warm-up is achieved (230 s), THC conversion efficiencies are as follows: Indolene, 94% with a standard deviation of 4.0 percentage points; Ultimate, 94% with a standard deviation of 3.8 percentage points; and low-sulfur fuel, 93% with a standard deviation of 5.0 percentage points. The CO conversion efficiencies are Indolene, 99% with a standard deviation of 2.7 percentage points; Ultimate, 98% with a standard deviation of 1.8 percentage points; and low-sulfur fuel, 98% with a standard deviation of 4.3 percentage points.

The NO<sub>x</sub>-conversion efficiencies show a less definite warm-up than the THC and CO efficiencies do. Before 200 s, there is considerable variation in the curves of the three fuels. After 230 s, efficiencies are generally higher than the earlier efficiencies, and there is less variation between the curves of the three fuels. However, the differences between the three fuels are greater than the differences between the fuels for the THC and CO curves. After 230 s, the NO<sub>x</sub>-conversion efficiencies are Indolene, 63% with a standard deviation of 20 percentage points; Ultimate, 65% with a standard deviation of 18.8 percentage points; and low-sulfur fuel, 73% with a standard deviation of 15.8 percentage points. The low-sulfur fuel has a higher NO<sub>x</sub>-conversion efficiency than the other fuels because its engine-out hydrocarbon emissions are higher than those of the other fuels, and its engine-out hydrocarbon emissions contain a relatively high percentage of aromatics. The aromatics in the lean NO<sub>x</sub> catalyst are particularly effective at reducing NO<sub>x</sub>.

Figure 32 shows the conversion efficiencies for Phase 2 for the three fuels. THC conversion efficiencies are Indolene, 98% with a standard deviation of 1.2 percentage points; Ultimate, 98% with a standard deviation of 0.7 percentage points; and low-sulfur fuel, 97% with a standard deviation of 1.7 percentage points. CO conversion efficiencies are Indolene, 99% with a standard deviation of 0.8 percentage points; Ultimate, 98% with a standard deviation of 1.1 percentage points; and low-sulfur fuel, 99% with a standard deviation of 1.8 percentage points. NO<sub>x</sub> conversion efficiencies are Indolene, 74% with a standard deviation of 11.3 percentage points; Ultimate, 75% with a standard deviation of 9.7 percentage points; and low-sulfur fuel, 83% with a standard deviation of 8.8 percentage points.

Catalyst conversion efficiencies for Phase 3 are shown in Figure 33. THC conversion efficiencies follow roughly the same curve for the three fuels, although the values for low-sulfur fuel dip lower than those for other fuels. Dips in THC efficiency are related to accelerations. THC conversion efficiencies are Indolene, 95% with a standard deviation of 3.9 percentage points; Ultimate, 95% with a standard deviation of 4.3 percentage points; and low-sulfur fuel, 94% with a standard deviation of 6.4 percentage points. CO conversion efficiencies are Indolene, 97% with a standard deviation of 5.4 percentage points; Ultimate, 94% with a standard deviation of 11.1 percentage points; and low-sulfur fuel, 93% with a standard deviation of 11.5 percentage points.

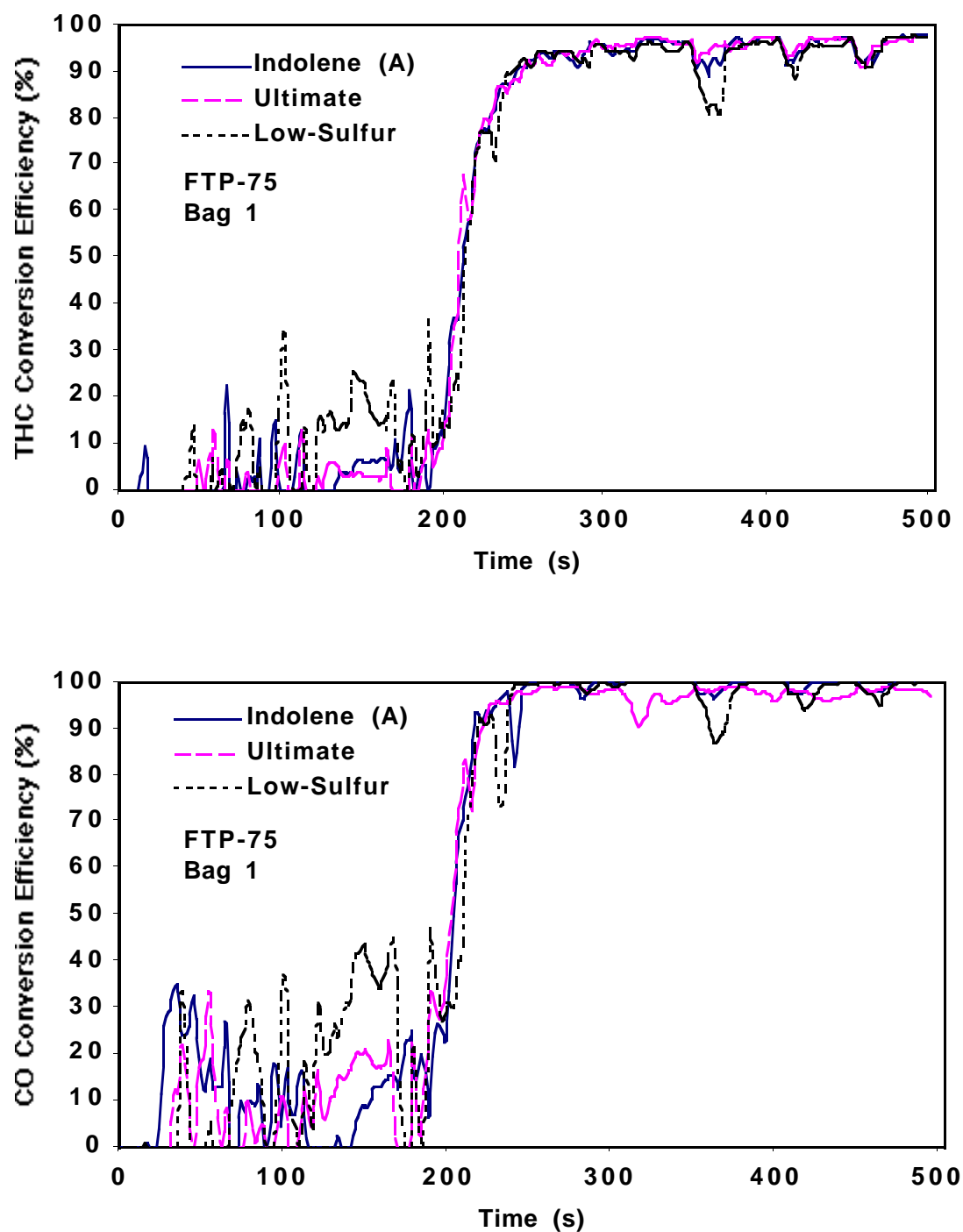
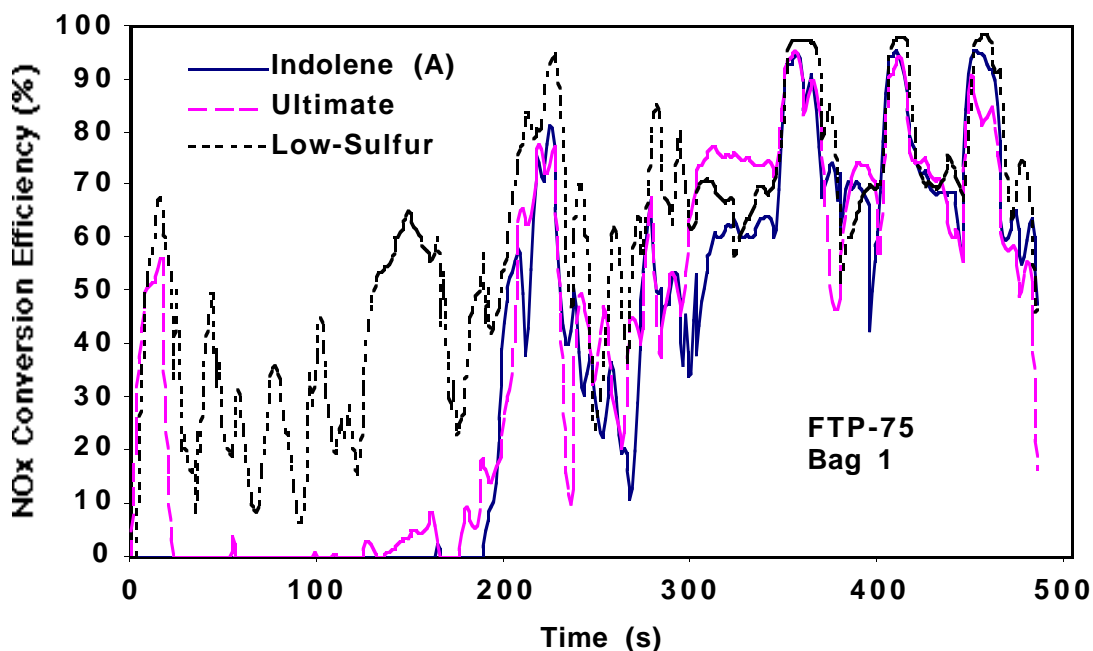


FIGURE 31 Catalyst Conversion Efficiencies for THC, CO, and NO<sub>x</sub> for Three Gasolines during First Phase of FTP (Bag 1)



**FIGURE 31 (Cont.)**

The  $\text{NO}_x$  conversion efficiencies are Indolene, 65% with a standard deviation of 17.1 percentage points; Ultimate, 70% with a standard deviation of 16.3 percentage points; and low-sulfur fuel, 72% with a standard deviation of 19.0 percentage points. Accelerations cause dips in the conversion efficiencies. Another reason for the variation in efficiencies (indicated by the large standard deviations) is that the lean  $\text{NO}_x$  catalyst is ineffective whenever the exhaust contains a substantial amount of oxygen. An example of this condition is the period of  $\text{NO}_x$  conversion efficiency of less than 50% between 1625 and 1650 s in bag 3, which corresponds to the highest speed (approximately 57 mph). During this period, engine-out  $\text{NO}_x$  emissions are relatively high, as shown in Figure 20. The engine operates in the stratified-charge mode, and the exhaust contains unconsumed oxygen. Such a condition makes chemical reduction of  $\text{NO}_x$  difficult.

Catalyst conversion efficiencies for the two vehicles are compared in Figures 34, 35, and 36 for Phases 1, 2, and 3, respectively. Both vehicles ran on Indolene. Figure 34 shows the catalyst warm-up characteristics of the two vehicles. The PFI catalyst begins to warm up at about 60 s after startup, while the SIDI catalyst requires about 200 s. The PFI catalyst is connected directly to the outlet of the exhaust manifold, but the SIDI catalyst is under the floor of the vehicle. After the catalyst has fully warmed up (80 s for the PFI catalyst and 230 s for the SIDI catalyst), the average THC conversion efficiency of the SIDI vehicle is 94% with a standard deviation 4.0 percentage points, while that of the PFI vehicle is 86% with a standard deviation of 10.6 percentage points. The average CO conversion efficiency after warm-up of the SIDI vehicle is 99% with a standard deviation of 2.7 percentage points, while that of the PFI vehicle is 86% with a standard deviation of 11.6 percentage points. The SIDI vehicle can achieve higher



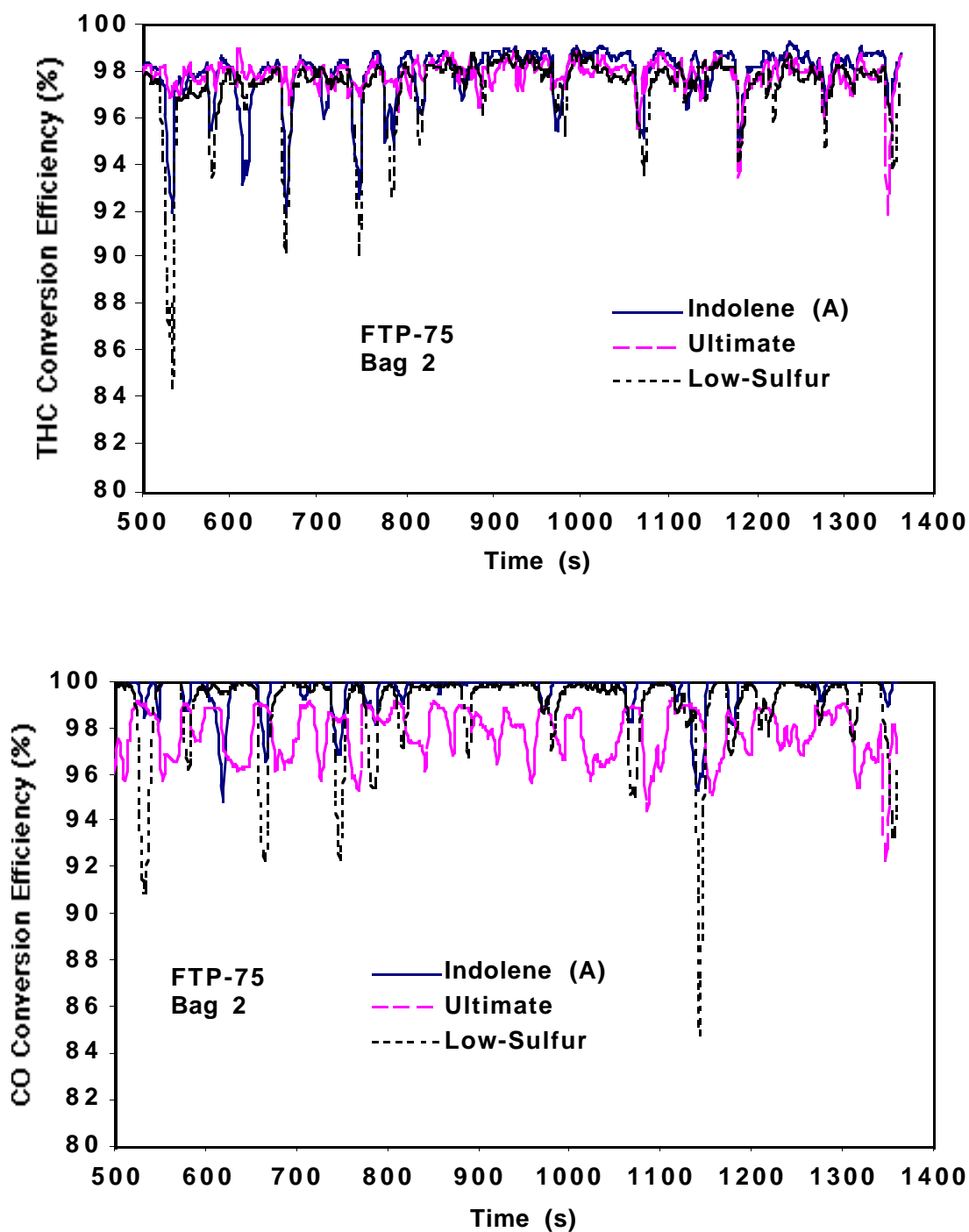
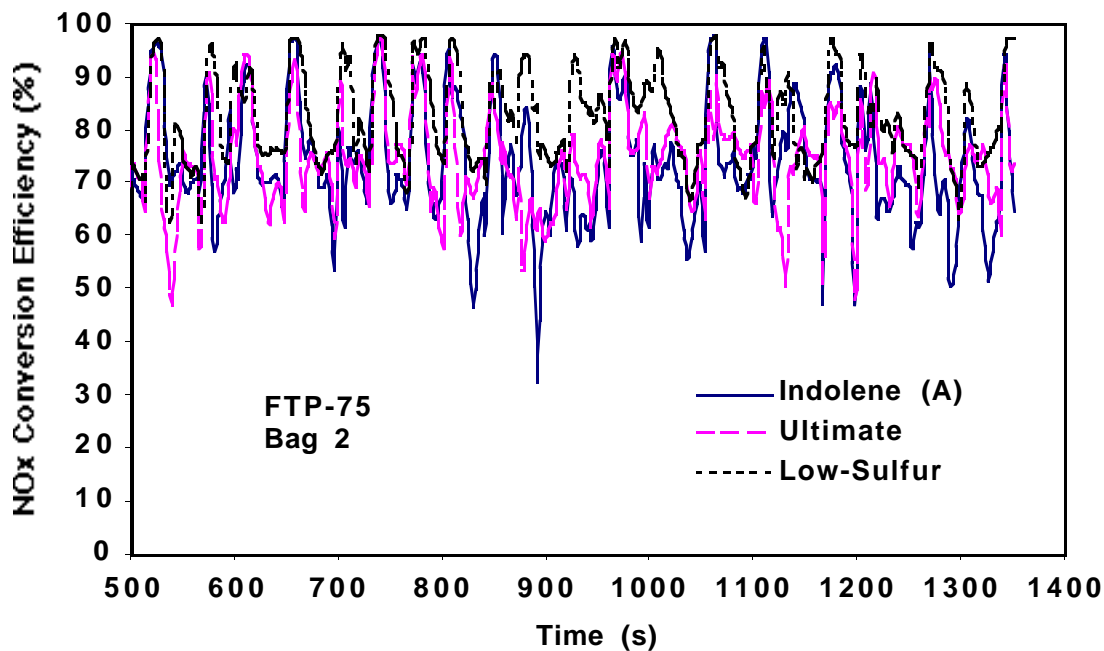


FIGURE 32 Catalyst Conversion Efficiencies for THC, CO, and NO<sub>x</sub> for Three Gasolines during Second Phase of FTP (Bag 2)



**FIGURE 32 (Cont.)**

conversion efficiencies for THC and CO than the PFI vehicle can because the exhaust of the former contains more oxygen.

Warm-up characteristics for the  $\text{NO}_x$  conversion catalyst are similar to those for the THC and CO catalyst; the PFI vehicle requires about 60 s to warm up, while the SIDI vehicle requires about 200 s. After warm-up, the PFI vehicle achieves  $\text{NO}_x$  conversion efficiencies of 86% with standard deviation of 13.2 percentage points, while the SIDI vehicle achieves 63% with a standard deviation of 20 percentage points. In both cases, dips in the conversion efficiency suggest that the catalyst is overwhelmed by  $\text{NO}_x$  during hard accelerations. The SIDI vehicle has a lower  $\text{NO}_x$  conversion efficiency because the excess oxygen in the exhaust works against the chemical reduction of the nitrogen oxides.

Figure 35 shows the catalytic conversion efficiencies for Phase 2 of the FTP. The average THC conversion efficiency for the SIDI vehicle is 98% with a standard deviation of 1.2 percentage points, while that for the PFI vehicle is 90% with a standard deviation of 2.9 percentage points. The average CO conversion efficiency for the SIDI vehicle is 99% with a standard deviation of 0.8 percentage points, while that for the PFI vehicle is about 95% with a standard deviation of 6.0 percentage points. Dips in the conversion efficiencies correspond to accelerations. The higher oxygen content of the SIDI exhaust favors more efficient oxidation of hydrocarbons and carbon monoxide.

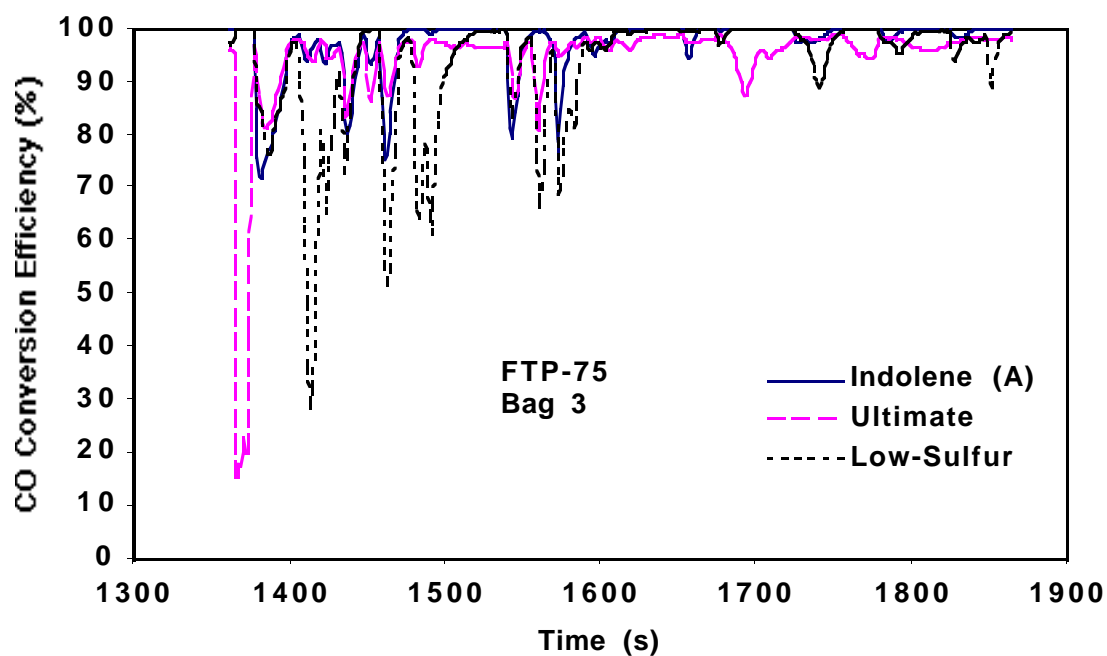
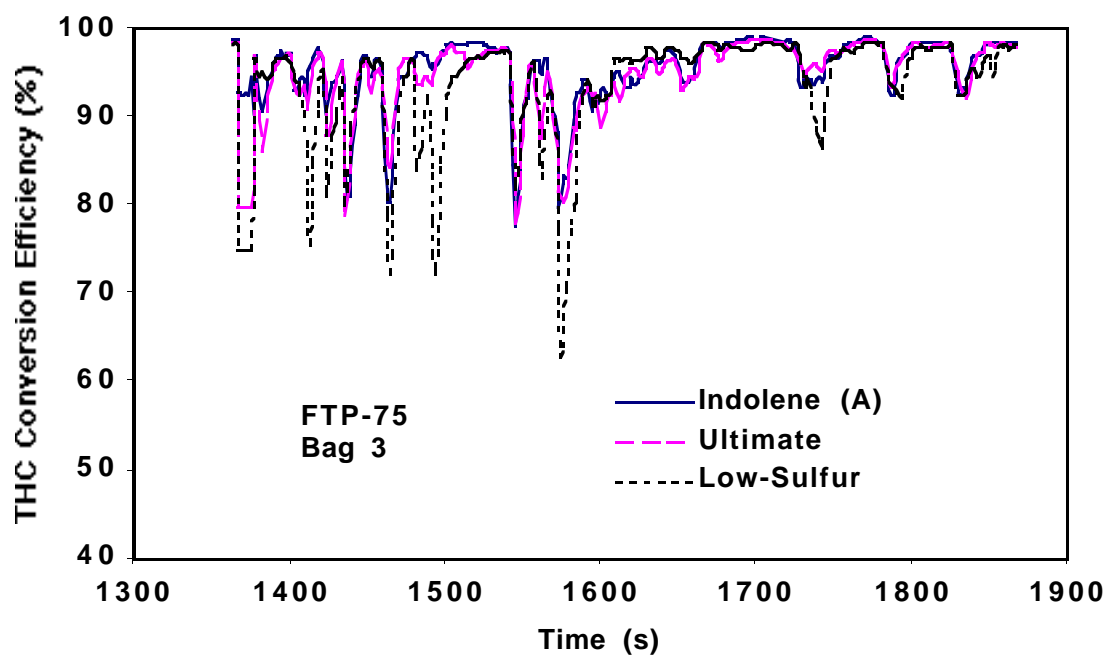
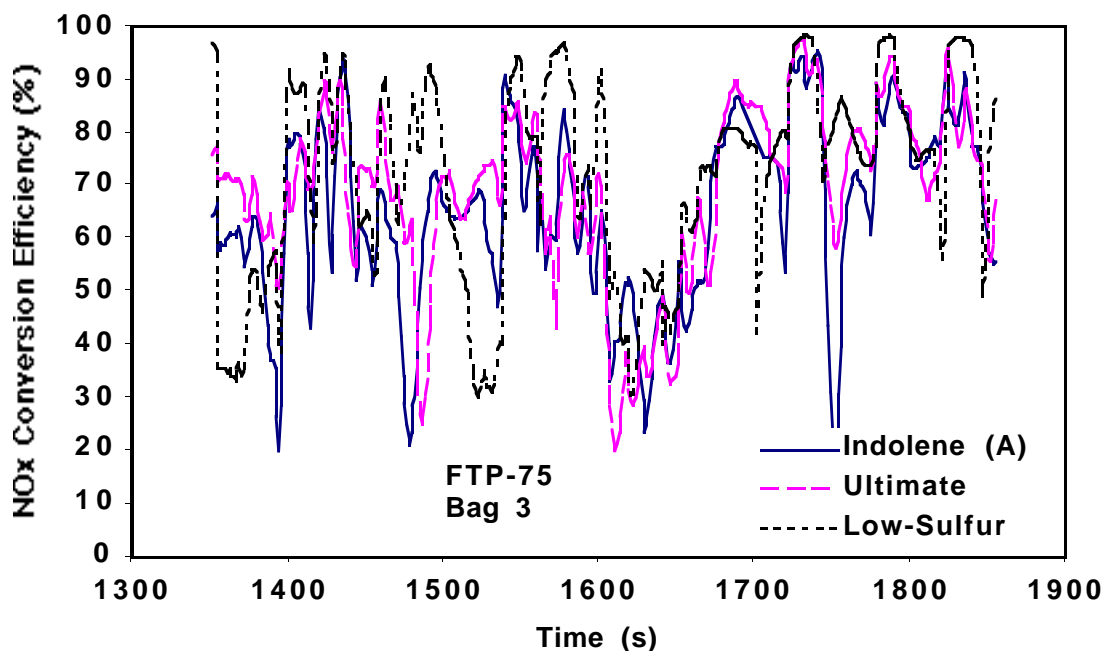


FIGURE 33 Catalyst Conversion Efficiencies for THC, CO, and NO<sub>x</sub> for Three Gasolines during Third Phase of FTP (Bag 3)



**FIGURE 33 (Cont.)**

The average  $\text{NO}_x$  conversion efficiency for the SIDI vehicle is 74% with a standard deviation of 11.3 percentage points, while that for the PFI vehicle is 89% with a standard deviation of 8.5 percentage points. Dips in the conversion efficiency correspond to accelerations. The higher oxygen content of the SIDI exhaust makes chemical reduction of nitrogen oxides more difficult.

Catalytic conversion efficiencies for Phase 3 of the FTP are shown in Figure 36. The average THC conversion efficiency for the SIDI vehicle is 95% with a standard deviation of 3.9 percentage points, while that for the PFI vehicle is 88% with a standard deviation of 13.3 percentage points. The average CO conversion efficiency for the SIDI vehicle is 97% with a standard deviation of 5.4 percentage points, while that for the PFI vehicle is 90% with a standard deviation of 16.2 percentage points. Dips in conversion efficiency correspond to accelerations. This is particularly severe in the CO conversion efficiency for the PFI vehicle. The PFI catalyst appears to have cooled off during the 10-minute soak between Phases 2 and 3 while the SIDI catalyst retained its heat. This is believed to be the reason for low THC, CO, and  $\text{NO}_x$  conversion efficiencies for the PFI catalyst at the beginning of this phase of the test.

The average  $\text{NO}_x$  conversion efficiency of the SIDI vehicle is 65% with a standard deviation of 17.1 percentage points, while that of the PFI vehicle is 82% with a standard deviation of 22 percentage points. As above, dips in conversion efficiency correspond to accelerations. A dip in SIDI  $\text{NO}_x$  conversion efficiency corresponds to the high-speed part of this phase (speeds of 50 mph or more between 1589 and 1662 s). This was described in the discussion of Figure 33.

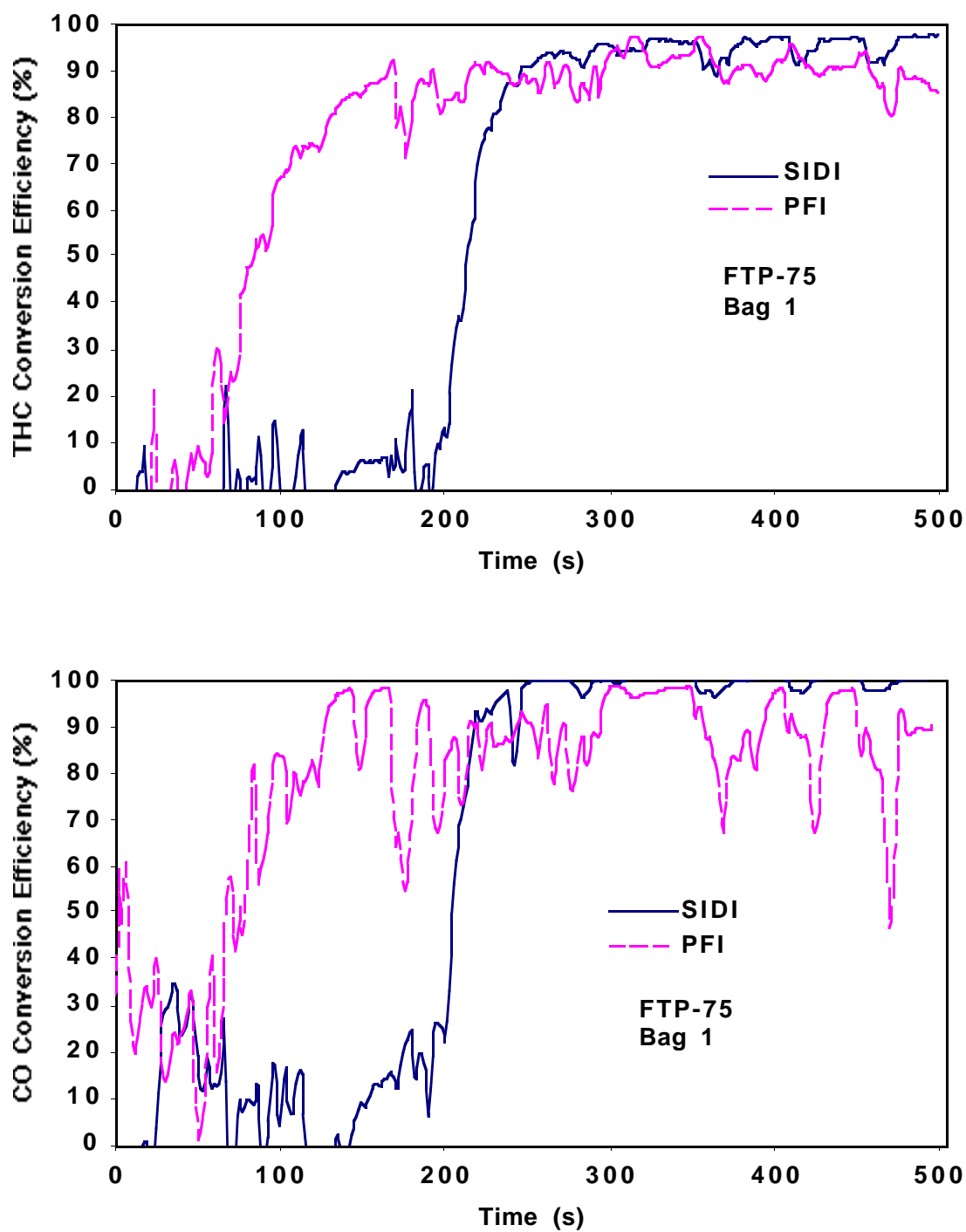


**FIGURE 34 Catalyst Conversion Efficiencies for THC, CO, and NO<sub>x</sub> during First Phase of FTP (Bag 1)**

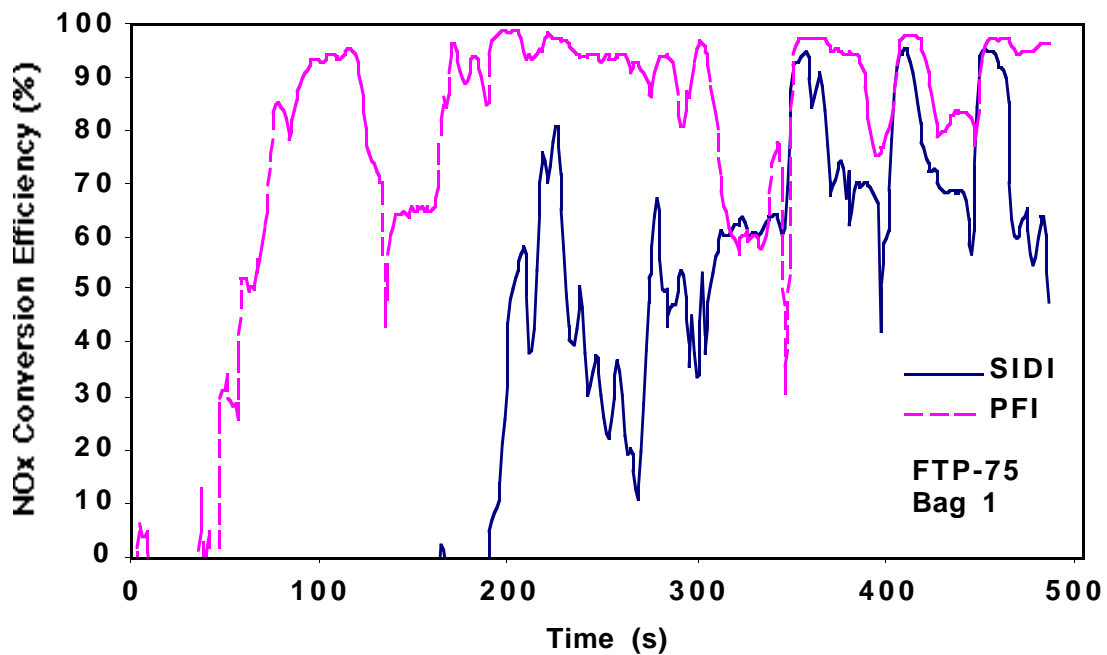


**FIGURE 34 (Cont.)**

Catalytic converter inlet temperatures during Phase 1 of the FTP are shown in Figure 37. The temperature profiles of the two vehicles are similar, except that the temperatures of the PFI converter are about 200 K hotter than those of the SIDI converter. A 650-K line drawn on the graph intersects the PFI temperature curve at 60 s and the SIDI temperature curve at 200 s. Since these times correspond to the warm-up of the catalyst, as shown in Figure 34, 650 K is the temperature required to activate the catalyst. Figure 37 also illustrates the effect on catalyst temperature of a close-coupled catalyst (PFI vehicle) vs. an under-the-floor catalyst (SIDI vehicle).

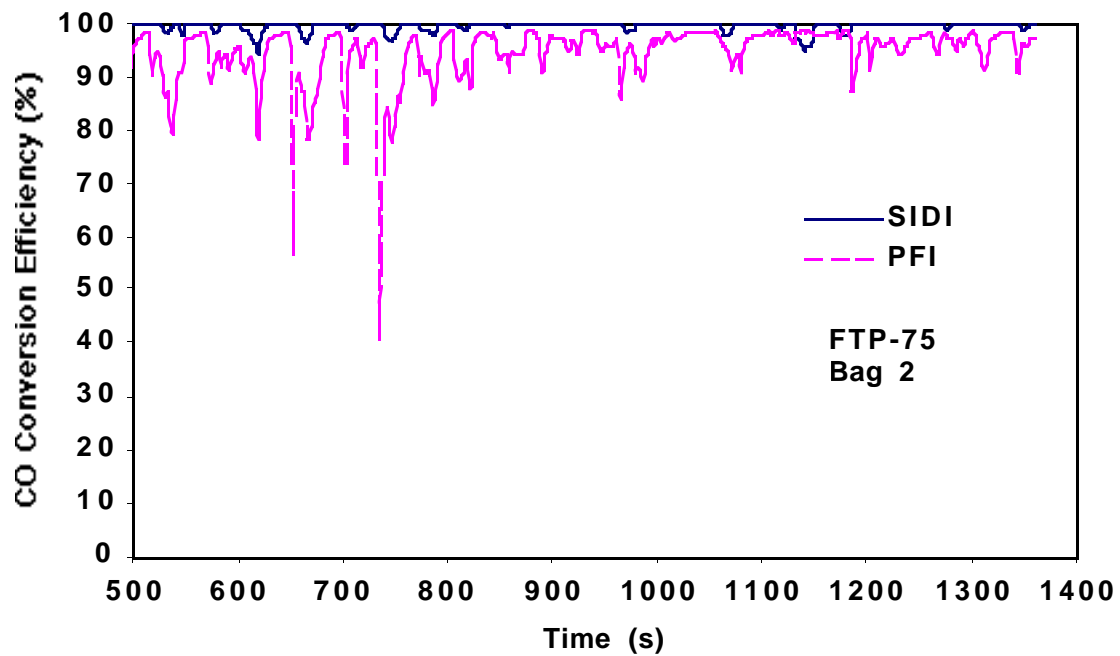
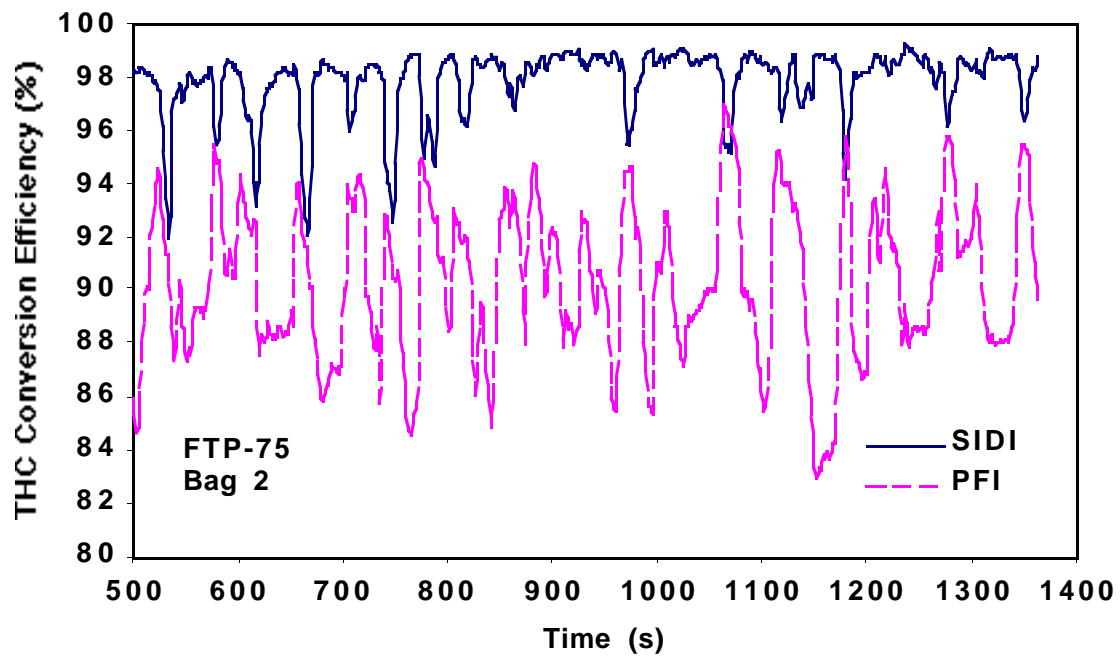


FIGURE 35 Catalyst Conversion Efficiencies for THC, CO, and NO<sub>x</sub> during Second Phase of FTP (Bag 2)

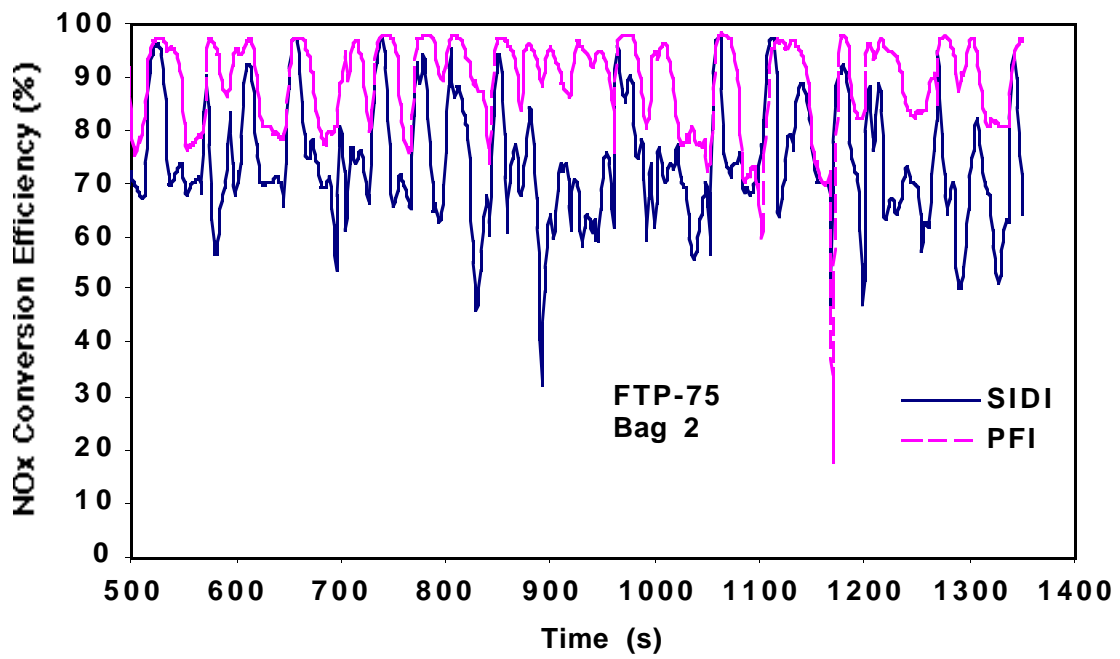


FIGURE 35 (Cont.)



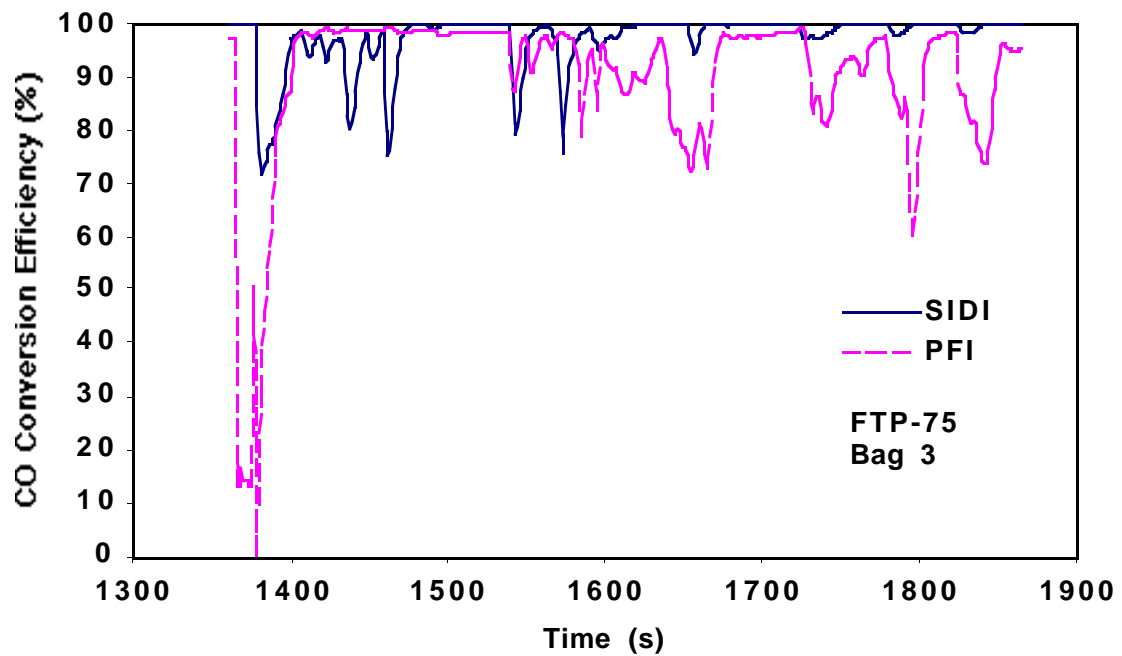
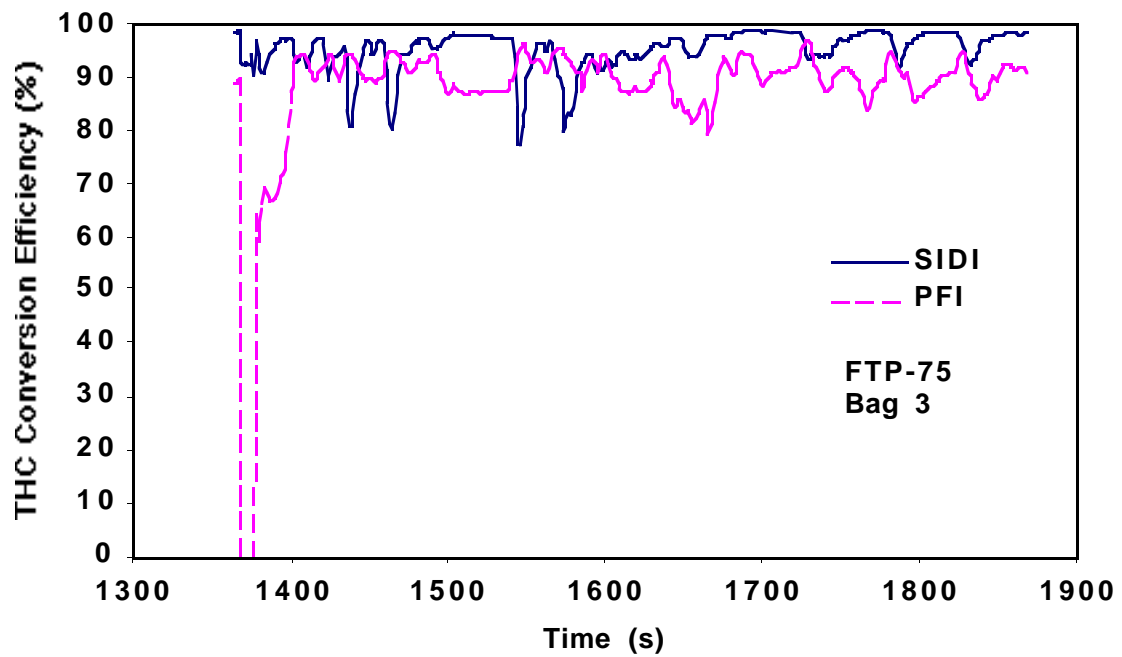


FIGURE 36 Catalyst Conversion Efficiencies for THC, CO, and NO<sub>x</sub> during Third Phase of FTP (Bag 3)

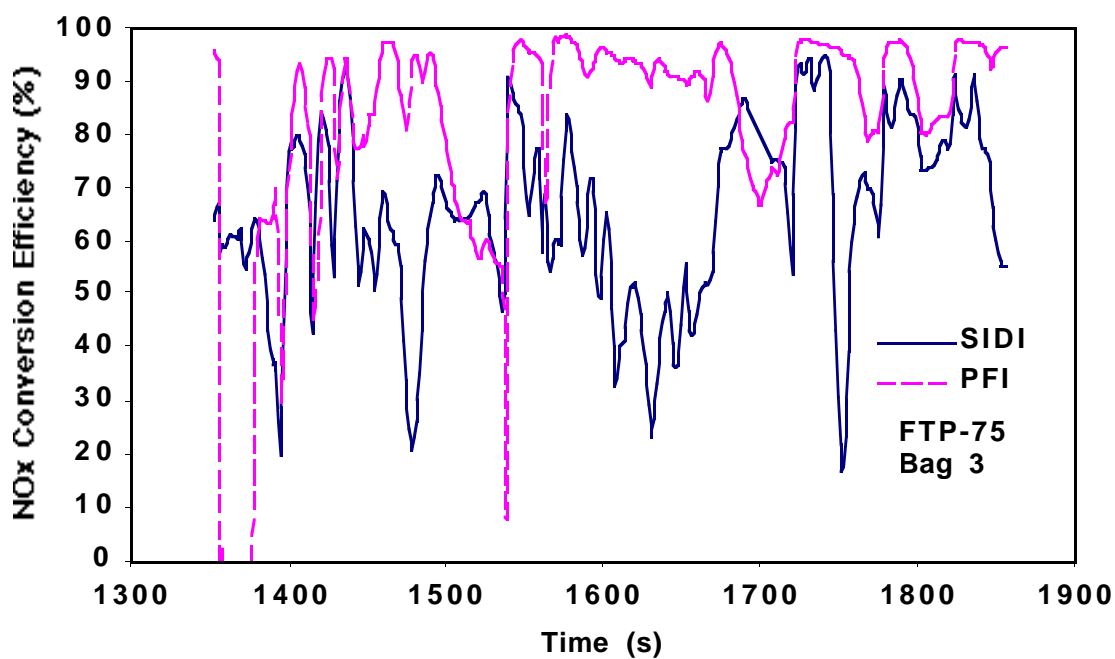


FIGURE 36 (Cont.)

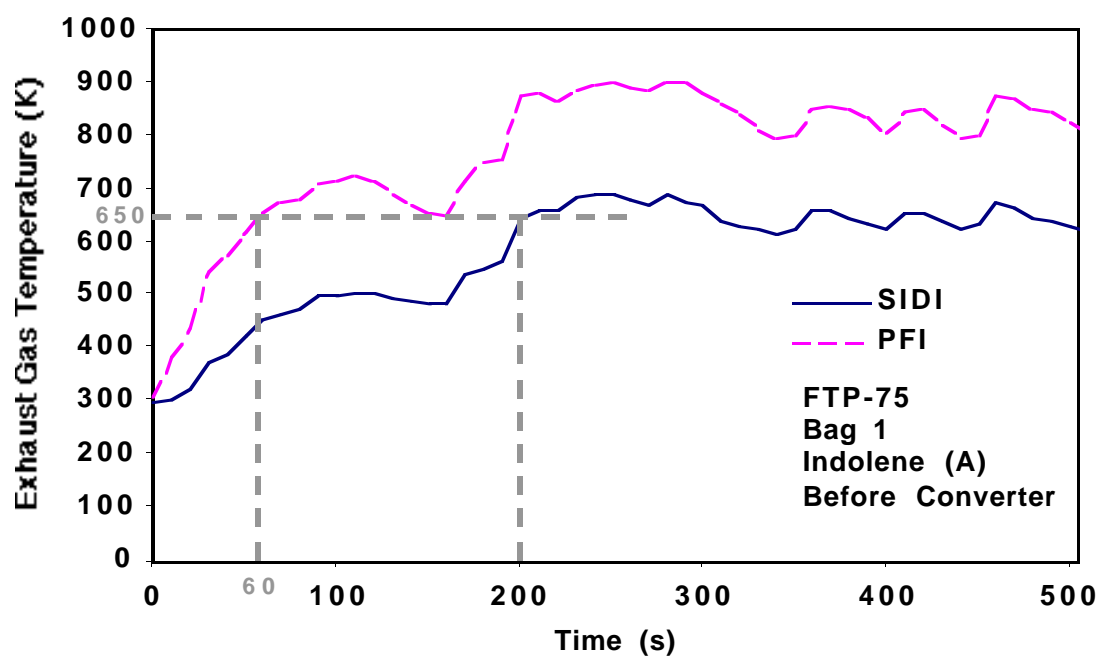


FIGURE 37 Converter Inlet Temperatures during First Phase of FTP (Bag 1)

## 4 Conclusions

### 4.1 Fundamental Conclusions

SIDI vehicles exhibit higher fuel economy and lower greenhouse-gas emissions than PFI vehicles do. How SIDI vehicles compare with CIDI vehicles will be determined by future tests.

SIDI engines emit more unburned hydrocarbons than PFI engines do. Catalytic oxidation of the hydrocarbons is aided by the excess oxygen in the exhaust. Thus, it may be possible to design a catalyst system that will meet the PNGV goals for hydrocarbons.

SIDI engines emit less carbon monoxide than PFI engines do. The SIDI vehicle with its current catalyst system meets the PNGV goal for carbon monoxide emissions.

SIDI engines emit more  $\text{NO}_x$  than PFI vehicles do. Catalytic reduction of  $\text{NO}_x$  by the selective-reduction catalyst is inhibited by the oxygen in the exhaust. This is a significant challenge that must be overcome before the PNGV goals can be met. However, the  $\text{NO}_x$  catalyst is reasonably effective when the engine operates in the homogeneous-charge mode. The similar challenge facing CIDI engines may prove more difficult, because the CIDI engine cannot operate in a homogeneous-charge mode.

SIDI engines emit measurable amounts of particulate matter. The PNGV goal for PM can be met if the SIDI vehicle employs an oxidation catalyst and if a low-sulfur fuel, such as RFG, is used. How SIDI vehicles compare with CIDI vehicles in this respect will be determined by future tests, but the CIDI engine is expected to have greater difficulty in meeting the PNGV goal for PM.

The mechanisms of mixture formation for both the stratified-charge and the homogeneous-charge modes are not well understood. Is it desirable to avoid fuel impingement on the piston? How can fuel impingement on the piston and cylinder walls be avoided? How does the boiling curve of the fuel affect mixture formation? How can excessively rich mixtures in the core of the stratified charge and excessively lean mixtures at the fringes be avoided? What types of fuel injectors form the best mixture?

In-cylinder air motion, which is closely related to mixture formation, is also not well understood. In-cylinder air motions influence how the air-fuel mixture forms and is transported to the spark plug. How much turbulence is necessary?

## 4.2 Fuel Economy and Greenhouse Gas Emissions

One of the main reasons for investigating the SIDI engine for use in PNGV vehicles is fuel economy. The PNGV goal is to achieve up to 80 mpg in a family-sized car. The five-passenger Mitsubishi station wagon with its SIDI engine achieved up to 53 mpg in the highway fuel economy cycle and up to 34 mpg in the FTP. The wagon's fuel economy was up to 24% better than that of the PFI vehicle, although the latter is smaller.

The SIDI engine achieves its high fuel economy by eliminating most of the pumping losses associated with throttling the intake manifold. The Mitsubishi engineers have chosen not to completely eliminate the intake throttle; such elimination would imply that the air/fuel ratio could exceed 50:1 under light loads. Instead, they have limited the air/fuel ratio to a maximum of about 30:1, according to their published papers. This achieves most of the fuel economy benefit and makes engine control easier. In our measurements, we found that air/fuel ratios of about 24:1 were typical in the stratified-charge mode. Another factor in the high fuel economy of the engine is its unusually high 12.0:1 compression ratio.

Greenhouse gas ( $\text{CO}_2$ ) emissions are proportional to the amount of fuel burned. Thus, the high fuel economy of the SIDI engine implies greenhouse gas emissions as much as 25% lower than those of the PFI engine.

## 4.3 Mass Emissions

The Mitsubishi was designed to meet Japanese emissions standards, which differ considerably from those of the U.S. FTP. The Japanese test consists of steady-state measurements with a warm engine, while the FTP consists entirely of transients that begin with a cold engine. Consequently, the failure of the Mitsubishi to meet both the current U.S. emissions standards and the PNGV goals is not surprising. Another difference is that Japanese gasolines are limited to 30 ppm sulfur content, while U.S. fuels have no limitations on sulfur content (except in California). The limited sulfur content of the Japanese fuel allows Mitsubishi more flexibility in the choice of catalyst. Sulfur content also affects particulate emissions, which are not regulated for gasoline vehicles in Japan but are included in the PNGV goals. In contrast, the Neon meets both the current U.S. emissions regulations and the PNGV goals.

The Mitsubishi running on Indolene (A) emits 2.8 times the PNGV goal for NMHC (0.125 g/mi) and 3.5 times the PNGV goal for  $\text{NO}_x$  (0.2 g/mi). However, it easily meets the PNGV goal for CO emissions (1.7 g/mi). The two main reasons for the failure to meet the PNGV goals for hydrocarbons and  $\text{NO}_x$  are that (1) the engine emits more hydrocarbons and  $\text{NO}_x$  than an optimized PFI engine does, and (2) the catalytic converter takes too long to warm up. The vehicle's ability to meet the PNGV goal for particulate matter is conditional on having an oxidation catalyst and a low-sulfur fuel.

The SIDI engine emits more unburned hydrocarbons than does the PFI engine because the former operates in a stratified-charge mode much of the time. Gradients of air/fuel ratio ranging from very lean to very rich exist throughout the combustion chamber. Both the rich and the lean ends of the gradient give rise to unburned hydrocarbons. Another source of hydrocarbon emissions is fuel-spray impingement on the piston and, possibly, the cylinder walls. Flames are quenched by the surfaces, so fuel on or near those surfaces does not participate in combustion. This effect is particularly severe if the fuel enters the crevice between the piston and the cylinder wall. The volatility of the fuel affects piston wetting. The relationship between fuel volatility and hydrocarbon emissions also appears to be affected by aromatic content of the fuel. Premium Ultimate, which had the highest volatility of the gasolines tested (Reid vapor pressure (RVP) of 12.62 psi) and relatively high aromatic content (50.2%), had low hydrocarbon emissions; the low-sulfur fuel, which had low volatility (RVP of 7.92 psi) and high aromatic content (63.9%), had the highest hydrocarbon emissions. However, RFG, which had lower volatility (RVP of 6.9 psi) than the low-sulfur fuel and low aromatic content (27.2%), had the lowest hydrocarbon emissions. Thus, a high aromatic content can be tolerated if the fuel volatility is high, but a low-volatility fuel requires a low aromatic content. The PFI engine, in contrast, has a homogeneous fuel-air mixture that is optimized by the engine control unit to give low engine-out hydrocarbon emissions.

The SIDI engine also emits more  $\text{NO}_x$  than the PFI engine does, for two reasons. In the stratified-charge mode, the gradients of air/fuel ratio include some nearly stoichiometric regions where the flame temperature will be near the maximum. The high flame temperature favors  $\text{NO}_x$  formation. The 12.0:1 compression ratio, which favors good fuel economy, also favors  $\text{NO}_x$  formation. At the same time, the oxygen content of the exhaust in the stratified-charge mode inhibits catalytic reduction of  $\text{NO}_x$  by the selective-reduction catalyst. A  $\text{NO}_x$ -trap catalyst might provide better  $\text{NO}_x$  reduction, but periodic excursions into homogeneous-charge mode to regenerate the catalyst would penalize fuel economy. In addition,  $\text{NO}_x$ -trap catalysts are sensitive to sulfur poisoning. Thus, the engine designer is faced with a dilemma: Features that favor fuel economy also favor  $\text{NO}_x$  production.

Tailpipe  $\text{NO}_x$  emissions are affected by the aromatic content of the fuel and by the oxygen content of the exhaust. The low-sulfur fuel, which emits more engine-out aromatics than the other fuels, emits significantly less tailpipe  $\text{NO}_x$  than the other fuels do. Unburned aromatics reduce  $\text{NO}_x$  in the catalytic converter more effectively than do short-chain paraffins. The excess oxygen in the exhaust of the SIDI engine makes chemical reduction of nitrogen oxides more difficult than is the case with the PFI engine. The overall  $\text{NO}_x$  conversion efficiency for the SIDI vehicle is 68%, compared to 96% for the PFI vehicle.

The catalytic converter of the Neon requires about 60 s to warm up, while that of the Mitsubishi requires about 200 s. If the Mitsubishi catalytic converter warmed up in 60 s instead of 200 s, the weighted-average hydrocarbon emissions could be decreased by about 36%, the weighted-average CO emissions could be decreased by about 38%, and the weighted-average  $\text{NO}_x$  emissions could be decreased by about 16%. This change alone would decrease the NMHC emissions from 2.8 times the PNGV goal to 1.8 times the PNGV goal. Similarly, a faster warm-up would decrease  $\text{NO}_x$  emissions from 3.5 times the PNGV goal to 3 times the PNGV goal. With

other modifications, the vehicle might be able to meet the PNGV emissions goals. Meeting the  $\text{NO}_x$  emissions goal will be more difficult than meeting the hydrocarbon emissions goal.

Particulate mass, as measured at present, consists primarily of three components: solid particles, absorbed hydrocarbons, and condensed sulfuric acid. An oxidation catalyst can remove a significant fraction of the unburned hydrocarbons from the exhaust stream and prevent their being absorbed by the solid particles. Low-sulfur fuel produces less sulfur trioxide, which hydrolizes to form sulfuric acid. The use of both an oxidation catalyst and low-sulfur fuel may be necessary to meet the PNGV goal for particulate mass emissions.

#### 4.4 Second-by-Second Emissions

Engine-out emission peaks generally correspond to accelerations in second-by-second measurements. Peaks of THC and  $\text{NO}_x$  are generally higher for the SIDI engine than for the PFI engine because (1) gradients of air/fuel ratio in the SIDI engine have regions of high THC and  $\text{NO}_x$  formation; (2) a 12.0:1 compression ratio for the SIDI engine vs. a 9.8:1 compression ratio for the PFI engine gives higher combustion temperatures, hence increased  $\text{NO}_x$  formation; and (3) there is less intake-manifold throttling in the SIDI engine, which leads to higher cylinder pressures and temperatures in the SIDI engine compared to the PFI engine. In the first 120 s of operation,  $\text{NO}_x$  peaks are higher for the PFI engine than for the SIDI engine because the cold-start enrichment of the PFI engine provides less accurate control of the air/fuel ratio. Peaks of CO are generally lower for the SIDI engine than for the PFI engine because the preferred operating mode for the PFI engine is slightly leaner than stoichiometric ( $\lambda > 1$ ).

The catalyst in the SIDI vehicle requires about 200 s to warm up, compared to about 60 s for the catalyst in the PFI vehicle. Locating the SIDI catalytic converter under the floor vs. locating the PFI catalytic converter near the exhaust manifold is mainly responsible for the difference in warm-up time. Because the SIDI catalyst is located farther from the engine, it operates about 20°C cooler than the PFI catalyst does. This may have been done to protect the selective-reduction  $\text{NO}_x$  catalyst from excessive temperature. The SIDI engine operates in the homogeneous-charge mode for the entire 200 s of the warm-up period. If the SIDI catalyst warm-up time could be reduced from 200 s to 60 s without affecting other catalyst characteristics,  $\text{NO}_x$  emissions in the FTP cycle might be reduced by 21%. This would not be sufficient, by itself, to meet the PNGV  $\text{NO}_x$  goal of 0.2 g/mi.

After the SIDI catalyst has warmed up, conversion of THC and CO in the oxidizing exhaust of the stratified-charge mode is effective. Peaks in THC and CO emissions occur when the engine reverts to homogeneous-charge mode during accelerations.  $\text{NO}_x$  conversion is less effective in the stratified-charge mode because of the oxidizing exhaust. This is especially true during high speed cruising (for example, the 56-mph cruise between the 1589- and 1639-s marks in Phase 3 of the FTP), where the engine operates in stratified-charge mode.

The oxygen traces show that the SIDI engine operates in the homogeneous-charge mode during (1) the first 200 s of a cold start and (2) strong accelerations. It operates in the stratified-charge mode during (1) idle, (2) cruising, and (3) decelerations.

#### **4.5 Hydrocarbon Speciation**

The catalyst in the SIDI vehicle appears to destroy aromatic compounds more effectively than the catalyst in the PFI vehicle does. Evidence of aromatic destruction is seen in the tailpipe olefin content of the exhaust, which is a higher percentage of the exhaust with the SIDI vehicle than with the PFI vehicle. Although the PFI vehicle has a higher percentage of aromatics in its exhaust compared to the SIDI vehicle, the absolute quantity of aromatics is less with the PFI vehicle. The top 20 exhaust species for each engine-out and tailpipe condition and for each fuel are shown in the Appendix

#### **4.6 Ozone-Forming Potential**

Ozone-forming potential is primarily a function of fuel volatility and aromatic content. During Phase 1 of the FTP, the fuel with the highest volatility in the SIDI engine will tend to have the lowest ozone-forming potential. During Phases 2 and 3, when the engine is warm, the aromatic content of the fuel becomes important. The fuel with high aromatic content will have high ozone-forming potential. As noted above, the low-sulfur fuel has tailpipe  $\text{NO}_x$  emissions that are 40% less than those of Indolene (A). Thus, there is a trade-off between ozone-forming potential and  $\text{NO}_x$  emissions.

The SIDI catalyst is more effective at oxidizing aromatics than the PFI catalyst is. This can be seen in Figure 30 for bags 2 and 3. The slow catalyst warm-up of the SIDI vehicle causes it to have a higher ozone-forming potential than the PFI vehicle for bag 1 and the weighted average have.

#### **4.7 Catalyst Efficiency and Warm-Up Time**

The under-the-floor catalyst of the SIDI vehicle requires 200 s to warm up, compared to 60 s for the close-coupled catalyst of the PFI vehicle. During the first 200 s, the SIDI vehicle is operated in the homogeneous-charge mode with a corresponding loss of fuel economy. Reasons for operating in the homogeneous-charge mode for the first 200 s may include the following:

1. The engine emits less hydrocarbons and  $\text{NO}_x$  in the homogeneous-charge mode than in the stratified-charge mode.

2. The engine exhaust is hotter in the homogeneous-charge mode, which favors faster catalyst warm-up.
3. Driveability considerations may dictate the use of the homogeneous-charge mode immediately after startup.

A catalyst that is tolerant of the temperatures required for a close-coupled catalyst is needed to improve catalyst warm-up time. The lean- $\text{NO}_x$  catalyst must be placed upstream of the oxidation catalyst so it can take advantage of the engine-out hydrocarbons that act as reductants for the nitrogen oxides. Moving the lean- $\text{NO}_x$  catalyst next to the exhaust manifold would also allow the oxidation catalyst to be moved closer to the exhaust manifold. The result would be improved conversion efficiencies for THC and CO as well as for  $\text{NO}_x$ .

Both  $\text{NO}_x$  catalysts and oxidation catalysts that operate over a wider temperature range should be developed. The SIDI exhaust has a wider temperature range than that of the PFI engine. At full load, the SIDI exhaust is as hot as that of the PFI engine, but at light load excess air dilutes and cools the combustion products from the former, compared to the PFI exhaust. Thus, catalysts that can operate over the widest possible temperature range are desirable.

After the catalyst reaches operating temperature, its THC and CO conversion-efficiency percentages are in the high 90s. The excess exhaust oxygen when the engine operates in the stratified-charge mode aids oxidation of hydrocarbons and carbon monoxide. However, the same exhaust oxygen makes chemical reduction of nitrogen oxides more difficult. Even after the catalyst has warmed up,  $\text{NO}_x$  conversion-efficiency percentages range from the low 60s to the low 70s.  $\text{NO}_x$  conversion is particularly difficult during high-speed cruising. Under those conditions, the engine operates in the stratified-charge mode and produces a relatively large amount of  $\text{NO}_x$ . At the same time, the concentration of exhaust oxygen is unfavorable to chemical reduction of  $\text{NO}_x$ .



## 5 References

1. Noma, K., et al., 1998, "Optimized Gasoline Direct Injection Engine for the European Market," SAE Paper No. 980150, Society of Automotive Engineers, Warrendale, Pa.
2. Pentikäinen, J., M. Wensing, S. Juutinen, K.-U. Münch, and A. Leipertz, 1998, "Gasoline: Influence of Fuel-Oxygen on NO<sub>x</sub> Emissions," SAE Paper No 981366, Society of Automotive Engineers, Warrendale, Pa.
3. Heywood, J. B., 1998, *Internal Combustion Engine Fundamentals*, McGraw-Hill, New York, N.Y., p. 592.
4. Heywood, J. B., 1998, *Internal Combustion Engine Fundamentals*, McGraw-Hill, New York, N.Y., pp. 567-592.

## Appendix: Test Results for Top 20 Hydrocarbon Species

This appendix addresses the top 20 hydrocarbon species for the conditions tested. Hydrocarbons are arranged in descending order of concentration, on the basis of the FTP weighted averages.

### Mitsubishi, Indolene (A), Engine-Out

Name	Bag 1 Species (g/mi)	Bag 2 Species (g/mi)	Bag 3 Species (g/mi)	FTP Wtd. Avg. (g/mi)
Toluene	5.343E-01	5.618E-01	3.909E-01	0.5072
Ethene	2.192E-01	1.901E-01	1.534E-01	0.1859
2,3,4-Trimethylpentane	1.814E-01	2.019E-01	1.296E-01	0.1769
2,2,4-Trimethylpentane (Iso-octane)	1.759E-01	1.925E-01	1.296E-01	0.1710
Propene	1.886E-01	1.539E-01	1.299E-01	0.1545
n-Butane	8.369E-02	9.655E-02	8.404E-02	0.0902
Benzene	9.704E-02	8.774E-02	6.021E-02	0.0819
m-Xylene	8.867E-02	8.674E-02	6.195E-02	0.0801
n-Pentane	6.126E-02	7.242E-02	4.924E-02	0.0634
1,3,5-Trimethylbenzene	4.128E-02	4.626E-02	3.320E-02	0.0415
2,2,5-Trimethylhexane	4.177E-02	4.602E-02	3.105E-02	0.0408
Ethylbenzene	4.399E-02	3.999E-02	3.809E-02	0.0403
2-Methylpentane	4.050E-02	4.339E-02	2.731E-02	0.0382
2,4-Dimethylpentane	3.602E-02	4.043E-02	2.805E-02	0.0360
2,3-Dimethylbutane	3.241E-02	3.723E-02	2.536E-02	0.0328
o-Xylene	3.229E-02	3.492E-02	2.340E-02	0.0311
Ethyne	1.410E-01	0.000E+00	0.000E+00	0.0303
2-Methyl-2-Butene	3.001E-02	3.720E-02	1.785E-02	0.0301
1-Butene	0.000E+00	0.000E+00	1.017E-01	0.0290
2-Methyl-1-Butene	2.321E-02	3.390E-02	2.008E-02	0.0277

### Mitsubishi, Indolene (A), Tailpipe

Name	Bag 1 Species (g/mi)	Bag 2 Species (g/mi)	Bag 3 Species (g/mi)	FTP Wtd. Avg. (g/mi)
Toluene	2.226E-01	3.210E-03	3.847E-03	0.0506
2,2,4-Trimethylpentane (Iso-octane)	1.472E-01	6.710E-03		0.0350
2,3,4-Trimethylpentane	1.218E-01	7.160E-03	1.759E-02	0.0348
Ethene	1.049E-01	0.000E+00	0.000E+00	0.0226
Propene	9.385E-02	0.000E+00	0.000E+00	0.0202

Ethyne	8.035E-02	2.307E-03	0.000E+00	0.0184
n-Butane	3.265E-02	3.880E-03	1.157E-02	0.0123
Benzene	4.710E-02		2.934E-03	0.0110
n-Pentane	1.993E-02	2.978E-03	5.558E-03	0.0074
m-Xylene	3.412E-02	0.000E+00	0.000E+00	0.0073
2,3-Dimethylbutane	1.399E-02	0.000E+00	7.431E-03	0.0051
2,2,5-Trimethylhexane	1.900E-02	1.712E-03	0.000E+00	0.0049
2,4-Dimethylpentane	1.937E-02		2.343E-03	0.0048
2,3-Dimethylhexane	1.954E-02	0.000E+00	1.576E-03	0.0047
Ethylbenzene	1.958E-02	0.000E+00	0.000E+00	0.0042
2-Methylpentane	1.532E-02	0.000E+00	3.002E-03	0.0041
Ethane	0.000E+00	3.752E-03	6.956E-03	0.0039
2-Methyl-2-Butene	1.442E-02	0.000E+00	1.579E-03	0.0036
Ethylcyclopentane	1.338E-02	0.000E+00	2.327E-03	0.0035
o-Xylene	1.204E-02	1.301E-03	9.990E-04	0.0035

### Mitsubishi, Premium Ultimate, Engine-Out

Name	Bag 1 Species (g/mi)	Bag 2 Species (g/mi)	Bag 3 Species (g/mi)	FTP Wtd. Avg. (g/mi)
2,3,4-Trimethylpentane	2.281E-01	2.608E-01	1.957E-01	0.2352
2,2,4-Trimethylpentane (Iso-octane)	2.179E-01	2.485E-01	1.837E-01	0.2235
Ethene	2.030E-01	1.801E-01	1.619E-01	0.1798
Toluene	1.788E-01	1.938E-01	1.456E-01	0.1768
Propene	1.887E-01	1.710E-01	1.522E-01	0.1694
n-Butane	1.174E-01	1.414E-01	1.342E-01	0.1342
4-Methylheptane	4.328E-01	5.513E-03	4.302E-03	0.0970
1-Butene	1.866E-01	0.000E+00	1.504E-01	0.0830
m-Xylene	8.156E-02	8.850E-02	6.330E-02	0.0798
n-Pentane	6.754E-02	8.332E-02	6.418E-02	0.0745
Benzene	6.381E-02	5.893E-02	4.395E-02	0.0557
2,2,5-Trimethylhexane	5.144E-02	5.717E-02	4.278E-02	0.0518
2,4-Dimethylpentane	3.574E-02	4.343E-02	3.255E-02	0.0387
2,3-Dimethylbutane	3.493E-02	4.314E-02	3.162E-02	0.0381
n-Hexane	2.172E-02	5.622E-02	1.382E-02	0.0367
1,3,5-Trimethylbenzene	3.191E-02	3.799E-02	2.665E-02	0.0335
o-Xylene	3.311E-02	3.687E-02	2.753E-02	0.0334
2-Methylpentane	3.038E-02	3.404E-02	2.736E-02	0.0313
2-Methyl-2-Butene	2.934E-02	3.463E-02	1.871E-02	0.0290
Ethylbenzene	3.011E-02	3.005E-02	2.327E-02	0.0281

### Mitsubishi, Premium Ultimate, Tailpipe

Name	Bag 1 Species (g/mi)	Bag 2 Species (g/mi)	Bag 3 Species (g/mi)	FTP Wtd. Avg. (g/mi)
2,3,4-Trimethylpentane	8.676E-02	3.740E-03	1.103E-02	0.0237
Ethene	8.120E-02	3.111E-03	5.367E-03	0.0205
2,2,4-Trimethylpentane (Iso-octane)	8.328E-02	3.066E-03		0.0194
Propene	7.424E-02	0.000E+00	1.185E-03	0.0163
Toluene	6.806E-02	1.199E-03	3.074E-03	0.0161
Ethyne	6.072E-02	0.000E+00	0.000E+00	0.0131
n-Butane	3.720E-02	1.068E-03	1.350E-02	0.0124
n-Pentane	2.377E-02	4.775E-03	4.514E-03	0.0088
m-Xylene	3.135E-02	2.036E-03	2.720E-03	0.0085
Benzene	2.916E-02		2.393E-03	0.0070
2,2,5-Trimethylhexane	1.947E-02	1.227E-03	2.554E-03	0.0055
o-Xylene	1.274E-02	1.691E-03	1.501E-03	0.0040
2,4-Dimethylpentane	1.403E-02		1.987E-03	0.0036
1,2,4,5-Tetramethylbenzene	3.127E-03		9.977E-03	0.0035
2-Methylpentane	1.008E-02	1.471E-03	1.498E-03	0.0033
2,3-Dimethylbutane	1.310E-02	0.000E+00	1.698E-03	0.0033
2-Methyl-2-Butene	1.126E-02	6.371E-04	1.463E-03	0.0032
Ethylbenzene	1.250E-02	0.000E+00	6.180E-04	0.0029
Ethane	0.000E+00	1.898E-03	6.627E-03	0.0028
2,3-Dimethylhexane	1.088E-02	0.000E+00	1.594E-03	0.0028

### Mitsubishi, Low-Sulfur Gasoline, Engine-Out

Name	Bag 1 Species (g/mi)	Bag 2 Species (g/mi)	Bag 3 Species (g/mi)	FTP Wtd. Avg. (g/mi)
Toluene	1.495E+00	1.568E+00	1.234E+00	1.4571
2,3,4-Trimethylpentane	1.543E-01	1.827E-01	1.315E-01	0.1620
2,2,4-Trimethylpentane (Iso-octane)	1.391E-01	1.633E-01	1.158E-01	0.1446
Ethene	1.495E-01	1.231E-01	1.111E-01	0.1254
Propene	1.444E-01	1.274E-01	1.044E-01	0.1245
Benzene	1.227E-01	9.489E-02	7.782E-02	0.0960
n-Butane	7.128E-02	9.606E-02	7.795E-02	0.0856
Ethyne	0.000E+00	8.062E-02	6.768E-02	0.0596
n-Pentane	5.537E-02	6.405E-02	5.084E-02	0.0584
1-Butene	0.000E+00	0.000E+00	1.344E-01	0.0383
Ethylbenzene	4.409E-02	3.175E-02	2.908E-02	0.0336
m-Xylene	3.752E-02	3.014E-02	2.579E-02	0.0305
1,3,5-Trimethylbenzene	3.171E-02	2.530E-02	3.402E-02	0.0292

2,2,5-Trimethylhexane	2.719E-02	2.972E-02	2.248E-02	0.0271
2,3-Dimethylbutane	2.329E-02	3.053E-02	2.030E-02	0.0261
2,4-Dimethylpentane	2.303E-02	2.780E-02	1.853E-02	0.0241
n-Propylbenzene	2.076E-02	1.807E-02	2.170E-02	0.0197
2-Methyl-2-Butene	1.766E-02	2.211E-02	1.511E-02	0.0192
2-Methyl-1-Butene	1.404E-02	2.187E-02	1.244E-02	0.0175
2-Methylpentane	1.664E-02	1.806E-02	1.471E-02	0.0168

### Mitsubishi, Low-Sulfur Gasoline, Tailpipe

Name	Bag 1 Species (g/mi)	Bag 2 Species (g/mi)	Bag 3 Species (g/mi)	FTP Wtd. Avg. (g/mi)
Toluene	1.241E+00	1.546E-01	4.687E-02	0.3575
2-Methyl-1-Butene	2.051E-02	1.876E-01	0.000E+00	0.0982
2,3,4-Trimethylpentane	1.499E-01	1.772E-02	1.272E-02	0.0447
Propene	1.624E-01	1.694E-02	2.258E-03	0.0440
2,2,4-Trimethylpentane (Iso-octane)	1.373E-01	1.307E-02	1.161E-02	0.0394
Ethene	1.692E-01	1.597E-03	0.000E+00	0.0372
n-Dodecane	4.194E-02	5.162E-02	0.000E+00	0.0348
n-Butane	1.030E-01	1.268E-02	9.642E-03	0.0312
Benzene	8.193E-02	1.439E-02	1.669E-02	0.0296
n-Undecane	2.653E-02	3.310E-02	0.000E+00	0.0223
Ethyne	9.184E-02	0.000E+00	0.000E+00	0.0197
Ethane	0.000E+00	2.497E-02	5.025E-03	0.0139
n-Decane	1.331E-02	1.567E-02	1.941E-03	0.0112
1,3,5-Trimethylbenzene	3.198E-02	5.788E-03	1.851E-03	0.0103
t-2-Butene	2.722E-02	3.753E-03	6.642E-03	0.0096
n-Propylbenzene	0.000E+00	1.902E-02	0.000E+00	0.0095
m-Xylene	2.640E-02	6.537E-03	1.427E-03	0.0094
Ethylbenzene	2.611E-02	4.899E-03	2.768E-03	0.0089
2,3-Dimethylbutane	2.568E-02	4.547E-03	2.581E-03	0.0085
2,2,5-Trimethylhexane	2.550E-02	3.979E-03	2.304E-03	0.0081

### Neon, Indolene (A), Engine-Out

Name	Bag 1 Species (g/mi)	Bag 2 Species (g/mi)	Bag 3 Species (g/mi)	FTP Wtd. Avg. (g/mi)
Toluene	2.066E-01	1.515E-01	1.119E-01	0.1521
Ethene	1.061E-01	8.533E-02	7.458E-02	0.0867
Propene	8.374E-02	5.773E-02	5.360E-02	0.0621
Ethyne	0.000E+00	4.915E-02	5.861E-02	0.0413

Benzene	4.461E-02	3.695E-02	3.037E-02	0.0367
2,2,4-Trimethylpentane (Iso-octane)	4.142E-02	2.713E-02	2.041E-02	0.0283
2,3,4-Trimethylpentane	3.909E-02	2.420E-02	1.682E-02	0.0253
m-Xylene	3.556E-02	2.284E-02	2.048E-02	0.0249
Ethylbenzene	1.875E-02	1.375E-02	1.096E-02	0.0140
n-Pentane	1.475E-02	1.311E-02	9.208E-03	0.0124
n-Butane	1.491E-02	1.201E-02	9.934E-03	0.0120
1,3-Butadiene	1.626E-02	8.277E-03	1.110E-02	0.0108
1-Butene	0.000E+00	0.000E+00	3.775E-02	0.0108
1,3,5-Trimethylbenzene	1.588E-02	1.003E-02	7.469E-03	0.0106
Ethane	0.000E+00	1.908E-02	0.000E+00	0.0095
o-Xylene	1.228E-02	8.784E-03	6.596E-03	0.0089
t-2-Butene	1.430E-02	1.011E-02	0.000E+00	0.0081
2,4-Dimethyloctane	7.427E-03	1.227E-02	0.000E+00	0.0077
1,2,3-Trimethylbenzene	1.075E-02	6.378E-03	5.855E-03	0.0072
2-Methyl-1,3-Butadiene	7.646E-03	7.596E-03	5.943E-03	0.0071

### Neon, Indolene (A), Tailpipe

Name	Bag 1 Species (g/mi)	Bag 2 Species (g/mi)	Bag 3 Species (g/mi)	FTP Wtd. Avg. (g/mi)
Toluene	6.662E-02	1.895E-02	3.422E-03	0.0248
2,2,4-Trimethylpentane (Iso-octane)	2.280E-02	0.000E+00	3.229E-03	0.0058
2,3,4-Trimethylpentane	1.892E-02	0.000E+00	2.620E-03	0.0048
Ethene	2.219E-02	0.000E+00	0.000E+00	0.0048
Ethane	1.236E-02	0.000E+00	4.161E-03	0.0038
Propene	1.400E-02	0.000E+00	0.000E+00	0.0030
n-Propylbenzene	4.125E-03	3.957E-03	0.000E+00	0.0029
n-Butane	6.548E-03	1.582E-03	2.299E-03	0.0029
m-Xylene	1.216E-02	0.000E+00	5.945E-04	0.0028
Ethyne	1.076E-02	0.000E+00	0.000E+00	0.0023
Benzene	9.156E-03	0.000E+00	2.305E-04	0.0020
2,4-Dimethylpentane	5.136E-03	1.822E-03	0.000E+00	0.0020
n-Pentane	7.051E-03	0.000E+00	1.499E-03	0.0019
1,3,5-Trimethylbenzene	7.294E-03	0.000E+00	0.000E+00	0.0016
Ethylbenzene	6.009E-03	0.000E+00	0.000E+00	0.0013
o-Xylene	4.905E-03	0.000E+00	7.718E-04	0.0013
2,2,5-Trimethylhexane	5.618E-03	0.000E+00	0.000E+00	0.0012
2-Methyl-2-Butene	3.770E-03	1.876E-04	5.157E-04	0.0011
n-Dodecane	1.972E-03	1.171E-03	0.000E+00	0.0010
1,2,3-Trimethylbenzene	4.685E-03	0.000E+00	0.000E+00	0.0010

### Mitsubishi, Indolene (B), Tailpipe

Compound	Bag 1 (mg/mi)	Bag 2 (mg/mi)	Bag 3 (mg/mi)	FTP (mg/mi)	US06 (mg/mi)
Toluene	241.47	5.27	22.08	58.75	49.06
Methane	89.70	41.81	45.83	52.82	49.14
2-Methylbutane (Isopentane)	64.82	4.60	17.18	20.51	20.56
Ethylene	91.25	0.00	5.22	20.31	26.82
2,2,4-Trimethylpentane (Iso-octane)	69.07	2.99	12.49	19.26	16.84
Propene	73.85	0.00	4.59	16.54	19.17
1,2,4-Trimethylbenzene & t-Butylbenzene	57.63	2.23	4.84	14.41	8.30
Benzene	52.12	1.75	8.82	14.11	18.46
2-Methylpropene & 1-Butene	51.55	0.43	4.20	12.04	13.10
Acetylene (Ethyne)	56.23	0.00	0.00	11.64	1.83
m- & p-Xylenes	44.36	1.50	4.54	11.20	8.74
Other Unknown Materials	42.83	1.26	3.35	10.44	7.03
2,3,4-Trimethylpentane	34.64	1.24	5.35	9.28	7.10
2,3,3-Trimethylpentane	34.64	1.24	5.35	9.28	7.10
1-Methyl-3-Ethylbenzene	35.91	1.33	2.97	8.94	6.22
Formaldehyde	27.54	1.89	1.47	7.08	1.52
Ethylbenzene	28.54	0.77	2.13	6.89	4.87
n-Butane	17.84	1.61	8.51	6.86	6.44
n-Pentane	20.34	0.89	4.95	6.03	6.36
Ethane	19.64	0.00	6.95	5.97	8.73

### Mitsubishi, California Phase-2 Reformulated Gasoline, Engine-Out

Compound	Bag 1 (mg/mi)	Bag 2 (mg/mi)	Bag 3 (mg/mi)	FTP (mg/mi)	Highway (mg/mi)	SC03 (mg/mi)
m- & p-Xylenes	304.28	316.05	233.77	290.96	163.15	236.42
MTBE	218.66	236.39	194.49	221.18	125.24	177.04
Toluene	229.09	224.10	171.65	210.70	119.92	175.17
2,2,4-Trimethylpentane (Iso-octane)	163.11	178.05	129.27	161.53	88.12	129.62
Ethylene	196.78	156.20	138.49	159.75	104.20	152.63
2-Methylpropene & 1-Butene	173.40	154.51	138.11	153.91	115.08	146.38
2-Methylbutane (Isopentane)	147.59	164.85	137.53	153.75	102.66	130.21
Propene	165.02	134.04	121.02	136.89	95.26	127.22
2,3-Dimethylpentane	90.96	97.73	72.02	89.25	48.41	71.00
Ethylbenzene	93.97	94.98	70.88	88.14	49.48	69.85
o-Xylene	78.02	82.30	60.05	75.29	43.23	61.75
1,2,4-Trimethylbenzene & t-Butylbenzene	70.57	77.80	58.77	71.06	41.06	60.69
2-Methylpentane & 4-Methyl-cis-2-Pentene	66.61	76.91	57.15	69.33	42.29	57.60
Acetylene (Ethyne)	96.57	66.96	50.40	68.55	31.44	62.34
Benzene	83.06	68.07	55.44	67.71	37.89	59.32

Other Unknown Materials	58.83	68.29	68.14	66.29	45.93	72.73
Methane	88.94	56.87	48.06	61.10	29.36	60.41
1-Methyl-3-Ethylbenzene	61.62	64.31	48.78	59.48	33.27	48.93
2,3,4-Trimethylpentane	48.83	53.59	38.24	48.38	25.97	37.49
2,3,3-Trimethylpentane	48.83	53.59	38.24	48.38	25.97	37.49

### Mitsubishi, California Phase-2 Reformulated Gasoline, Tailpipe

Compound	Bag 1 (mg/mi)	Bag 2 (mg/mi)	Bag 3 (mg/mi)	FTP (mg/mi)	Highway (mg/mi)	SCO3 (mg/mi)
Methane	77.85	35.26	40.86	45.63	24.43	46.87
2,2,4-Trimethylpentane (Iso-octane)	80.30	2.58	12.26	21.36	5.44	10.69
Toluene	89.65	1.28	5.10	20.66	0.72	5.92
m- & p-Xylenes	87.20	1.34	4.93	20.14	0.81	5.18
Ethylene	81.73	0.00	2.68	17.69	0.61	3.04
2-Methylpropene & 1-Butene	72.61	0.46	4.71	16.59	0.30	5.22
2-Methylbutane (Isopentane)	57.81	1.65	12.03	16.15	5.32	9.99
Propene	68.60	0.00	2.61	14.95	0.31	2.61
MTBE	54.24	0.37	3.11	12.30	1.24	2.77
2,3-Dimethylpentane	37.52	0.97	5.29	9.74	2.07	4.92
Acetylene	44.43	0.00	0.00	9.22	0.00	0.59
Benzene	36.77	0.48	3.74	8.91	0.71	3.69
Ethylbenzene	34.79	0.68	1.59	8.01	0.31	1.84
Other Unknown Materials	31.32	1.18	2.00	7.66	0.77	0.84
Ethane	19.10	2.89	6.79	7.32	2.42	5.97
o-Xylene	29.55	0.77	1.66	6.99	0.27	1.79
1,2,4-Trimethylbenzene & t-Butylbenzene	28.11	1.04	1.62	6.81	0.28	1.61
2,3,4-Trimethylpentane	23.23	0.64	3.07	5.99	1.24	2.74
2,3,3-Trimethylpentane	23.23	0.64	3.07	5.99	1.24	2.74
2-Methylpentane & 4-Methyl-cis-2-Pentene	22.58	0.50	3.50	5.90	1.32	3.27